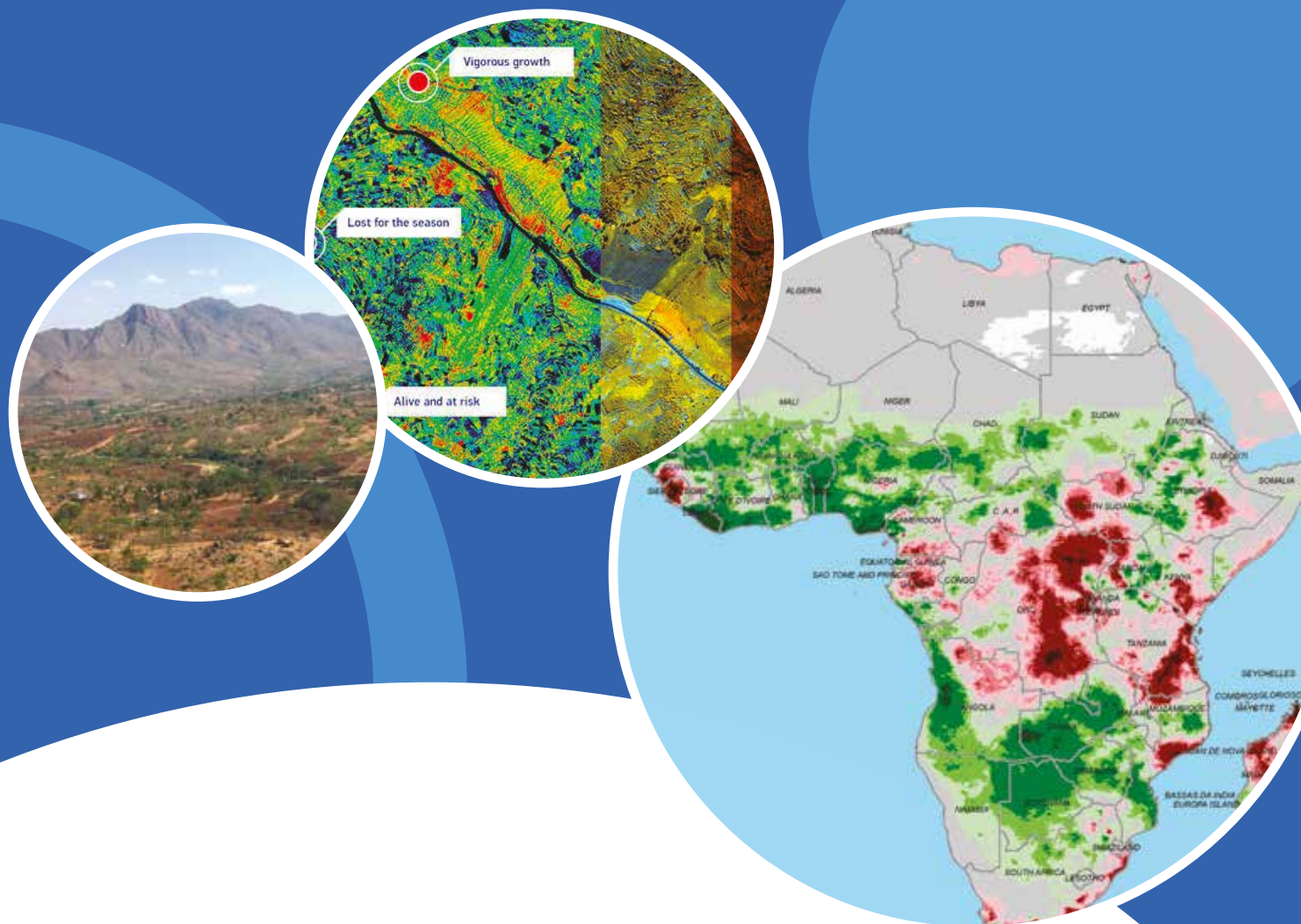


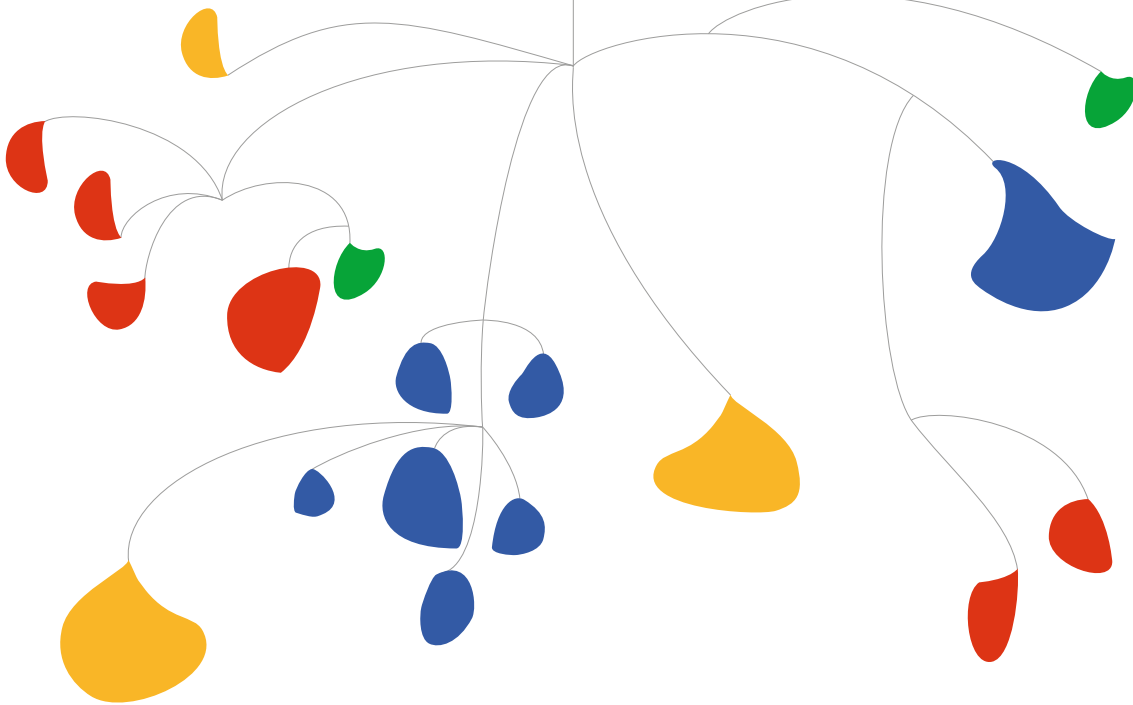


Food and Agriculture  
Organization of the  
United Nations



# REVIEW OF THE AVAILABLE REMOTE SENSING TOOLS, PRODUCTS, METHODOLOGIES AND DATA TO IMPROVE CROP PRODUCTION FORECASTS





# **REVIEW OF THE AVAILABLE REMOTE SENSING TOOLS, PRODUCTS, METHODOLOGIES AND DATA TO IMPROVE CROP PRODUCTION FORECASTS**

FOOD AND AGRICULTURE ORGANIZATION OF THE UNITED NATIONS

Rome, 2017

The designations employed and the presentation of material in this information product do not imply the expression of any opinion whatsoever on the part of the Food and Agriculture Organization of the United Nations (FAO) concerning the legal or development status of any country, territory, city or area or of its authorities, or concerning the delimitation of its frontiers or boundaries. The mention of specific companies or products of manufacturers, whether or not these have been patented, does not imply that these have been endorsed or recommended by FAO in preference to others of a similar nature that are not mentioned.

The views expressed in this information product are those of the author(s) and do not necessarily reflect the views or policies of FAO.

ISBN 978-92-5-109840-0

© FAO, 2017

FAO encourages the use, reproduction and dissemination of material in this information product. Except where otherwise indicated, material may be copied, downloaded and printed for private study, research and teaching purposes, or for use in non-commercial products or services, provided that appropriate acknowledgement of FAO as the source and copyright holder is given and that FAO's endorsement of users' views, products or services is not implied in any way.

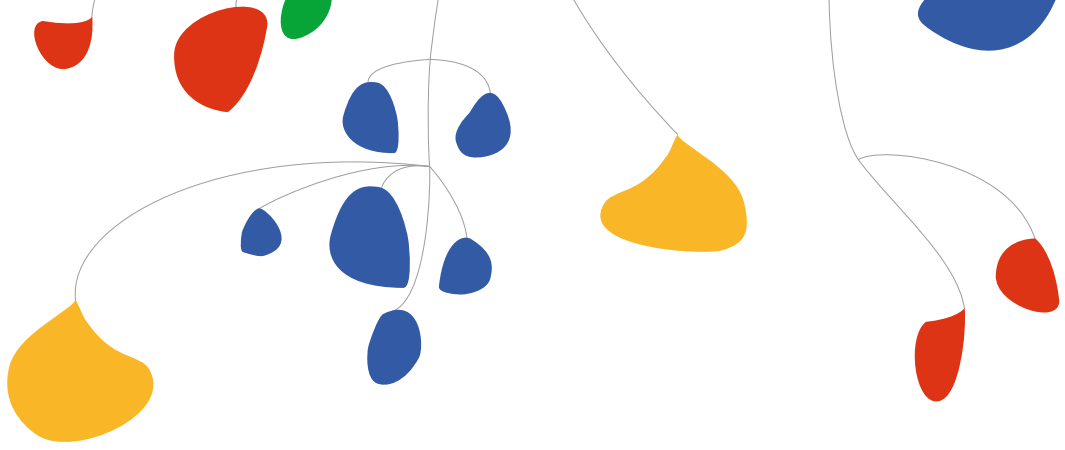
All requests for translation and adaptation rights, and for resale and other commercial use rights should be made via [www.fao.org/contact-us/licence-request](http://www.fao.org/contact-us/licence-request) or addressed to [copyright@fao.org](mailto:copyright@fao.org).

FAO information products are available on the FAO website ([www.fao.org/publications](http://www.fao.org/publications)) and can be purchased through [publications-sales@fao.org](mailto:publications-sales@fao.org).

This publication has been printed using selected products and processes so as to ensure minimal environmental impact and to promote sustainable forest management.

**Layout:** Laura Monopoli

**Cover photos:** © FAO/ Jacques Delincé



# Contents

<b>Acknowledgements</b>	<b>iv</b>
<b>Acronyms</b>	<b>v</b>
<b>Figures</b>	<b>vii</b>
<b>Executive summary</b>	<b>ix</b>
<b>Chapter 1</b>	
<b>Introduction</b> .....	<b>1</b>
<b>Chapter 2</b>	
<b>Review methodology</b> .....	<b>3</b>
<b>Chapter 3</b>	
<b>Literature review</b> .....	<b>5</b>
<b>3.1</b> Overview of the application of RS in crop forecasting	5
<b>3.2</b> RS methodologies currently used in crop production forecasts	9
<b>3.2.1</b> Yield forecast with RS	9
<b>3.2.2</b> RS and crop yield estimation	13
<b>3.2.3</b> Link between crop models and RS for yield forecasting	14
<b>3.2.4</b> Applications in EWS	19
<b>3.2.5</b> Combining optical and microwave RS	22
<b>3.3</b> Geoportals and RS data and products on agricultural crop production and forecasting	24
<b>3.3.1</b> Free RS portals, tools, data and products	25
<b>3.3.2</b> RS portals, tools, data and products available for a fee	59
<b>3.3.3</b> Other RS platforms that support agricultural applications	62
<b>3.4</b> National agencies mandated to generate crop production statistics	62
<b>3.4.1</b> National institutional RS capacities and competencies in the pilot countries	62
<b>Chapter 4</b>	
<b>Key findings and conclusions</b> .....	<b>73</b>
<b>References</b> .....	<b>75</b>

# Acknowledgements

This publication was prepared by Erick Khamala, a consultant engaged to develop guidelines on utilizing existing remote sensing tools, data, products, portals and methodologies to improve crop production forecasts at the Statistics Division (ESS) of the Food and Agriculture Organization of the United Nations (FAO).

The invaluable contributions of FAO staff – Y. Seid and C. Duhamel, as well as Gideon Galu, Regional Scientist of the Famine and Early Warning Systems Network (FEWS NET) – kindly provided during the preparation of this review are gratefully acknowledged.

This publication was prepared with the financial support of the Bill & Melinda Gates Foundation provided through FAO Project MTF-GLO-359-BMG on “Strengthening agricultural market information systems globally and in selected countries, using innovative methods and digital technology;” which is implemented in the context of the G20 AMIS Initiative.

# Acronyms

<b>AMC</b>	Antecedent Moisture Conditions
<b>AMIS</b>	Agricultural Management Information System
<b>ARC</b>	African Rainfall Climatology
<b>ASI</b>	Agricultural Stress Index
<b>AVHRR</b>	Advanced Very High Resolution Radiometer
<b>BERM</b>	Basin Excess Rainfall Map
<b>CHARM</b>	Collaborative Historical African Rainfall Model
<b>cm</b>	centimetre
<b>CN</b>	Curve Number
<b>CSM</b>	Crop Simulation Model
<b>DMC</b>	Disaster Monitoring Constellation
<b>DMCii</b>	Disaster Monitoring Constellation International Imaging
<b>DMP</b>	Dry Matter Productivity
<b>DRSRS</b>	Directorate of Resource Surveys and Remote Sensing (Kenya)
<b>ECMWF</b>	European Centre for Medium-Range Weather Forecasts
<b>ECV</b>	Essential Climate Variable
<b>EO</b>	Earth Observation
<b>ESA</b>	European Space Agency
<b>EROS (Center)</b>	Earth Resources Observation and Science Center (USGS)
<b>ET</b>	Evapotranspiration
<b>ETa</b>	actual evapotranspiration
<b>EU</b>	European Union
<b>EWS</b>	early warning system
<b>fAPAR</b>	fraction of Absorbed Photosynthetically Active Radiation
<b>FCover</b>	Fraction of Vegetation Cover
<b>FEWS NET</b>	Famine Early Warning System Network
<b>GCOS</b>	Global Climate Observing System
<b>GEO</b>	Group on Earth Observations
<b>GEOS</b>	Global Earth Observation System of Systems
<b>GEOGLAM</b>	GEO Global Agricultural Monitoring initiative
<b>GFS</b>	Global Forecast System (NOAA)
<b>GIEWS</b>	Global Information and Early Warning System on Food and Agriculture
<b>GIS</b>	Geographic Information System
<b>GMES</b>	Global Monitoring for Environment and Security
<b>GPS</b>	Global Positioning System
<b>GSD</b>	Ground Sample Distance
<b>GTS</b>	Global Telecommunication System
<b>ITF</b>	Inter-Tropical Front
<b>JRC</b>	Joint Research Centre (EU)
<b>km</b>	kilometre
<b>KMD</b>	Kenya Meteorological Department
<b>LACIE</b>	Large Area Crop Inventory Experiment

<b>LAI</b>	Leaf Area Index
<b>LST</b>	Land Surface Temperature
<b>LUE</b>	Light-Use Efficiency
<b>m</b>	metre
<b>MoA</b>	Ministry of Agriculture
<b>MODIS</b>	Moderate Resolution Imaging Spectroradiometer
<b>MI</b>	Moisture Index
<b>NASA</b>	National Aeronautics and Space Administration's
<b>NDVI</b>	normalized difference vegetation index
<b>NDWI</b>	Normalized Difference Water Index
<b>NIR</b>	near-infrared
<b>nm</b>	nanometre
<b>NOAA</b>	National Oceanic and Atmospheric Administration
<b>PDF</b>	Probability Distribution Function
<b>PAR</b>	Photosynthetically Active Radiation
<b>PRM</b>	Physical Reflectance Model
<b>RFE</b>	Rainfall Estimate
<b>RS</b>	remote sensing
<b>SAR</b>	Synthetic Aperture Radar
<b>SPI</b>	Standard Precipitation Index
<b>SPOT</b>	Satellite Pour l'Observation de la Terre
<b>SDD</b>	Stress Degree Day
<b>SSEBop</b>	Operational Simplified Surface Energy Balance
<b>SV</b>	State Variable
<b>TCI</b>	Temperature Condition Index
<b>SCS</b>	Soil Conservation Service
<b>SSA</b>	sub-Saharan Africa
<b>USDA</b>	US Department of Agriculture
<b>USGS</b>	US Geological Survey
<b>VHI</b>	Vegetation Health Index
<b>VI</b>	Vegetation Index
<b>VCI</b>	Vegetation Condition Index
<b>VHR</b>	Very High Resolution
<b>VPI</b>	Vegetation Productivity Index
<b>WHC</b>	Water Holding Capacity
<b>WRSI</b>	Water Requirement Satisfaction Index

# Figures

<b>Figure 1.</b>	Interaction of visible and NIR radiation with a healthy leaf.....	6
<b>Figure 2.</b>	Spectral signatures of soil, vegetation and water, and spectral bands of LANDSAT 7 .....	7
<b>Figure 3.</b>	Flowchart of the Belgian crop monitoring and yield forecasting system (B-CGMS) .....	19
<b>Figure 4.</b>	Conceptual framework of the WRSI .....	22
<b>Figure 5.</b>	Seasonal global ASI product for the second dekad of July 2016 .....	26
<b>Figure 6.</b>	Seasonal global Progress of Season product for the second dekad of July 2016 .....	27
<b>Figure 7.</b>	Seasonal global mean VHI product for the second dekad of July 2016 .....	27
<b>Figure 8.</b>	Global NDVI anomaly product for the second dekad of July 2016.....	28
<b>Figure 9.</b>	Global VCI product for the second dekad of July 2016 .....	28
<b>Figure 10.</b>	Global VHI product for the second dekad of July 2016.....	29
<b>Figure 11.</b>	Crop condition map synthesizing information for all Early Warning Crop Monitor crops as of 28 July 2016.....	30
<b>Figure 12.</b>	Africa's RFE 2.0 daily product for 24 June 2013 .....	32
<b>Figure 13.</b>	Map of the three windows used to package RFE 2.0 daily data .....	33
<b>Figure 14.</b>	Global one-day data for the first day of the seven-day period .....	34
<b>Figure 15.</b>	Global seven-day accumulation data for the first day of the seven-day period .....	34
<b>Figure 16.</b>	Maps of the number of rain days and relative anomaly.....	35
<b>Figure 17.</b>	Maps of maximum consecutive dry days and relative anomaly.....	36
<b>Figure 18.</b>	Maps of total accumulated rainfall and relative anomaly.....	36
<b>Figure 19.</b>	Maps of number of days since rain and relative anomaly .....	37
<b>Figure 20.</b>	Excess rainfall map for the first dekad of August 2016 at catchment level .....	38
<b>Figure 21.</b>	Excess rainfall map for the first dekad of August 2016 at river level .....	39
<b>Figure 22.</b>	Maps of daily runoff and anomaly as of 10 August 2016 .....	41
<b>Figure 23.</b>	ITF position map for the third dekad of July 2016, also showing the position during the previous dekad and the long-term average .....	42
<b>Figure 24.</b>	MI map of the first dekad of August 2016.....	43
<b>Figure 25.</b>	MI/SW difference images of the first dekad of August 2016 .....	44
<b>Figure 26.</b>	Monthly ETa anomaly product for July 2016.....	46
<b>Figure 27.</b>	SPI products for accumulation periods.....	48
<b>Figure 28.</b>	S10 NDVI product of the first dekad of May 2006.....	51
<b>Figure 29.</b>	VPI illustration, showing an example of high NDVI and high probability.....	52
<b>Figure 30.</b>	VPI product for Sudan for the second dekad of August 2016.....	53
<b>Figure 31.</b>	The DMP product for Sudan for the second dekad of August 2016. ....	55
<b>Figure 32.</b>	The NDWI product of the first dekad of July 2006.....	56
<b>Figure 33.</b>	Integrated crop production forecasting systems.....	63



# Executive summary

Timely and reliable agricultural production forecasts are critical to make informed food policy decisions and to enable rapid responses to emerging food shortfalls (Jayne *et al.*, 2010; Rashid *et al.*, 2010). Agricultural forecasts are increasingly important in national planning in sub-Saharan Africa (SSA) due to highly variable yield, production and consumption trends, which are in turn occasioned by high climate variability and change, rapidly increasing populations, and limited financial capacity to cope with frequent food insecurity crises.

In most SSA countries, the agricultural sector holds great importance. For instance, in countries such as Kenya, Senegal and Zimbabwe, this sector contributes between 20 and 30 percent of national Gross Domestic Product (GDP). Further, between 60 and 75 percent of the SSA's rural population depends on agricultural production for food and income sources. However, the majority of these rural populations depend on subsistence farming; characterized by small farm holdings and low farm inputs, this result in low productivity.

Further, in SSA countries, national governments tend to allocate less than five percent of their budgets to the agricultural sector, far below the percentage of 10 percent agreed by the Comprehensive Africa Agriculture Development Programme (CAADP). This has significantly contributed to several problems: agricultural productivity in key food sources ranking well below global average; challenges in implementing and sustaining reliable agricultural production monitoring and forecasting systems; and delayed and inappropriate decision- and policy-making at subnational to national levels that often result in catastrophic humanitarian crises and, as a consequence, costly and unsustainable mitigation measures.

It is against such a background that this review examines the current status of the remote sensing (RS) tools, products, methodologies and data that can help to improve agricultural crop production forecasting systems. The review is structured in three parts:

- A description of the methodology used for this review
- A literature review that covers four core areas, namely: an overview of the application of RS in crop production forecasting; the RS methodologies currently used in crop production forecasting; insight into the available geoportals and RS data and products on crop production forecasting; and an analysis of the national agencies mandated to generate crop production statistics in the three pilot countries of Kenya, Senegal and Zimbabwe
- A discussion on the key findings and the conclusions

The overview of the application of RS in crop forecasting begins by defining RS and describing the key biophysical elements of the plants and crops that are useful to it, particularly in the context of spectral vegetation indices, which help to measure vegetation activity while at the same time taking into account the variability occasioned by vegetation characteristics such as Leaf Area Index (LAI), vegetation cover, etc. The application of RS in yield forecasting and crop yield estimation is then discussed, including the use of RS-driven crop models. Early warning systems (EWS) that leverage on RS to provide warnings on aspects relating to crop

production are highlighted. The subsection ends by illustrating the importance of combining the use of optical and microwave RS: their complementarity strengthens crop production forecasting, helping to circumvent each other's inherent limitations.

In examining the geoportals and RS/Earth Observation (EO) data and products that support agricultural production, forecasting and early warning information, the review discusses both those RS tools, data and products that can be used free of charge as well as their commercially available counterparts. The geoportals and tools providing RS data and products without charge include: the GIEWS Earth Observation portal, the GeoGLAM website, the FEWS NET data portal of the US Geological Survey (USGS), the VEGETATION/Proba-V data portals, the GEONETCast network, the EUMETSAT data portal, and the Copernicus - Sentinels Scientific data hub. On the other hand, commercially available RS data include DigitalGlobe imagery, imagery from Airbus Defence and Space, imagery from Planet Labs/BlackBridge (RapidEye), imagery from DMCii, and other RS platforms such as aerial photography, LiDAR and drones.

The analysis of the national agencies mandated to generate crop production statistics was performed for two of the three pilot countries, Kenya and Senegal. The analysis considered various factors, among which institutional infrastructure, technical and financial resources, statistical methods and practices, availability and reliability of statistical information, information user needs, packaging, and dissemination. The analysis for Zimbabwe will be conducted in time for publication in a subsequent review.

The key findings of this review are the following:

- There have been significant improvements in global remotely sensed observations, products and services, in terms of sensors and spatial and temporal resolution.
- There are several readily available, good-quality suites of agricultural drought monitoring and early warning products.
- Most RS products and services are freely available on dedicated geoportals, even though their use and applications in the pilot countries is still very limited.
- The RS products available must be validated and fine-tuned for wider application within the countries of interest.
- Africa's information technology (IT) and communications systems are at different levels of development, but have significantly improved in the past decade and are generally capable of accessing and downloading low- to moderate-resolution RS data and products.
- There are shortcomings and gaps in the institutional capacity to integrate RS products with field agroclimatic information for the purpose of supporting a timely, reliable and cost-effective agricultural crop forecasting system.
- The technological transfer is unsustainable, due to uncoordinated and ad hoc funding by development partners; in most cases, this ends with the project, which tends to be merely replicated afresh without recognizing and building on earlier initiatives.
- Kenya, Senegal and Zimbabwe display disparities in terms of institutional progress in using RS products and services, which accurately reflects the challenges inherent in the African context. The success of the implementation of the Agricultural Management Information System (AMIS) pilot project would inform the future scaling-up of improved agriculture forecasting systems across the continent.

Based on these findings, and in light of the increasing demand for timely and reliable crop production forecast estimates, this review recommends two main actions:

- As a first step, ensure the full participation and engagement of key stakeholders and technical partners in the process of prioritized capacity development. This should be achieved through needs assessments, data and information exchange protocols throughout the entire course of the implementation of the pilot project. This activity could be fast-tracked by engaging national consultants, who would be supported by the staff of the FAO Country Offices and of the ministries of agriculture (MoAs) of the countries concerned.
- Develop an inventory database of the recommended RS data and products, among those tested in the pilot countries.





# Introduction

Timely and reliable crop production forecasts are crucial to making informed food policy decisions and enabling rapid responses to emerging food shortfalls. This is especially true in the sub-Saharan Africa (SSA) region, which is becoming highly vulnerable to food insecurity. In this region, the drivers for food insecurity are both climatic and non-climatic, and are often aggravated by subjective and unreliable crop production forecasting systems. In light of increasing interseasonal crop production variability, occasioned by highly unpredictable climate, increasing food consumption and limited financial resources, decision-makers continue to need reliable crop production forecasts that are capable of providing them with adequate lead time for resource allocation and facilitating appropriate responses and contingency planning.

Agricultural production forecasting is the science of estimating potential production with adequate lead time. In the SSA region, several approaches for agricultural production forecasting are currently in use and range from fairly subjective methods to more statistically objective techniques, depending on the technical and financial resources available. In recent years, new approaches have been developed that geospatially integrate field and satellite observations with simple crop models, to generate timely and more reliable agricultural production forecasts.

In examining and assessing the current status of agricultural production forecasting systems, this review focuses on the review and documentation of the Remote Sensing (RS) tools, products, methodologies and data that can be used to improve agricultural crop production forecasts in the SSA in general and in the three pilot countries of Kenya, Senegal and Zimbabwe in particular. The review further seeks to determine core institutional capacities and competencies in the pilot countries.

The review is structured as follows. Section 2 broadly describes the methodology, including the specifications and standards used. Section 3 provides an overview of the application of RS in agricultural crop forecasting, and specifically examines the RS tools, products, methodologies and data that can be used to improve agricultural crop production forecasts. It also considers the geoportals and platforms that offer RS data and products on agricultural crop production, as well as tools and methodologies for processing the same, and analyses the RS capacities in the main national agencies mandated to regularly generate reliable agricultural production statistics. Section 4 sets out the key findings and conclusions.



## Review methodology

The methodology adopted to compile this review is based on two broad activities. First, a literature review provides an overview of the application of RS in agricultural crop forecasting, highlighting which RS approaches and methodologies that can be used to improve agricultural crop production forecasts, as well as the geoportals and RS tools, data, and products for processing crop production forecasts. The review further assesses the RS capacities of the national agencies charged with the responsibility of generating crop production statistics in Kenya, Senegal and Zimbabwe. The second activity is the compilation of key findings from the literature review.

The methodology is pillared on the specifications and standards that guided the preparation of this review. First, the literature reviewed was from authentic sources that comprised authoritative institutions and published material (papers, books, etc.). Second, only authentic and authoritative geoportals and platforms were reviewed. Third, the review focused not only on access to freely available RS data sets and products, but also on other RS data sets and products currently available through EO satellite sensors, aircraft-based sensors, drones, etc. Fourth, the methodologies reviewed for deriving crop production forecasts include approaches based on RS and in situ data collection, collation and processing, including the use of Geo-Information and Communication Technologies (Geo-ICTs).





## Literature review

This literature review has four main components. The first component provides an overview of the application of RS in agricultural crop forecasting. The second component highlights the RS methodologies currently used in agricultural crop production forecasts. The third component gives insight into the available geoportals and RS data and products on crop production forecasting, while the fourth component examines national agencies mandated to generate crop production statistics in the three pilot countries of Kenya, Senegal and Zimbabwe.

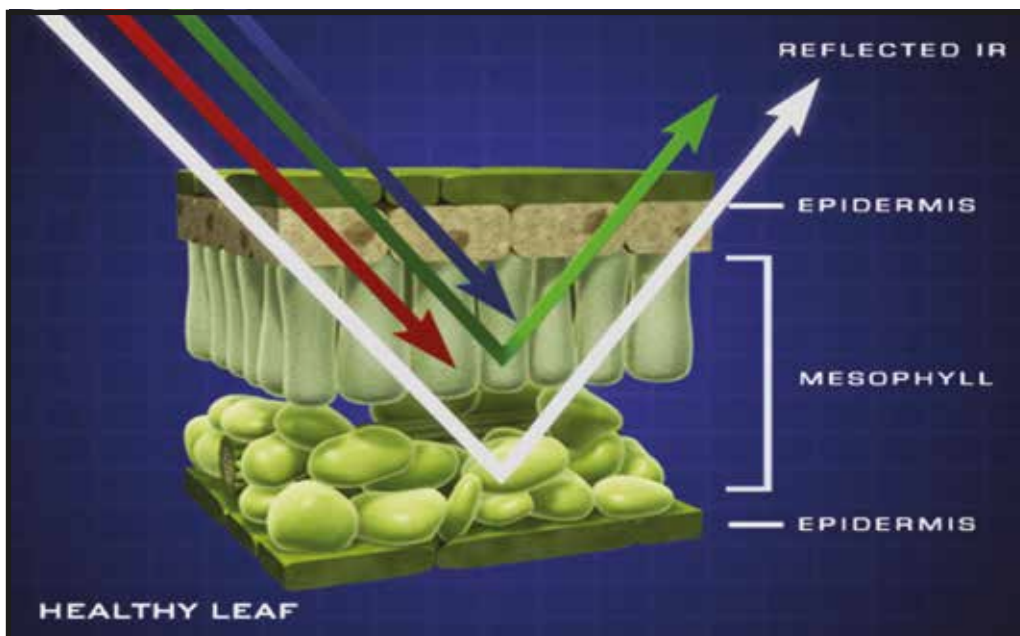
### 3.1 Overview of the application of RS in crop forecasting

RS is the science of acquiring information about an object through the analysis of data obtained by a device that is not in contact with the object (Lillesand and Keifer, 1994). Remotely sensed data can take many forms, including variations in force distribution, acoustic wave distribution or electromagnetic energy distribution. The data can be obtained from a variety of platforms, such as satellites, aircrafts, unmanned aerial or underwater vehicles, and handheld radiometers. Remotely sensed data may be gathered by various devices such as sensors, cameras, and video recorders. The instruments used for measuring electromagnetic radiation are called sensors. Sensors are passive when they do not have their own source of radiation and are sensitive to radiation from external sources, such as the Sun; they are active when they have a built-in source of radiation.

Leaves do not absorb all wavelengths of sunlight; they absorb the blue and red wavelengths and reflect green light (Campbell, 1996). The reflection of visible radiation is mainly a function of leaf pigments, while the near-infrared (NIR) radiation is reflected by the leaves' internal mesophyll structure. NIR radiation passes through the first layer of the leaf (the palisade tissue); when it reaches the mesophyll and the internal leaf cavities, it is either reflected

upwards (reflected radiation) or downwards (transmitted radiation). The behaviour of the reflected NIR is also a function of the Leaf Area Index (LAI), cell turgor, leaf thickness, and leaf internal air and water content. Human eyes perceive a leaf to be green because wavelengths in the green region of the spectrum are reflected by pigments in the leaf, while the other visible wavelengths are absorbed. In addition, components in plants reflect, transmit, and absorb different portions of the NIR radiation that are invisible to human sight. Reflected NIR radiation can be sensed by satellites, thus allowing scientists to study vegetation from Space. Healthy vegetation, while reflecting green light energy, absorbs blue and red light energy to fuel photosynthesis and create chlorophyll (Figure 1). A plant with more chlorophyll will reflect more NIR energy than an unhealthy plant. Thus, analysing a plant's spectrum for both absorption and reflection in visible and in NIR wavelengths can provide information about the plant's health and productivity.

**FIGURE 1. Interaction of visible and NIR radiation with a healthy leaf.**

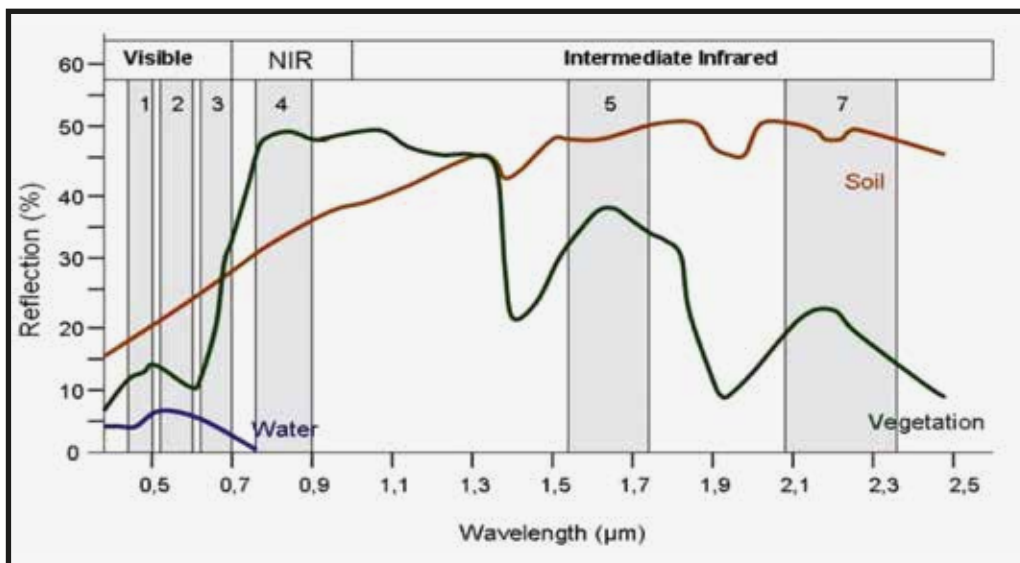


Source: Cans.

As a result of the mechanism described above, healthy crops will show high values of reflectance in the NIR spectrum and low values in the visible spectrum. During senescence and in crops subjected to stress (such as disease, pests, or nitrogen and water shortages), the lower chlorophyll content allows for the expression of other leaf pigments, such as carotenes and xanthophyll, which causes a broadening of the green reflectance peak at 550 nanometres (nm) and an increase in the visible light reflectance (Pinter *et al.*, 2003). At the same time, there is a decrease in relative reflectance in the NIR, due to the lesser absorption of visible light in the leaves (Asner, 1998). The soil reflectance increases monotonically from the visible to the NIR regions of the electromagnetic spectrum, and its slope varies according to soil type (Huete, 1987). In the visible region, leaf reflectance is lower than soil reflectance,

whereas in the NIR, leaf reflectance is higher than soil reflectance (Figure 2). This behaviour helps to explain the utility of these reflectance measurements in agricultural applications and the separation of crops from soil (Bausch, 1993). The spectral reflectance of soil is a function of soil constituents (soil organic matter, iron oxides, etc.) and soil roughness (such as particle and aggregate size) (Rondeaux *et al.*, 1996).

**FIGURE 2. Spectral signatures of soil, vegetation and water, and spectral bands of LANDSAT 7.**



Source: Siegmund & Menz, 2005 (with modifications).

The RS of soil and crop can be an attractive alternative to the traditional methods of field scouting because it is capable of covering large areas rapidly and repeatedly, providing the spatial and temporal information necessary for sustainable soil and crop management. The potential of RS in agriculture is very high because it is able to draw inferences about soil and vegetation amount in a non-destructive manner.

Numerous spectral vegetation indices (VIs) have been developed to characterize vegetation canopies. Plant canopy reflectance factors and derived multispectral VIs are receiving increased attention in agricultural research as they are considered robust surrogates for traditional agronomic parameters. Spectral reflectance and the thermal emittance properties of soils and crops have been used extensively, to predict ecological variables such as percentage of vegetation cover, plant biomass, green LAI and other biophysical characteristics. VIs are strongly modulated by interactions between solar radiation and photosynthetically active plant tissues, and are thus also indicative of dynamic biophysical properties related to productivity and surface energy balance.

Recent advances in the resolution and availability of RS imagery, coupled with a decrease in its associated costs, have enabled collection of timely information on soil and crop variability by examining VI spatial and temporal patterns. Precision agriculture applications rely on some form of VI to quantify spatial variability within a field.

Spectral VIs are mathematical combinations of different spectral bands, mostly in the visible and NIR regions of the electromagnetic spectrum. These numerical transformations are semi-analytical measures of vegetation activity and have been widely shown to vary not only with the seasonal variability of green foliage, but also across space, thus proving to be suitable for detecting within-field spatial variability. The main purpose of spectral VIs is to enhance the information contained in spectral reflectance data by extracting the variability due to vegetation characteristics (e.g. LAI, vegetation cover) and to minimize soil, atmospheric, and sun-target-sensor geometry effects (Moulin and Guerif, 1999). Spectral VIs enable a simple and convenient approach to extract information from remotely sensed data due to their ease of use, which facilitates the processing and analysis of large amounts of data acquired by satellite platforms (Govaerts *et al.*, 1999; Myneni *et al.*, 1995). Significant advances have been achieved in understanding the nature and proper interpretation of spectral VIs (Myneni *et al.*, 1995; Pinty *et al.*, 1993) and theoretical frameworks have been proposed to support the development of indices optimized for particular applications and sensors (Gobron *et al.*, 2000; Verstraete *et al.*, 1996).

Applications of VIs have ranged from leaf to global levels, and in the case of green LAI, efforts have been successful for several crops (Boegh *et al.*, 2002; Broge and Mortensen, 2002; Clevers, 1989; Colombo *et al.*, 2003; Curran, 1983a, 1983b; Xiao *et al.*, 2002). However, most VIs tend to be species-specific and therefore not robust when applied across different species, which naturally possess different canopy architectures and leaf structures.

The LAI is the ratio of leaf surface area to unit ground surface area (Breda, 2003). This index describes the potential surface area available for leaf gas exchange between the atmosphere and the terrestrial biosphere (Cowling and Field, 2003). Therefore, it is an important parameter that controls many biological and physical processes of the vegetation, including the interception of light and water (rainfall and fog), the attenuation of light through the canopy, transpiration, photosynthesis, autotrophic respiration, and carbon and nutrient (nitrogen, phosphorus, etc.) cycles. LAIs obtained across a range of spatial scales – from individual plants to entire regions or continents (Bonan, 1993; Running, 1990; Running and Coughlan, 1988; Sellers *et al.*, 1986) – has been used extensively in interactive models of land surface processes (Field and Avissar, 1998; Pielke *et al.*, 1998). As with other canopy structural properties, the LAI can be separated into its photosynthetic and non-photosynthetic components. The portion of LAI composed of green leaf area (i.e. the green LAI) is the photosynthetically functional component. Two main types of approach have been developed to estimate green LAI remotely: (i) inversions of canopy radiative transfer models (Fang *et al.*, 2003; Knyazikhin *et al.*, 1998a, 1998b; Weiss *et al.*, 1999); and (ii) identifying empirical relationships between green LAI and spectral VIs (Chen and Cihlar, 1996; Curran, 1983a, 1983b; Jordan, 1969; Myneni *et al.*, 1997; Wiegand *et al.*, 1979). While the two approaches relatively complement one another (Pinty *et al.*, 2009), it is difficult to obtain optimal parameterized solutions for radiative transfer model inversions (Fang *et al.*, 2003). Therefore, VIs are more widely used, due to their ease of computation.

Thus, spatial variability can be identified economically and rapidly through the use of remotely sensed images of the crop field, image processing, Geographic Information System (GIS) analysis and modelling, and Global Positioning Systems/Global Navigation Satellite Systems

(respectively, GIS and GNSS). Higher-end image processing techniques are followed to enhance precision.

## **3.2 RS methodologies currently used in crop production forecasts**

### **3.2.1 Yield forecast with RS**

Hatfield (1983) divided the models used for yield forecast from RS into spectral models (Tucker *et al.*, 1980); albedo models (Idso *et al.*, 1978), and thermal models (Idso *et al.*, 1977; Walker and Hatfield, 1979). Horie *et al.* (1992) identified three models used to forecast crop growth and yield from RS: the empirical regression model, the biomass production model as a function of absorbed or intercepted solar radiation, and the stress-degree-day model.

The meteorological models used for forecasting yield are mainly based on two variables, temperature and precipitation, because these are related to crop yields (Barnett and Thompson, 1982) and can be easily obtained from meteorological stations or satellite measurements. These two input variables can be used separately or in combination with one another, and as daily or monthly variables.

Meteorological models are generally a simple regression that entail three main methods: time series; based on changes in space and time; and based on changes in space (Lobell and Burke, 2010). Fisher (1924) used a statistical approach to successfully predict wheat yield as a function of growing season rainfall. In rain-fed agricultural regions, rainfall is the most important factor affecting crop growth and yield. French and Schultz (1984) proposed rainfall-based models to calculate the upper limit of potential yield. In Australia, this approach is still used by farmers and consultants. Robertson and Kirkegaard (2005) noted that the use of these models may lead to overestimating the yield, because the formula does not account for rainfall distribution, runoff, drainage or access to stored soil water. Fitzpatrick and Nix (1969) used the ratio of actual to potential evapotranspiration to forecast wheat yield. However, Unger (1966) concluded that to successfully use agrometeorological models for yield estimation, it is necessary to take into account the daily effects of temperature, soil moisture, the energy balance of the crop, or any of the yield components. Rudorff and Batista (1990) concluded that when these models are applied at regional level, they cannot fully simulate the various crop growing conditions within the region.

Today, the application of agrometeorological models is more common due to the integration with RS. Doraiswamy *et al.* (2003) reported one of the first examples of an effort to forecast production through satellite RS and measured meteorological observations on the ground. The Large Area Crop Inventory Experiment (LACIE) project, launched in 1974, used satellite RS to forecast wheat production in the major wheat-producing countries. For example, in 1977, LACIE forecasted a 30 percent reduction of spring wheat production in the former Soviet Union, an estimate that came close to the official figures released after the harvest (Myers, 1983). The models used in LACIE were statistical models, in which yield is modelled

as a function of air temperature and rainfall (Doraiswamy *et al.*, 2003). Tucker *et al.* (1980) used this approach to relate yield and the normalized difference vegetation index (NDVI), while Shibayama and Munakata (1986) used reflectance data collected during the grain filling period to forecast rice yield.

RS data obtained from the National Oceanic and Atmospheric Administration's Advanced Very High Resolution Radiometer (NOAA-AVHRR) has been used to monitor large-scale cropping systems and to forecast yield since the 1980s (Tucker *et al.*, 1985). Benedetti and Rossini (1993) used the AVHRR-satellite-derived NDVI data for wheat forecasting and monitoring in a region of Italy. The authors derived a simple linear regression model for wheat yield estimation and forecasting based on NDVI images captured during the wheat grain filling period. They validated their results against official data, and found good correlations between the two. Doraiswamy *et al.* (2003) used the AVHRR NDVI data as proxy inputs to an agrometeorological model for the estimation of wheat yield at two different spatial resolutions in North Dakota. Kogan *et al.* (2012) estimated winter wheat, sorghum and corn yields three weeks before harvest using the AVHRR data. The errors of yield estimated were in the order of 8 percent, 6 percent and 3 percent, for wheat, sorghum and corn, respectively.

In African countries bordering the Mediterranean Sea, Maselli and Rembold (2001) used the NDVI derived from the AVHRR platform to estimate cereal production. Meroni *et al.* (2013) used SPOT (Satellite Pour l'Observation de la Terre) imagery and a statistical model to quantify wheat yield in northern Tunisia, and concluded that where crop conditions must be quantified without ground measurements for calibration, the biomass proxies are preferred. In Senegal, Rasmussen (1999) used the AVHRR data to estimate millet yield using the NDVI integrated during the reproductive phase of millet development. He also investigated whether it was possible to reduce both the interannual and environmental variability by taking into account areas where production levels were homogeneous. Ray *et al.* (1999) used the Indian Remote Sensing (IRS) satellite to estimate cotton yields at district level, using the relationship between actual evapotranspiration and non-irrigated cotton yield. The use of low-resolution satellite images, along with their high temporal frequency, broad geographical coverage, and low costs per area, renders these images as a good choice for yield estimation; several reported findings confirm this conclusion. In Western Australia, Smith *et al.* (1995) used the AVHRR satellite images to estimate wheat yield in over 70 percent of the state's wheat-growing area. The authors concluded that the high correlation with the NDVI taken during the growing season indicated the capability to correctly forecast wheat yield well ahead of the end of the growing season.

Another frequently used satellite sensor is the National Aeronautics and Space Administration's (NASA) Moderate Resolution Imaging Spectroradiometer (MODIS), which has better spectral and spatial resolution than the AVHRR (Doraiswamy *et al.*, 2001; Ren *et al.*, 2008; Funk and Budde, 2009; Becker-Reshef *et al.*, 2010). AVHRR and MODIS have high-frequency observations; however, for both, the spatial resolutions are rather coarse. For example, MODIS data are available at resolutions of 250 m, 500 m, and 1 000 m, depending on the product chosen (Justice *et al.*, 1998), while the AVHRR data have a spatial resolution of 1.1 km for local coverage and 4 km for global coverage (Kidwell, 1998). Bolton and Friedl (2013) used satellite data from MODIS to develop empirical models for maize and soybean yield

forecast in central United States. The MODIS Enhanced Vegetation Index (EVI) displayed a better ability to predict maize yield than the NDVI, and the use of crop phenology information from MODIS improved the model predictability. Although MODIS has a relatively lower spatial resolution (250 m, 500 m and 1 000 m), the authors showed that MODIS was still able to identify the agricultural areas without affecting the model's output, compared to the crop-type maps developed by the US Department of Agriculture (USDA) with a higher spatial resolution. Kogan *et al.* (2013) used NDVI values from MODIS, at a spatial resolution of 250 m to forecast wheat yield in Ukraine. In Kenya, MODIS was used to derive images for six sugarcane management zones, over nine years, to estimate the sugarcane yield for each zone. Because of the zoning, the different management strategies were taken into account using the temporal series of the NDVI, which was normalized by means of a weighting method that includes sugarcane growth and the NDVI's time series. The challenge lies in estimating the yield of smallholder farms, where the fields are often smaller than the spatial resolution (250 m) of the MODIS data used.

Landsat is a satellite with better spatial resolution (30 m). It has been used for the purposes of yield forecast (Rudorff and Batista, 1990; Thenkabail *et al.*, 1994). However, the Landsat temporal resolution is lower than those of NOAA-AVHRR and MODIS. This may be problematic if frequent observations at sensitive crop growth stages are necessary. Idso *et al.* (1980) used Landsat and crop senescence to forecast grain yield. This was achieved by means of the concept of crop albedo variations during the growing season (Idso *et al.*, 1977, 1978). Wheat field albedo always decreased from the time of heading to the beginning of senescence. When a crop was subject to water stress, senescence appeared earlier compared to well-watered crops. Thus, Idso *et al.* (1980) used the senescence rates and their correlation with grain yield to forecast production. Rudorff and Batista (1990) estimated sugarcane in Brazil using RS and an agrometeorological model based on a model developed by Doorenbos and Kassam (1979) in which yield is related to a multiple regression technique used to integrate the VI obtained from Landsat data and the yield from the agrometeorological model. These estimations explained the yield variations of 69, 54, and 50 percent, respectively, in the three growing seasons analysed. The authors also tested the accuracy of sugarcane yield estimations using RS on the agrometeorological model only. The results were poorer compared to the combinations of both (Rudorff and Batista, 1990).

Recent studies have used a combination of data with higher spatial resolution, from Landsat, and data with higher temporal frequency, from MODIS or AVHRR (Genovese *et al.*, 2001; Becker-Reshef *et al.*, 2010; Mkhabela *et al.*, 2011). To generalize these models and ensure their reliability, the use of physiological concepts was introduced. One of the most frequently used concepts is the Photosynthetically Active Radiation (PAR).

The PAR is defined as the amount of light available for photosynthesis, which ranges between 400 and 700 nm (McKree, 1972). Monteith (1977) proposed a simple model that relates crop biomass, at any moment of crop growth, with the PAR accumulated. This model has been further validated by experimental evidence (Shibles and Weber, 1966; Gallagher and Biscoe, 1978; Kumar and Monteith, 1982; Sinclair and Horie, 1989; Daughtry *et al.*, 1992; Gower *et al.*, 1999). Bastiaanssen and Ali (2003) combined the PAR model with the light use efficiency model developed by Field *et al.* (1995) and the surface energy model of Bastiaanssen *et al.*

(1998), to estimate crop growth and forecast crop yield using the AVHRR data for wheat, rice, sugarcane and cotton. The authors concluded that although the resolution of AVHRR is too coarse for the purposes of field scale estimation, it nevertheless provides useful yield forecasts.

Forecasting crop yield in suboptimal growing conditions is more difficult. However, the use of RS and physiological concepts such as the PAR may be of assistance in gaining real-time information on crop growing conditions at any stage during the crop growing season (Clevers, 1997). The use of PAR estimated from RS was used to predict sugar beet yield in Europe. The model's parameters were not empirical estimates; rather, they were derived using physiological concepts. Another important crop parameter, the LAI, was linked with remotely sensed data. The LAI is considered to be an important factor in describing several processes, such as crop evapotranspiration, photosynthesis and yield (Price and Bausch, 1995). The LAI is also a good indicator of canopy ground cover; for this reason, RS has been used to link LAI (Richardson and Wiegand, 1977; Tucker *et al.*, 1979) and greenness (Rice *et al.*, 1980).

The VIs and greenness are linearly related to the PAR absorption rate of crop canopies (Hatfield *et al.*, 1984; Asrar *et al.*, 1985; Wiegand *et al.*, 1979; Wiegand and Richardson, 1990). Therefore, the crop-absorbed PAR can be estimated from remotely sensed VIs or greenness and the PAR observed at ground stations. This approach has been used for several crops, to remotely estimate yields with satisfactory results (Asrar *et al.*, 1985; Wiegand *et al.*, 1989; Wiegand and Richardson, 1990). However, the method produces a potential crop yield rather than an actual one, and it is assumed that the radiation conversion efficiency and the harvest index are constant. The radiation conversion efficiency is affected by nitrogen deficiency (Sinclair and Horie, 1989) and water stress, while harvest index is influenced by water or temperature stress during the reproductive and grain-filling stages (Horie, 1987). Casanova *et al.* (1998) used VIs and PAR to estimate the LAI and biomass, and concluded that the estimation of biomass is more reliable than the estimation of the LAI. Indeed, at early growth stages, the low LAI and high soil reflectance makes it difficult to isolate the plant signal, thereby affecting the relationships between the spectral and canopy biophysical properties (Huete, 1988). Later in the season, high LAI values cause some VIs to lose sensitivity to crop stress. Carlson and Ripley (1997) found that when LAI values ranged between three and six, the NDVI became ineffective. Daughtry *et al.* (2000) demonstrated that the LAI is the main variable affecting VIs, for the estimation of leaf chlorophyll concentration.

The other model used to integrate RS and yield forecasts is based on canopy temperature measurements. The rationale behind this approach is that water stress causes elevated plant temperatures, which negatively affect plant photosynthesis and crop yield (Idso *et al.*, 1977; Idso, 1968). Idso *et al.* (1978) refer to this model as the Stress Degree Day (SDD), in which canopy yield is inversely and linearly related to the accumulated SDD over a given period of time during crop development. Idso *et al.* (1977) demonstrated that the differences in canopy-air temperatures at midday (SDD) were related to yield when cumulated over a period of time. This model was used as a base for forecasting crop yield and crop water status by means of RS. However, the difference in leaf and air temperatures is strongly influenced by the air's vapour pressure deficit and by soil moisture; therefore, the application of the SDD is somewhat limited to environments where the vapour pressure deficit is relatively constant

(Horie, 1992). Jackson *et al.* (1981) improved the SDD by creating the Crop Water Stress Index (CWSI), which takes the effects of vapour pressure deficit into account. Gardner *et al.* (1981) proposed a Temperature-Stress-Day (TSD) index, which compares canopy and field temperatures at an unknown stress level and for a fully-watered field with the same crop. Reginato *et al.* (1978) found that for the purposes of yield prediction, the cumulative SDD for grain crops is calculated from head appearance and awns to the end of plant growth. Idso *et al.* (1978) integrated the SDD concept with that of growing degree days (GDD), to better predict both grain yield and the end of crop growth.

Yield forecasts through RS and models have been made for several cropping systems. For vineyards, the final yield was evaluated using high spatial resolution RS to estimate canopy vigour and yield components (Hall and Wilson, 2013). RS techniques have been extensively used in research for yield forecast, but played only a small part in understanding the cause of spatial yield variability.

Although it has been argued that RS may not be suitable for applications in developing countries due to the stratified agricultural systems and very small farm sizes generally prevailing there, and that this difficulty is likely to persist in the near future because of RS's inability to estimate yield in mixed agriculture systems, the increased availability of multispectral high-spatial-resolution satellite and airborne RS data (including drone-acquired data) at reasonable costs makes this technique a viable and interesting alternative for the purposes of yield forecasting.

### 3.2.2 RS and crop yield estimation

RS can provide valuable information on yield assessment and reveal spatial variation across the field. Two approaches exist for yield estimation: the first is a direct method, in which predictions are derived directly from RS measurements. The second is an indirect one, where remotely sensed data are incorporated into simulation models for crop growth and development, either as within-season calibration checks of model output (LAI, biomass), or in a feedback loop used to adjust model starting conditions (Maas, 1988). The direct method for yield prediction using RS can be reflectance- or thermal-based. Both methods have been successfully applied to various crops, such as corn, soybean, wheat and alfalfa (Tucker *et al.*, 1979; Tucker *et al.*, 1981; Idso *et al.*, 1977; Pinter *et al.*, 1981). In his survey of 82 different varieties of wheat, Hatfield (1981) was unable to identify a consistent relationship between spectral indices and yield. To predict wheat and sorghum yields, Hatfield (1983) coupled frequent spectral reflectance and thermal observation within a more physiological method, which required thermal infra-red (TIR) daily measurements during the grain-filling period to estimate crop stress (Hatfield, 1983). Shanahan *et al.* (2001) demonstrated that the corn pollination period was not a good growth stage during which to estimate yield, because of the various factors that can influence the tassel emergence date. Yang *et al.* (2000) found similar results, concluding that images taken at grain filling can provide good relationships between VIs and the yield.

The reliability of imagery for use in yield estimation decreases the sooner it is captured prior to harvest, because there are more opportunities for factors such as stress to influence yield. Aase and Siddoway (1981) had cautioned that the relationships of spectral indices to yield depended upon normal crop grain-filling conditions. Similar results were found by Basso *et al.* (2004), who noted that the NDVI images of a rain-fed durum wheat field showed different correlations to yield depending on the time that the image selected was captured. In this specific case, the spatial variability of the soil texture and of the soil water uptake by plants affected by drought was mutable, presenting different scenarios from that predicted by the NDVI estimation.

### 3.2.3 Link between crop models and RS for yield forecasting

Crop Simulation Models (CSMs) are computerized representations of crop growth, development and yield, simulated through mathematical equations as functions of soil conditions, weather and management practices (Hogenboom *et al.*, 2004). The strength of CSMs lies in their ability to extrapolate the temporal patterns of crop growth and yield beyond a single experimental site. CSMs can be used to gain new scientific knowledge of crop physiological processes, or to evaluate the impact of agronomic practices on farmers' incomes and environments. However, crop models are only an approximation of the real world, and many fail to take into account important factors such as weeds, diseases, insects, tillage and phosphorus (Jones *et al.*, 2001). Nevertheless, CSMs have played important roles in interpreting agronomic results, and they are increasingly being applied as decision support systems for farmers.

The models range from simple to complex. The purpose for which they are to be used determines, to a large extent, their complexity. Simple models are often used for yield estimation across large land areas, that is based on statistical information related to climate and historical yields; these models include little detail on the soil-plant system. More complex mechanistic models may provide detailed explanations of the soil-plant-atmosphere system; however, they require a large amount of input data, some of which may not be available.

Models can be broadly classified into two general groups: deterministic models and stochastic models. Deterministic models produce a specific outcome for a given set of conditions, assuming that all plants and soil within the simulation space are uniform. Stochastic models produce outcomes that incorporate the uncertainties associated with the simulations. These uncertainties may be due to the spatial variability of soil properties, weather conditions and other abiotic and biotic factors; they are not accounted for in a deterministic model. To overcome some of the problems arising from spatial soil variability, soil properties are subdivided into small homogenous units and results using deterministic models, and are then aggregated to provide the entire field yield. Stochastic models are required when there is uncertainty as to the accuracy of the input information. Generally, the crop growth system is more stochastic than deterministic, because many parts of the agroecosystem are heterogeneous. However, to date, CSMs using a stochastic approach have not been developed to a level that can be useful in decision-making, except where year-to-year variations in weather are accounted for using deterministic models. Deterministic CSMs can

be classified into three basic types: statistical, mechanistic, and functional. The number of data inputs and functions, and the degree of their sophistication, help to contrast the model types (Addiscott and Wagenett, 1985).

The integration of RS and CSMs for crop yield forecasting has been a subject of research for almost three decades, and is justified by the fact that RS is capable of quantifying crop status at any given time during the growing season, while CSMs can describe crop growth every day throughout the season (Maas, 1988). RS can indirectly provide measures for the canopy state variables used by the CSM, as well as spatial and temporal information about those variables, information that can then be used to adjust the model simulation. Ever since satellite data first became available to scientists, they have developed algorithms to estimate canopy state variables, such as the LAI, the Green Vegetation Fraction (GVF) and the Fraction of Absorbed Photosynthetically Active Radiation (fAPAR). One of the main integration procedures between RS and CSMs focuses on adjusting the LAI simulated with the crop models against that estimated by means of RS. The LAI is an important agronomic parameter, because water and carbon dioxide are exchanged between the plant and the atmosphere through the plant's leaves. In addition, the LAI is used to model crop evapotranspiration, biomass accumulation and final yield (Strachan *et al.*, 2005).

Researchers working on RS and CSM integration generally adopt three basic steps: (i) estimate canopy variables with RS; (ii) run the CSM; and (iii) use a proper integration method to adjust model runs. The first step may affect the subsequent results of the integration because, if the crop variable is not properly estimated, adjusting the model with a biased variable will lead to a wrong model evaluation. There are two ways of using RS for the estimation of canopy variables: through the use of statistical/empirical relationships; and the Physical Reflectance Models (PRMs) that simulate the interaction between solar beams (a definition of the concentrated stream of particle, such as the light flux) and the various canopy components by using physical laws in which the LAI can be entered as input obtained from the crop model (Dorigo *et al.*, 2007).

The first methods consist of building relationships between the crop variables and RS or VIs, such as that between the Weighted Difference Vegetation Index (WDVI) and the LAI (Clevers, 1989). Such models are built by means of simple or multiple regressions, stepwise multiple regressions, or partial least square regressions (Hansen and Schjoerring, 2003; Yoder and Pettigrew-Crosby, 1995). They are simple to build and to evaluate, and do not require a great deal of computational effort. Several studies have reported on the successful application of this technique, such as in the development of indices for the global estimation of crop parameters that are sensitive to high biomass levels, and less influenced by soil reflectance and atmospheric effects (Jiang *et al.*, 2008). The main limitation of empirical-statistical methods lies in the fact that, for every year of measurement in the same field or for different sites, the relationships must be recalibrated due to changes in soil reflectance, canopy type and architecture. Nevertheless, this approach has been successfully used for the validation of crop models in a precision agriculture context, because the simplicity of using NDVI data and their empirical relationship with yield help to characterize spatial patterns of crop growth variability; the crop model will only be validated in the areas defined by the RS map (Basso *et al.*, 2001).

The second method involves the use of PRMs, which can simulate reflectance of either leaf or of the overall canopy (Verhoef, 1984; Jacquemonod and Baret, 1990); for practical purposes, physical models that simulate canopy reflectance are preferred, because the measured reflectance is collected in the field on an area base. Canopy reflectance models are built on the radiative transfer theory, according to which the canopy is a turbid medium with leaves that are small and distributed randomly. Canopy reflectance models are usually inverted, to identify the best set of parameters that minimize the differences between the observed and simulated canopy reflectance. The methods used to find the best solution to the inversion are the iterative technique, look-up tables and artificial neural networks (Moulin *et al.*, 1998; Dorigo *et al.*, 2007). One problem of the inversion technique is that the solution does not produce a unique value, because the variables affecting the overall canopy spectral signature have synergic effects and compensating for this will affect the outcome (Fourty and Baret, 1997). For example, Baret and Guyot (1991) found that the modelled reflectance of sparse canopies with horizontal leaves was similar to that of dense canopies with vertical leaves.

Farmers in developed countries tend to use one or a few remotely sensed images for crop management, to retrieve canopy variables with empirical or statistical methods. This is more practical than the modelling approach, because it is simple and does not require extensive time, calculation or interpretation. Moreover, canopy reflectance models require knowledge about the nature of the inputs and the techniques required for the inversion, whereas in the statistical approach, only the variable of interest is taken into account. For example, taking remote observations before the application of N fertilization, and using a functional relationship between VIs and canopy N stress, is more practical for farmers and agronomists, who may find canopy reflectance models to be too complex. It must be acknowledged, however, that canopy reflectance models are an important tool for research purposes and for understanding the effects of both crop architecture and soil reflectance on the overall canopy spectral signature. Therefore, the two methods may be considered complementary: while scientists use physical modelling approaches to either design new indices or comprehend the patterns of crop spectral responses, agronomists can use the knowledge gained from models to derive empirical models to achieve better crop management (Cammarano, 2010). The other important step in integrating crop models and RS is the technique used to combine them. Maas (1988) analysed four ways to integrate RS and CSMs:

#### ***Method 1: Evaluation of driving variables.***

This technique is relatively simple and uses RS information to evaluate driving variables. Remote observations should be performed frequently during the growing season, or at least frequently enough to perform interpolation techniques, and thus obtain the daily values of the RS estimated variable. Therefore, a limitation of this technique is that remote observations are required for each time-step of the simulation, which is practically and economically unfeasible (Cammarano, 2010).

#### ***Method 2: Updating of the model State Variables (SVs).***

The daily State Variable (SV) values are simulated with the CSM and, when RS data become available, the new values are simply updated into the CSM. For example, many crop models

use the LAI to estimate biomass accumulation. The values of the LAI and biomass are simulated by the model and when the LAI estimated with RS is available. For this technique, the accuracy of the updated variable is a function of the latest remote observation and, because RS data carry some degree of error, the updated SV may present bias that cannot be minimized by more frequent remote observations. Another limiting factor is that in the model, all SVs should be updated after RS acquisition (Cammarano, 2010).

### **Method 3: Reinitialization of the model SVs.**

This technique modifies the initial condition of the SV in the crop model so that a new simulation will accord with RS observations. Indeed, different values for the SVs' initial conditions in the crop model could lead to different simulation scenarios. For example, when remote observations are available, the SV is estimated from RS, and discrepancies are likely to exist between the observed and simulated SVs. This effect is taken into account by considering the sum of the absolute errors between simulated and observed values. This leads to the creation of an error function. This function can be solved through an iterative numerical analysis technique (e.g. the secant method) and a new value for the SV can be found. This new value will replace the old value required to initialize the model. Reinitialization can be performed on one or more SVs, leading to a unidimensional or multidimensional solution for the problem. This method has been used to derive new values of the LAI and to calibrate the model (Maas, 1988). In the estimation of biomass and final yield, the reinitialization procedure leads to good results compared to previous integration strategies, because RS is used to modify the SV in the model and, at the same time, reduce the random error present in RS data. However, one limitation of this technique lies in the nature of the empirical relationship between RS and the LAI. For example, NDVI values tend to reach saturation levels at LAI values greater than three (Aparico *et al.*, 2000); the NDVI is therefore insensitive to changes in LAI after saturation point has been reached in dense canopies. Also, these relationships may have only local significance, and must be recalibrated for each new site.

### **Method 4: Re-parameterization of models.**

This is similar to Method 3, with the difference that the model parameters are modified after their estimation with RS observation. Typically, a model has more parameters than SVs and the minimizing procedure is more complicated, requiring more computational power. Indeed, while for reinitialization the error function is often two-dimensional, for the re-parameterization it will depend on the number of parameters involved. Therefore, the solution of the error function is multidimensional and all the parameters should receive the same relative amount of change (Cammarano, 2010). Since Maas (1988), many other conceptual models for the integration of RS and CSM have been proposed, such as the reviewed classification for integration, which also identifies an "assimilation" technique (Moulin *et al.*, 1998) in which RS is directly used to re-parameterize or reinitialize the model. In this case, the daily crop reflectance can be simulated with PRMs, and the differences in simulated and observed reflectance then minimized by adjusting the CSM's initial conditions or model parameters. An LAI simulated with a CSM is first used as input in the canopy reflectance model and then, once the errors between RS observed and simulated data are minimized, the new LAI value can be adjusted in the CSM. But with this method, the number of parameters that can be

adjusted is a function of the frequency and the timing of RS observations. Launay and Guerif (2005) used this assimilation procedure to spatially link the RS and the CSM. They found that in drought conditions, the CSM does not properly estimate the LAI, and its use in the canopy reflectance model will not improve method robustness.

One of the key requirements for a successful integration of RS and CSMs for in-season and between-season crop management is that the whole system – defined as RS observation, crop simulation and soil-crop-weather – must be properly understood. One of the most challenging problems in the use of both CSMs and RS is the interpretation, comprehension and evaluation of the results, to develop the agronomic management strategy that minimizes observed variability in crop production. Factors affecting crop growth, development and yield are well understood, and evidence of yield variability is normally provided but not explained (Cammarano, 2010). For instance, final yield is a function of the complex temporal interaction of several variables, such as genotype, crop population, management, weather and stress (Bachelor *et al.*, 2002). A CSM takes into account, to some extent, the above effects and the temporal effects of stresses on crop growth and development. However, the use of both model results and measured data to understand the causes of particular spatial and temporal crop variability, and how it can be managed from the agronomic, economic and environmental point of view, remains challenging.

Through the observation of VIs' spatial patterns, RS enables information on crop variability to be collected (Blackmer and White, 1998). Therefore, a strategy integrating RS and CSMs can be useful for in-season crop management, and offers an explanation of the causes of field variability and how this can be managed.

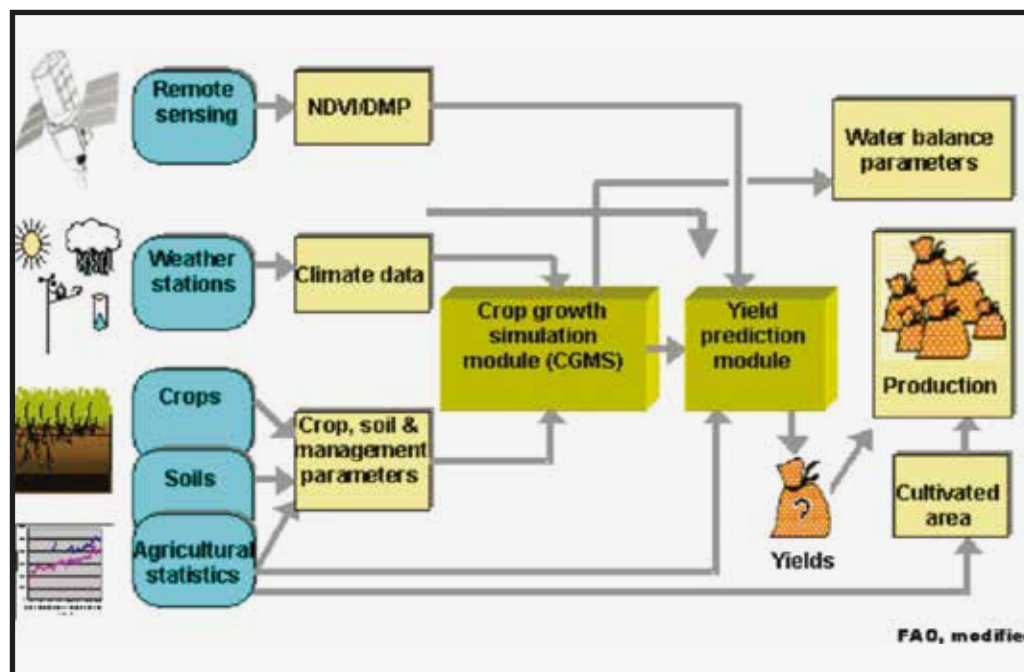
As a result, CSMs should be used with a view to understanding crop temporal variability, and RS images should be used to map the actual distribution of crop spatial variability at a given time during the growing season. An example of a spatial integration approach is described in Basso *et al.* (2001), in which a CROPGRO soybean model (Boote *et al.*, 1998) was used to validate three management areas across the field, individuated with an NDVI map by means of a supervised classification technique. Soil properties and average crop population were measured in each zone with targeted sampling, and subsequently used as inputs in the CROPGRO model. The model run was made only for three zones without calibration for the season, and the model simulated yield for these three zones with a root mean square error (RMSE) of 101 kg ha<sup>-1</sup> with an average measured yield of 3 000 kg ha<sup>-1</sup>. This technique has a twofold advantage: it reduces the costs of applying CSMs to precision agriculture; and the model inputs and model parameterization are scale-independent, because the scale is controlled by the observed variation in the field, which is the scale at which the model is applied (Bachelor *et al.*, 2002).

The other approach commonly adopted to link RS and CSMs is based on the concept that the biomass produced by a crop is a function of the amount of PAR absorbed, along with the air temperature and soil conditions. The amount of PAR absorbed is a function of the incoming radiation and a crop's capability to intercept this light. The latter is mainly a function of the LAI. The interceptive relationship between the LAI and PAR has been the subject of several reviews and studies (Asrar *et al.*, 1984; Gallo *et al.*, 1985; Tucker and Sellers, 1986; Sellers, 1987; Baret

and Guyot, 1991; Field *et al.*, 1995; Frouin and Pinker, 1995; Serrano *et al.*, 2000; Goetz *et al.*, 2005; Vina and Gitelson, 2005; Garbulsky *et al.*, 2011; Wang *et al.*, 2013). The first step that helped researchers to link RS and PAR was the equation developed by Monteith in 1977 to quantify the PAR absorbed by the crop (fAPAR) (Monteith, 1977). The fAPAR depends mostly on the canopy's LAI. Monteith (1977) proposed that an exponential relation existed between the LAI and the fAPAR. The fAPAR is quantified from the RS because the NDVI has been found to have a good predictive ability (Baret and Guyot, 1991). The close link between the NDVI and the fAPAR was confirmed in theoretical studies and, later, in experimental studies too (Sellers, 1985; Sellers *et al.*, 1997). The relationship between fAPAR and the NDVI is justified because the PAR intercepted and NDVI depend on the LAI, leaf pigment concentrations, leaf angle orientation, and soil reflectance features (Baret *et al.*, 1989; Huete, 1985).

Figure 3 illustrates a flowchart, modified by FAO, of Belgium's crop monitoring and yield forecasting system, which combines both RS and CSMs.

**FIGURE 3. Flowchart of the Belgian crop monitoring and yield forecasting system (B-CGMS).**



### 3.2.4 Applications in EWS

#### 3.2.4.1 EWS: an introduction. The ENSO

The application of EWS in agriculture must engage constant crop monitoring in a simple, timely and accurate manner and provide forecasts and impact assessments of the spatial and temporal variability of crop production at national and regional levels, as well as, to a large extent, the risk of famines. Most EWS use remotely sensed data for crop monitoring

and early screening for signs of drought, flood, and climate change impact. When analysed against historical trends, multiyear VI images of the growing season can help to identify years in which the crop was in better or worse conditions.

Seasonal NDVI patterns in East Africa have been associated with the El Niño/Southern Oscillation (ENSO) index. This index is derived from the atmospheric pressure patterns in the Pacific Ocean, the temperature anomalies of the ocean surface, and the anomalies in the outgoing long-wave radiation. If the ENSO information can be translated into practical advice and shared in a timely manner, farmers can adjust their management factors (such as planting, fertilization, irrigation) to bring about a positive impact on food security and crop production. For example, in Mexico, the economic gains of an EWS based on the ENSO has been estimated to consist in approximately US\$ 10 million per year (Adams *et al.*, 2003).

The El Niño events are also known to cause issues to farmers in Southeast Asia. For example, an El Niño event in Indonesia entails delayed rainfall and less planted rice areas, thus reducing the amount of rice produced for that growing season and increasing the risk of annual rice deficits (Naylor *et al.*, 2007). Predictions of these events over the next 50 years suggested that farmers should adopt new management strategies to cope with reduced rainfall during the important crop stages. The 1997-1998 El Niño events, which were considered to be among the strongest of the previous 50 years, was related to vegetation patterns monitored by the NDVI in Africa (Kogan, 1998). Naylor *et al.* (2007) concluded that increased investments in water storage, drought-tolerant crops, crop diversification, and EWS were viable adaptation strategies that Indonesian farmers could adopt to offset the negative effects of future El Niño events.

The Southern Oscillation is also known to affect crop yield in Australia. Rimmington and Nicholls (1993) discussed how wheat yields in Australia are correlated with the Southern Oscillation Index, which affects growing season rainfall. Information on the Southern Oscillation Index is generally available close to the sowing date, and can therefore provide interesting yield forecasts.

#### **3.2.4.2 Early drought warnings and yield**

It is crucial to forecast and prevent drought events in Africa because the lack of resources often means that a drought will lead to a severe reduction in production and to famine (Haile, 2005). For example, 17 million people in East Africa live in drought-prone zones, and the recent recurrence of drought poses these people at risk of food insecurity (Funk and Verdin, 2010). Using the Famine Early Warning System Network (FEWS NET), Funk *et al.* (2003) found that the agricultural areas of Ethiopia experienced a net decline in growing season rainfall over the years, and that Ethiopia is therefore facing increased food shortages. This was caused by the anomalous warming in the Indian Ocean, which caused dryness in East Africa. Funk *et al.* (2008) linked this warming, to some extent, to anthropogenic activities. Funk and Verdin (2010) argue that a combination of simple water and food balances remains a useful tool for quantifying the evolution of the risk, and, when coupled with spatial and temporal analysis, can be valuable in providing early warning information. For example, the spatial information of water per capita was used to derive information on the spatial patterns

of water availability per household (Funk *et al.*, 2005). This information was then used to derive three main zones of water security. The authors found a correlation between areas of low rainfall and water security, but also that the urbanization of those areas competed for the water used in agriculture. In particular, two points are interesting: first, that the vulnerable zones are increasing; second, there are some areas of water surplus.

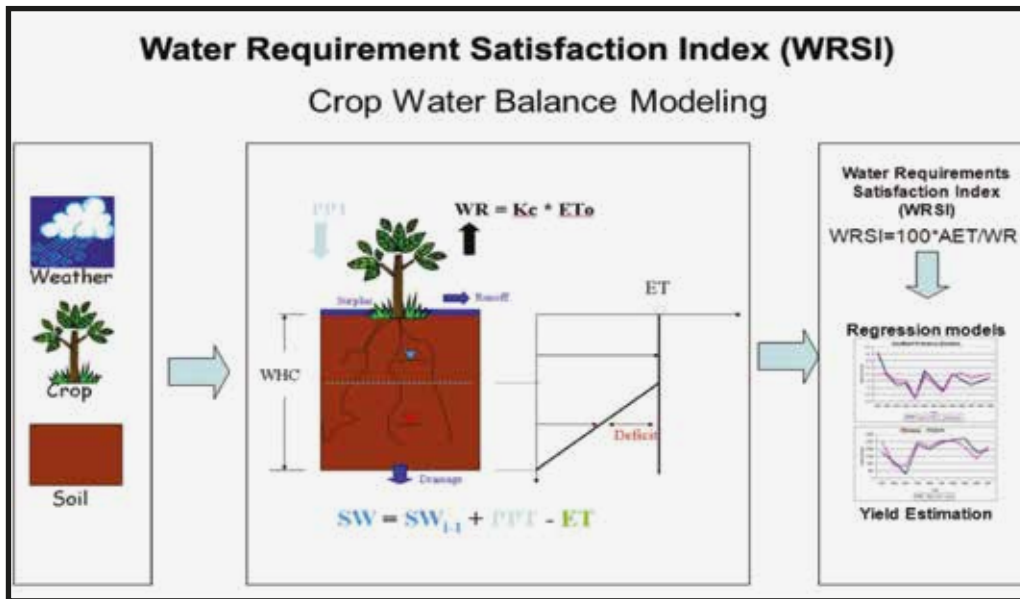
Ceccato *et al.* (2007) used RS to monitor variations in rainfall and crop growth, to help policymakers in sub-Saharan countries to quantify the risk of desert locusts and malaria outbreaks. The monitoring of crop yield, especially in rain-fed areas (as are many African countries), must also take into account the temporal and spatial variability of rainfall. The AVHRR-NDVI product has also been used to build a GIS for the detection of parasites, in East Africa, that can affect livestock and humans alike (Malone, 1998). In Burkina Faso, cereal production is a function of the amount and timing of rainfall during the growing season.

The use of CSMs, GIS, and RS has helped to build an EWS for production anomalies (Thornton *et al.*, 1997). One limitation of the use of CSMs in such locations is that the weather station networks are very sparse, which may lead to several gaps in data (Washington *et al.*, 2004); for this reason, most researchers focus their attention on the use of RS products, such as the Rainfall Estimate (RFE), to fill gaps in rainfall data. Drought events are also associated with sea temperature anomalies and anomalies in RS VIs. Referring to eight years of satellite data, Myemi *et al.* (1996) found correlations between the sea temperature of the Pacific Ocean and NDVI anomalies in rainfall patterns in the arid and semi-arid regions of Africa, Australia and South America. These results were also found by Anyamba and Eastman (1996). Using AVHRR-NDVI, these authors studied the trends followed by vegetation greenness in Africa and climate trends over four years, finding that in Southern Africa, there is a significant relationship with the ENSO. In addition, Anyamba and Eastman (1996) noted that there is no correlation with the ENSO in East Africa and the Sahel. Therefore, they concluded, the NDVI-ENSO is specific to certain regions of Africa.

Drought monitoring can also be performed through seasonal rainfall forecasts, which are becoming widely available in Africa (Goddard *et al.*, 2001). FAO has developed the Water Requirement Satisfaction Index (WRSI; Frere and Popov, 1986) to estimate the effects of rainfall on crop production in rain-fed areas. The WRSI uses decadal information on rainfall observations and soil water-holding capacity. The water demand is calculated using FAO's potential evapotranspiration approach (Allen *et al.*, 1998), while the supply is calculated from rainfall and soil water (see Figure 4). Spatial versions of the WRSI have been developed for Mozambique and other African countries, where RS-NDVI and point WRSI were used to derive spatial maps for EWS (Rojas and Amade, 1998). In Algeria, growing season rainfall has been used to carry out drought planning in an empirical manner; however, El Mourid and Watts (1989) have noted that in such areas, the approach is not optimal because there is no correlation between rainfall in autumn and in spring, the periods when crops are more sensitive to drought. Monnik (2000) discusses the EWS in South Africa, which has experienced an increase of drought extremes over the past two decades. For example, South Africa currently uses an EWS based on decile rainfall, water satisfaction index, the satellite NDVI, and crop and pasture models. The relationship of rainfall to seasonal NDVI has been also confirmed in other environments. In the dry areas of the Negev Desert in Israel,

this approach was used to quantify vegetation cover (Schmidt and Karnieli, 2000). Indeed, vegetation cover can be considered another factor that can be implemented in the EWS as a proxy for a desertification monitoring system. In the SSA, Symeonakis and Drake (2004) estimated vegetation cover and Rain-Use Efficiency (RUE) using the NDVI.

**FIGURE 4. Conceptual framework of the WRSI.**



### 3.2.4.3 EWS and climate change

Short-, medium- and long-term predictive approaches and methodologies exist that incorporate RS data and climatic data to simulate future agricultural productivity. These approaches and methodologies mostly leverage on historical land use or land cover data and climatic data to project potential future scenarios, thereby providing short-, medium- and long-term early warning information on agricultural production at global, regional and national scales as may be influenced by climate trends – mostly relating to rainfall and temperature. These types of early warning systems will not be explored in detail in this review; suffice it to note that they are important in providing a longer time perspective, that can be of great assistance in agricultural planning and development.

### 3.2.5 Combining optical and microwave RS

The intensity of reflectance from vegetation is commonly greater than from most inorganic materials. Consequently, vegetation appears bright in NIR wavelengths, mostly due to the sensitivity of these wavelengths to internal plant pigmentation. Radar sensors are able to capture plant structure and soil moisture content. As a result, both optical and radar sensors can contribute to measuring and monitoring crop conditions at different phenological stages, supporting the estimation of crop yields.

For optical and radar RS, crop classification can be challenging, as the difference among crop types in reflectance or backscatter can be minimal. In addition, differences in crop condition among fields of the same crop type can cause confusion, when separating crop by type. Multiple scattering within a canopy can be useful to discriminate crops using radar RS. Research relying upon radar data recorded on multiple dates has demonstrated that radar RS could play a very important role in agricultural applications (Zhang, 1999). In addition to the sensitivity of radar backscatter to crop canopy characteristics, given their all-weather capability, Synthetic Aperture Radar (SAR) sensors are a reliable option for crop monitoring. Nevertheless, much research remains necessary if the use of SAR is to be advanced to operational applications.

### **3.2.5.1 Crop type and crop condition**

If RS technologies are to be successfully applied for the purposes of crop classification, for each crop type, reflectance and backscatter signatures must be well defined. Difficulties arise when the signatures of different crops are not sufficiently unique, or when the variance in the signature within a single crop class is too large. Integration of optical and radar imagery is an attractive option. Indeed, both of these technologies offer complementary information on the crop canopy, and SAR sensors may fill the gap in optical acquisitions during periods of persistent cloud cover. End-of-season crop maps are also valuable; however, early-season crop area estimates provide additional value as they support in-season crop production and yield forecasting. The heterogeneity of corn-growing conditions in many countries makes it difficult to obtain accurate data for yield prediction. Small agricultural plots, irregular shapes, different sowing seasons and variations in crop cultivars are all contributing factors to classification errors. For this particular crop, accuracy can be increased by combining the information obtained from optical and radar satellite images.

Research has demonstrated that the timing of image acquisition is crucial to the success of crop mapping with optical imagery. Unless optical imagery is available during the key stages of crop development and when field data are collected, these images alone will not provide the information necessary for operational field-level crop monitoring. Acquisition of SAR data during key phenological stages is more reliable; consequently, these data are an important source of information for crop monitoring systems. SAR and SAR-optical solutions for crop monitoring have been explored in various regions of the world. A summary of these studies is given below.

By integrating optical and SAR imagery, McNairn *et al.* (2008) demonstrated that multitemporal satellites can successfully classify crops, for a variety of cropping systems. McNairn *et al.* (2009) further indicate that multitemporal TerraSAR-X data can provide a classification accuracy of 84 percent; application of a post-classification filter to remove noise in the map product, a final accuracy of 95 percent was obtained.

As explained above, SAR investigations have confirmed that microwaves are sensitive to both soil and crop characteristics. Results using multitemporal RADARSAT-1 imagery have confirmed that the C-HH backscatter can detect differences in crop type, crop growth stage and crop indicators, such as crop height, biomass and the LAI. Active microwave systems

have a significant advantage over optical systems, particularly for crop monitoring, since SAR acquisitions are not impeded by cloud cover. The multibeam modes associated with RADARSAT-1 also provide significant flexibility in terms of the timing, spatial resolution and incidence angle of the acquired imagery (McNairn *et al.*, 2000).

The availability of multipolarization data from a number of SAR sensors operating at different frequencies (X-Band from TerraSAR-X, C-Band from ASAR and RADARSAT-2 and L-Band from ALOS PALSAR) has significantly advanced the use of SAR for agriculture and land cover mapping. The multipolarized configurations provide more information relating to crop structure and crop condition. Using simulations of data in preparation for the availability of RADARSAT-2 data, the Canada Centre of Remote Sensing (CCRS) gathered airborne polarimetric imagery over several Canadian sites in 1998 and 1999. These data were used to evaluate the sensitivity of multipolarized SAR data, to characterize corn, wheat and soybean crops (McNairn *et al.*, 2000). Multiple polarizations were significantly advantageous in crop identification efforts, compared to the use of single or dual polarization. The most important polarization for crop classification was the linear cross polarization (HV or VH). Cross polarization responses are a result of multiple scattering from within a crop canopy. Differences in canopy architecture due to differences in crop type result in unique cross polarization signatures. In a study using C-HH RADARSAT-1 data, multiple dates of RADARSAT-1 imagery provided information on crop type and condition, with or without the integration of multispectral optical imagery. A regression analysis established that some indicators of crop vigour – in particular, the LAI and crop height – were correlated with backscatter. The success of this RADARSAT-1 study was attributed to the acquisition of the SAR data during the critical stages of reproduction and seed development crop growth (McNairn *et al.*, 2002).

### **3.3 Geoportals and RS data and products on agricultural crop production and forecasting**

Various geoportals, and RS and EO data and products, support agricultural production, forecasting and early warning information. This review focuses mainly on freely available RS tools, data and products used for agricultural crop production and forecasting. However, information will also be provided on relevant RS tools, data and products that are only available for a fee.

A geoportal is a type of web portal used to retrieve and access geographic information (geospatial information) and associated geographic services (display, editing, analysis, etc.) via the Internet. Most contemporary geoportals provide data and products, as well as processing tools and e-libraries. RS data are simply imagery acquired by Earth Observing satellites and high- or low-flying aircrafts (including drones) on phenomena occurring on land, in the sea or in the atmosphere. RS products comprise both remotely sensed imagery and data sets processed from the same, such as vegetation indices like the NDVI.

Sections 3.3.1 and 3.3.2 below describe some of the geoportals, tools, data and products available freely or for a fee.

### 3.3.1 Free RS portals, tools, data and products

Several freely available RS portals (geoportals), tools, data and products currently exist to serve the need for agricultural crop production and forecasting demands. These include but are not limited to those listed in sections 3.3.1.1 to 3.3.1.7 below.

#### 3.3.1.1 The Global Information and Early Warning System on Food and Agriculture (GIEWS) Earth Observation portal

<http://www.fao.org/giews/earthobservation/index.jsp?lang=en>

The Global Information and Early Warning System on Food and Agriculture (GIEWS) monitors the condition of major food crops across the world to assess production prospects. To support analysis and supplement ground-based information, the GIEWS utilizes RS data, which can provide valuable insight on water availability and vegetation health during cropping seasons. In addition to rainfall estimates and the NDVI, the GIEWS and FAO's Climate, Energy and Tenure (NRC) Division have developed the Agricultural Stress Index (ASI), a quick-look indicator for early identification of agricultural areas that are probably affected by dry spells or, in extreme cases, drought.

The GIEWS Earth Observation portal packages and provides data at global and country level. The data relating to African countries may be accessed via five regions: Central Africa, Eastern Africa, North Africa, Southern Africa and Western Africa.

The seasonal indicators are designed to enable easy identification of areas of cropped land where the likelihood of water stress (drought) is high. The indices are based on RS data on vegetation and land surface temperature, combined with information on agricultural cropping cycles derived from historical data, and a global crop mask. The final maps highlight anomalous vegetation growth and potential drought in crop zones during the growing season. The satellite data used to calculate the mean Vegetation Health Index (VHI) and the ASI is the 10-day (dekadal) vegetation data from the METOP-AVHRR sensor, at a resolution of 1 km (since 2007). Data at a resolution of 1 km for the 1984–2006 period were derived from the NOAA-AVHRR data set which was captured at a resolution of 16 km. The crop mask is a modified version of an EC-JRC data set that compiles several different sources of land cover data, including GlobCover V2.2, Corine-2000 and AfriCover, as well as the SADC data set and the USGS Cropland Use Intensity Data Set.

The vegetation indicators (the NDVI anomaly, the Vegetation Condition Index, or VCI, and the VHI) provide alternative measurements of relative vegetation health. These indices can be used to monitor areas where vegetation may be stressed, as a proxy to detect potential drought. The precipitation indicators present a global analysis of absolute (mm) and relative (percentage) rainfall levels per dekad, in addition to long-term average precipitation levels (mm). All three vegetation indicators are based on 10-day (dekadal) vegetation data from the METOP-AVHRR sensor at a resolution of 1 km (since 2007). Data at a resolution of 1 km for the 1984–2006 period were derived from the NOAA-AVHRR data, which were set at a resolution of 16 km. Precipitation estimates for all African countries (except Cabo Verde and

Mauritius) are taken from NOAA/FEWSNet; for the remaining countries, the data is obtained from the European Centre for Medium-Range Weather Forecasts (ECMWF).

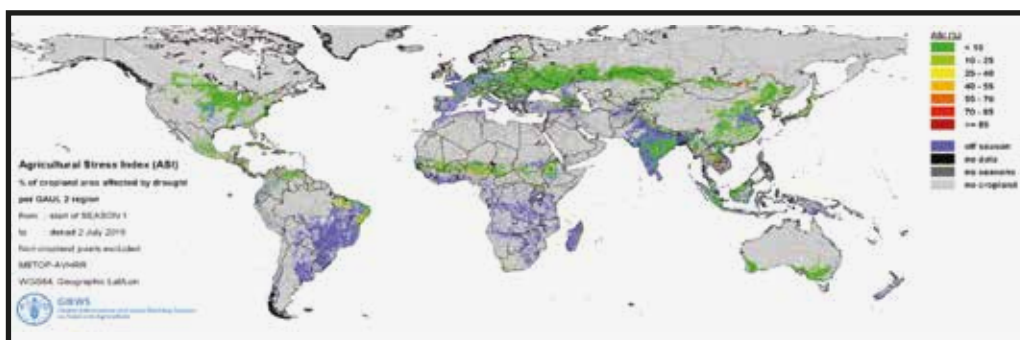
The country-level maps and graphs depict the latest 36-month period for each seasonal, vegetation and precipitation indicator. The data are presented by dekad and month. All three country-level vegetation indicators are based on 10-day (dekadal) vegetation data from the METOP-AVHRR, NOAA-AVHRR and NOAA, FEWSNet and the ECMWF.

The data and products available through the GIEWS Earth Observation portal are briefly described below. The data are grouped into Seasonal Global Indicators, Global Indicators and Country Indicators.

### SEASONAL GLOBAL INDICATORS

**Agricultural Stress Index (ASI).** This index is based on the integration of the VHI in the temporal and spatial dimensions, which are critical in assessing a drought event in agriculture. To calculate the ASI, the first step is a temporal averaging of the VHI, assessing the intensity and duration of dry periods occurring during the crop cycle at pixel level. The second step determines the spatial extent of drought events by calculating the percentage of pixels in arable areas with a VHI value below 35 percent (value that Kogan, 1995, identified as a critical threshold in assessing the extent of drought). Finally, each administrative area is classified according to the percentage of its affected area, to facilitate rapid interpretation of results.

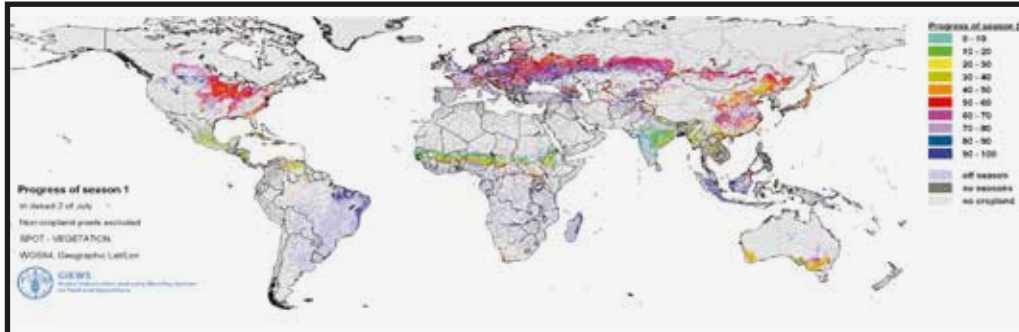
**FIGURE 5. Seasonal global ASI product for the second dekad of July 2016.**



Source: GIEWS Earth Observation geoportal.

**Progress of Season.** This indicator illustrates the development of the crop growing season. For any dekad in a given year, the Progress of Season map indicates how far the season has progressed, represented by a value comprised between 0 and 100 percent (50 percent is the midpoint of the growing season). Season progress is based on the long-term average of vegetation phenologies for each pixel. This simplification implies that crop phenologies are static and, therefore, that the growing seasons progress at a constant rate every year.

**FIGURE 6. Seasonal global Progress of Season product for the second dekad of July 2016.**

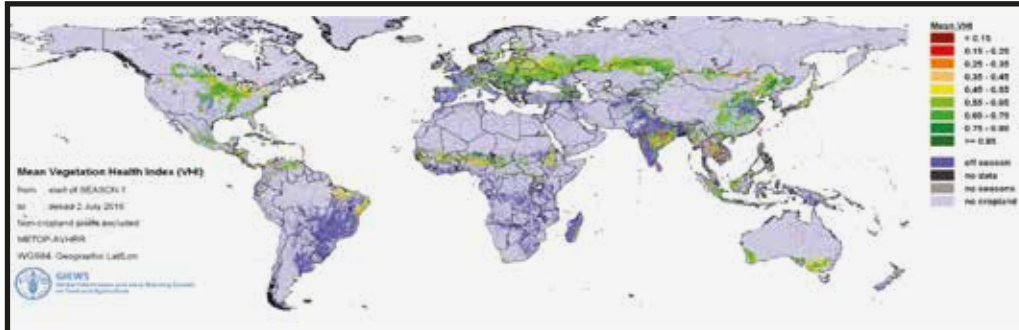


Source: GIEWS Earth Observation geoportal.

**Mean Vegetation Health Index (VHI).**

This Index an average of the dekadal VHI values over the crop growing season to date. The mean VHI is a good indicator of drought at pixel level. To facilitate analysis, non-cropland is masked over the mean VHI maps.

**FIGURE 7. Seasonal global mean VHI product for the second dekade of July 2016.**

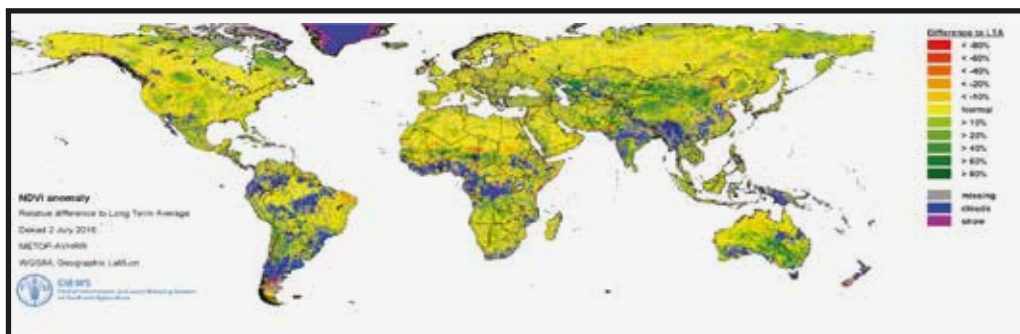


Source: GIEWS Earth Observation geoportal.

**GLOBAL INDICATORS**

**NDVI Anomaly.** The NDVI measures the greenness of ground cover, and is used as a proxy to indicate the density and health of vegetation. NDVI values range from + 1 to -1: high positive values correspond to dense and healthy vegetation, while a low or negative NDVI value indicates poor vegetation conditions or sparse vegetative cover. The NDVI anomaly indicates the variation of the current dekade compared to the long-term average, where a positive value (for example, 20 percent) signifies enhanced vegetation conditions compared to the average, while a negative value (for instance, -40 percent) indicates comparatively poor vegetation conditions.

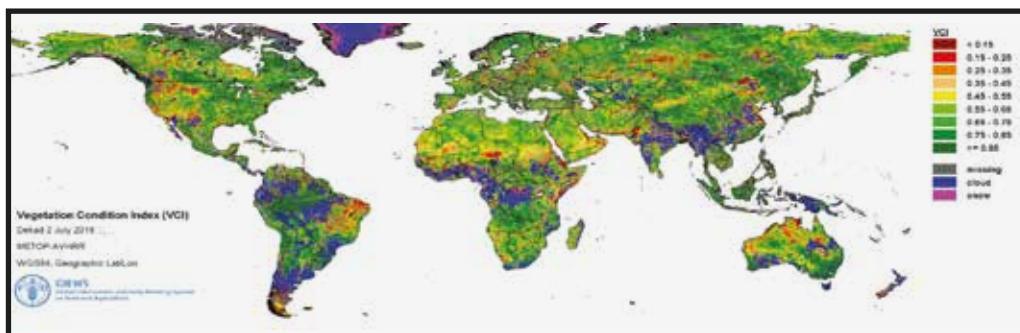
**FIGURE 8. Global NDVI anomaly product for the second dekad of July 2016.**



Source: GIEWS Earth Observation geoportal

**The VCI.** This indicator relates the current dekadal NDVI to its long-term minimum, normalized by the historical range of NDVI values for the same dekad. The VCI was designed to separate the weather-related component of the NDVI from its ecological element.

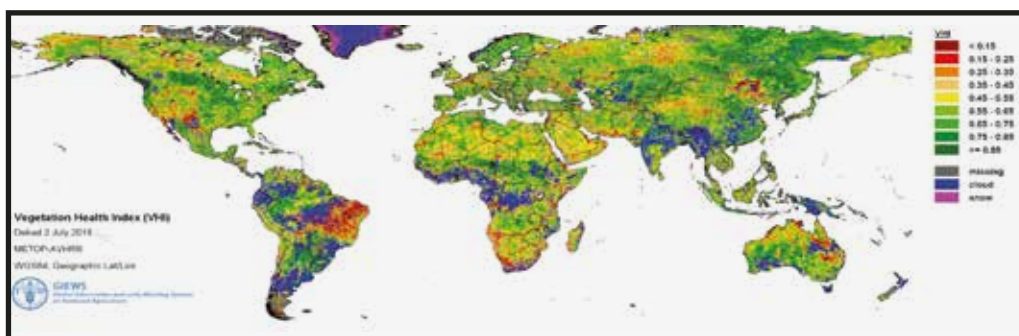
**FIGURE 9. Global VCI product for the second dekad of July 2016.**



Source: GIEWS Earth Observation geoportal

**The VHI.** This is a composite index and the elementary indicator used to compute the ASI. It combines both the VCI and the Temperature Condition Index (TCI). The TCI is calculated using an equation similar to that applied for the VCI, but relates the current temperature to the long-term maximum, on the assumption that higher temperatures tend to cause a deterioration in vegetation conditions. A decrease in the VHI following, for example, a decline in the VCI (relatively poor green vegetation) and an increasing TCI (warmer temperatures) signify stressed vegetation conditions, and over a longer period are indicative of drought. When computing the VHI, its two components (VCI and TCI) are given equal weight. The VHI images are computed for the two main seasons and in three modalities: dekadal, monthly and annual.

**FIGURE 10. Global VHI product for the second dekad of July 2016.**



Source: GIEWS Earth Observation geoportal

### **COUNTRY INDICATORS**

On the GIEWS Earth Observation portal, the country indicator products are classified under four main categories: seasonal indicators, vegetation indicators, precipitation indicators, and graphs (GAUL Level 1). The data date back to July 2013.

Seasonal indicators are further divided into six subcategories: ASI-Season 1, ASI-Season 2, Mean-VHI-Season 1, Mean-VHI-Season 2, ASI-Annual Summary–Season 1, and ASI-Annual Summary–Season 2. Vegetation indicators are divided into three subcategories: NDVI Anomaly, VCI and VHI. Precipitation indicators are classified in two subcategories: Estimated Precipitation and Estimated Precipitation Anomaly. Graphs (GAUL Level 1) are divided into three subcategories: NDVI, Estimated Precipitation and Accumulated Precipitation. With reference to the pilot countries of Kenya, Senegal and Zimbabwe, these data sets are accessible at the following links:

- **Kenya:**  
<http://www.fao.org/giews/earthobservation/country/index.jsp?lang=en&code=KEN>
- **Senegal:**  
<http://www.fao.org/giews/earthobservation/country/index.jsp?lang=en&code=SEN#>
- **Zimbabwe:**  
<http://www.fao.org/giews/earthobservation/country/index.jsp?lang=en&code=ZWE>.

#### **3.3.1.2 GeoGLAM**

<http://www.geoglam-crop-monitor.org/>

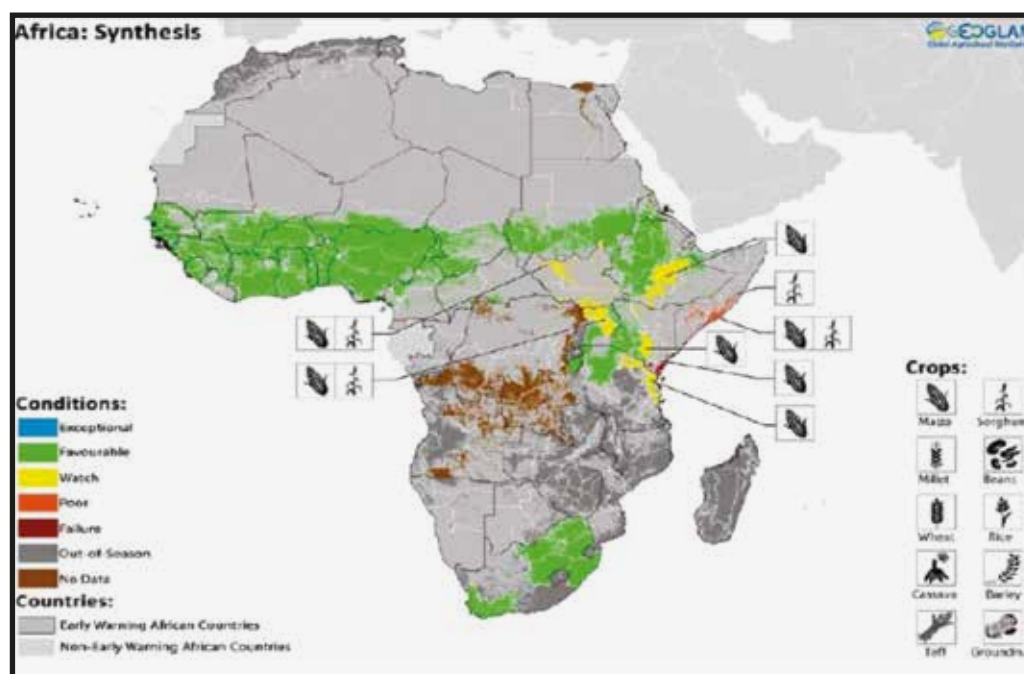
The Group on Earth Observations (GEO, a partnership between governments and international organizations) developed the Global Agricultural Monitoring (GEOGLAM) initiative, in response to growing calls for improved agricultural information. The goal of GEOGLAM is to strengthen the international community's capacity to produce and disseminate relevant, timely and accurate forecasts of agricultural production at national, regional and global scales through the use of EO, which include satellite and ground-based observations. This initiative is designed to build on existing agricultural monitoring programs and initiatives at national,

regional and global levels and to enhance and strengthen them through international networking, operationally focused research, and data and method sharing.

Both GEOGLAM and AMIS were endorsed by the G20 Heads of States' Declaration issued in November 2011, in which GEOGLAM was tasked with the coordination of "satellite monitoring observation systems in different regions of the world in order to enhance crop production projections and weather forecasting data." Within this framework, GEOGLAM developed the Crop Monitor reports, which provide assessments on global crop condition in support of the AMIS market monitoring activities. The first issue of the Crop Monitor appeared in the September 2013 issue of the AMIS Market Monitor.

The objective of the Crop Monitor is to provide AMIS with an international and transparent multisource, consensus assessment of crop growing conditions, status, and agroclimatic conditions that are likely to impact global production. This activity covers the four primary crop types (wheat, maize, rice, and soybean) within the main agricultural regions of AMIS countries. These assessments have been produced operationally since September 2013 and are published in the AMIS Market Monitor Bulletin. The Crop Monitor provides cartographic and textual summaries of crop conditions as of the twenty-eighth day of each month, according to crop type (Figure 11).

**FIGURE 11. Crop condition map synthesizing information for all Early Warning Crop Monitor crops as of 28 July 2016.**



In the first issues of the Crop Monitor, the crop condition maps were based on the EO-derived NDVI depicting crop growth anomalies. Starting with the May 2014 issue, GEOGLAM has been releasing a more informative set of maps and pie charts that depict crop stage, crop

conditions by region, and the climatic drivers affecting these conditions.

### 3.3.1.3 USGS FEWS NET Data Portal

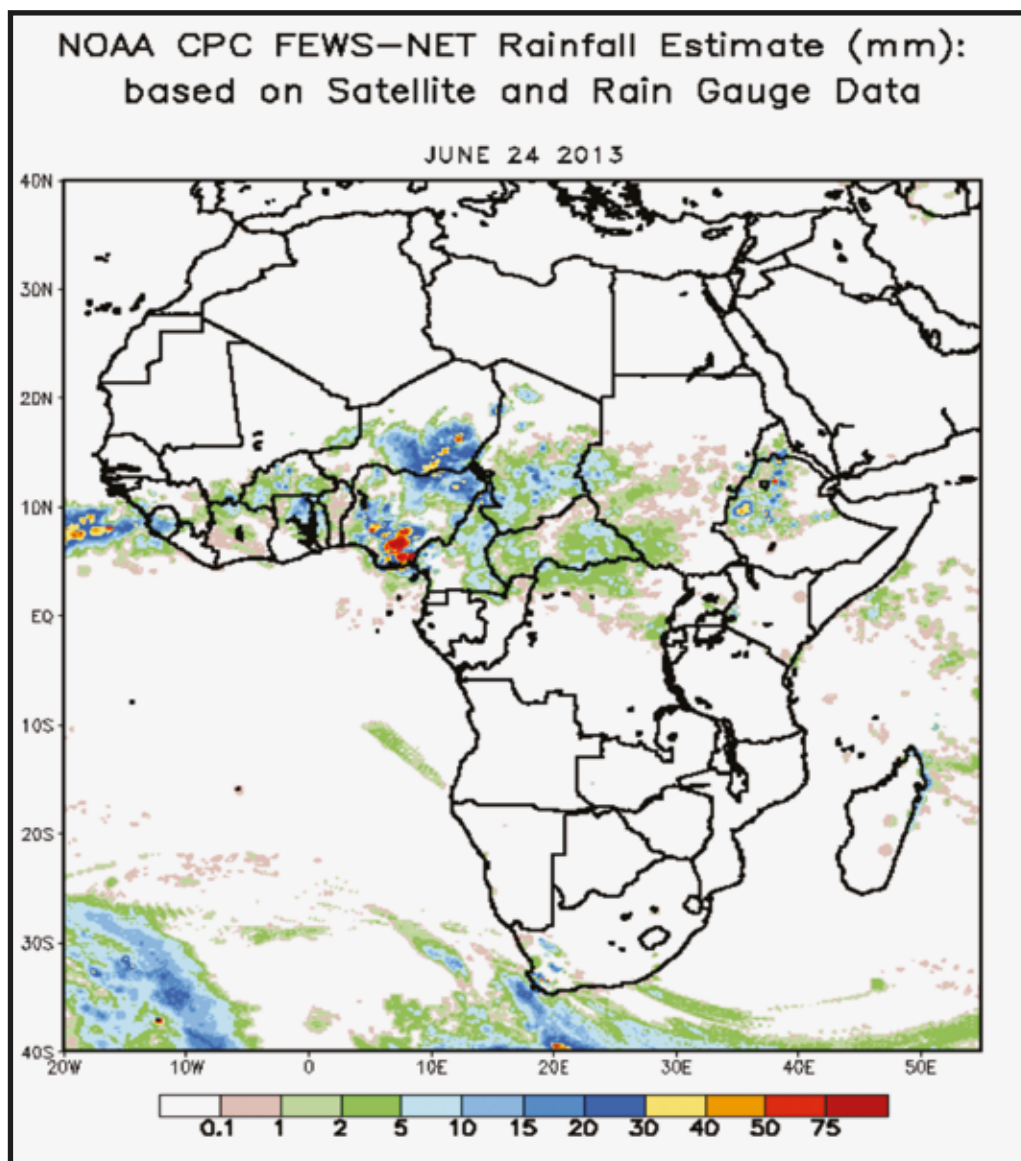
<http://earlywarning.usgs.gov/fews>

The USGS FEWS NET Data Portal provides access to software tools, geospatial data, satellite image products, and derived data products in support of FEWS NET drought monitoring efforts throughout the world. This portal is provided by the USGS FEWS NET Project, which is part of the Early Warning Focus Area at the USGS Earth Resources Observation and Science (EROS) Center. The data on Africa may be found in the portal's Africa Data Portal, formerly the Africa Data Dissemination Service (ADDS). The Africa Data Portal provides RS and modelled geospatial data and information for monitoring agrometeorological conditions throughout Africa. A diverse array of daily and dekadal products are available at both continental and regional levels (East Africa, North Africa, Southern Africa and West Africa).

The data and products relevant to agricultural crop production and forecasting that are available on the FEWS NET data portal include the following:

- **NOAA Daily RFE 2.0 Data.** As of 1 January 2001, RFE version 2.0 was implemented by the NOAA Climate Prediction Center (CPC). Created by Ping-Ping Xie, the algorithm replaced the dekad-based 1.0 version that was operational from 1995 through 2000 (Herman *et al.*, 1997). RFE 2.0 uses additional techniques to obtain better estimates of precipitation, while continuing to use cloud top temperature and station rainfall data that formed the basis of RFE 1.0. Infrared data is acquired from a Meteosat geostationary satellite at 30-minute intervals, and areas depicting cloud top temperatures of less than 235K are used to estimate convective rainfall. Data taken from approximately 1 000 stations of the World Meteorological Organization's (WMO) Global Telecommunication System (GTS) data provide accurate rainfall totals, and are assumed to be the true rainfall near each station. RFE 1.0 used an interpolation method to combine Meteosat and GTS data for daily precipitation estimates, and warm cloud information was included to obtain dekadal estimates. The two new satellite rainfall estimation instruments that are incorporated into RFE 2.0 are the Special Sensor Microwave/Imager (SSM/I) aboard the Defence Meteorological Satellite Program satellites, and the Advanced Microwave Sounding Unit (AMSU). Both estimates are acquired at 6-hour intervals and have a resolution of 0.25 degrees. RFE 2.0 obtains the final daily rainfall estimation using a two-part merging process, and then adds daily totals to produce dekadal estimates. All the satellite data are first combined using a maximum likelihood estimation method. The GTS station data are then used to remove bias (see Figure 12). Warm cloud precipitation estimates are not included in RFE 2.0. RFE data are available for public download mainly in binary format, but it may also be downloaded in GeoTiff format. With regard to Africa, the entire collection is available through the FEWS NET Bulk RFE Data Download page at <http://earlywarning.usgs.gov/fews/datadownloads/Continental Africa/Dekadal RFE>.

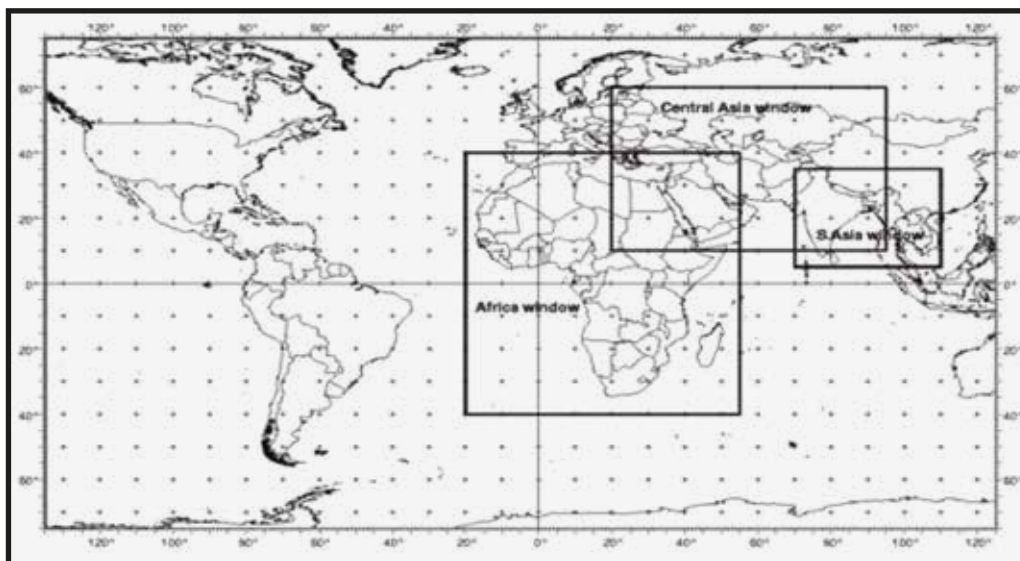
FIGURE 12. Africa's RFE 2.0 daily product for 24 June 2013.



For the FEWS NET project, the RFE 2.0 daily data are compiled over three geographic areas, or windows. As illustrated in Figure 13, the windows and their boundary coordinates are:

- Africa continental window: -20 to +55 longitude by -40 to +40 latitude
- Central Asia window: +20 to +95 longitude by +10 to +60 latitude
- South Asia window: +70 to +110 longitude by +5 to +35 latitude

**FIGURE 13. Map of the three windows used to package RFE 2.0 daily data.**



The daily data for each region are downloaded from NOAA/CPC and converted (to the nearest whole mm) into ArcInfo integer \*.bil images, which are then zipped and staged to the EROS's anonymous FTP server, from which users may access them. This server is available at <ftp://edcftp.cr.usgs.gov/edcuser/fewsips>. All data remain on the server for eight days before being auto-deleted. The Africa window data may be found under the Africa sub-directory. The naming convention for the daily image zip file is "rain\_YYYYJDA.tar.gz", where "YYYY" stands for the four-digit year and "JDA" for the one- to three-digit day of the year. Each daily rainfall file is a UNIX \*.tar.gz file which contains the ArcInfo \*.bil image and related files (i.e. .bil, .blw, .hdr, .stx, .clr) for the day. The entire African collection is available through the FEWS NET Bulk RFE Data Download page, which may be accessed at: <http://earlywarning.usgs.gov/fews/datadownloads/Continental Africa/Dekadal RFE>.

- **NOAA Daily GFS Forecast Data.** The Global Forecast System (GFS) precipitation data are provided on a daily basis by the NOAA Climate Prediction Center (<http://www.cpc.ncep.noaa.gov/>), for the purpose of near real-time usage by national and international relief agencies and the general public. The users of these data include the USGS, the US Agency for International Development (USAID), the Joint Agricultural Weather Facility (JAWF) and national meteorological centres in Africa, Asia and South America. The data are disseminated in binary format and in the form of shape and .tiff files, to meet the needs of the GIS community. The data have seven individual 24-hour accumulated precipitation amounts (indicated in mm), at a resolution of 0.25 degrees. The data have global extent and correspond to the seven forecast days, with an additional dataset indicating the grand total of accumulated seven-day precipitation (in mm). Thus, each forecast field represented has eight Geotiff files and eight shape files. All of these files are zipped into a single file (each day). Each "day" goes from 00Z to 00Z.

Graphics are provided for both global and regional levels, on the basis of the original data. The global extent graphics illustrate the situation at the first day of the seven-day period (Figure 14), and for the total seven-day accumulation (Figure 15). The regional or country-specific graphics show the data for individual days for the first six of the seven-day forecasts, and are displayed in conjunction with the past six days of rainfall estimates.

**FIGURE 14. Global one-day data for the first day of the seven-day period.**

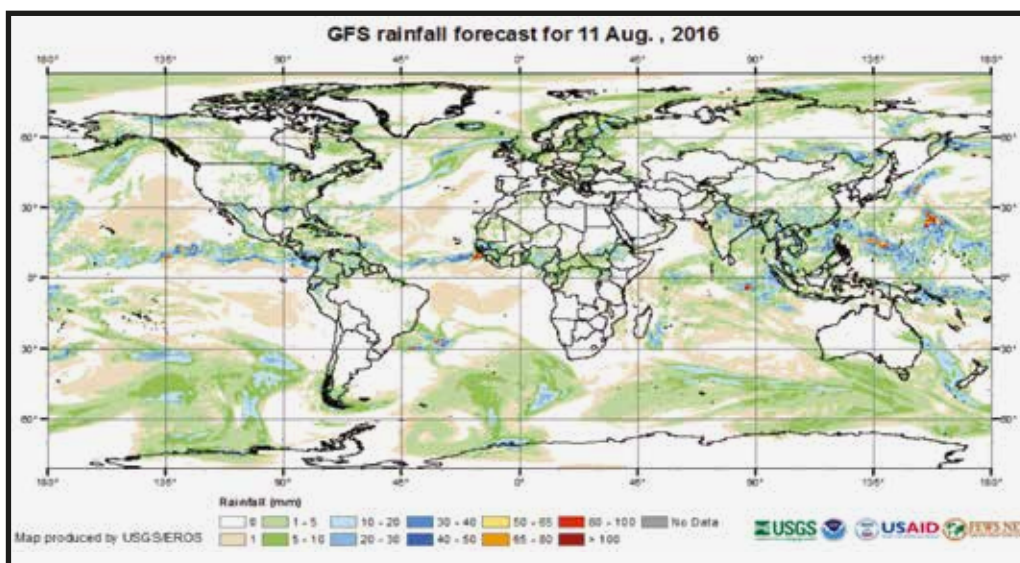
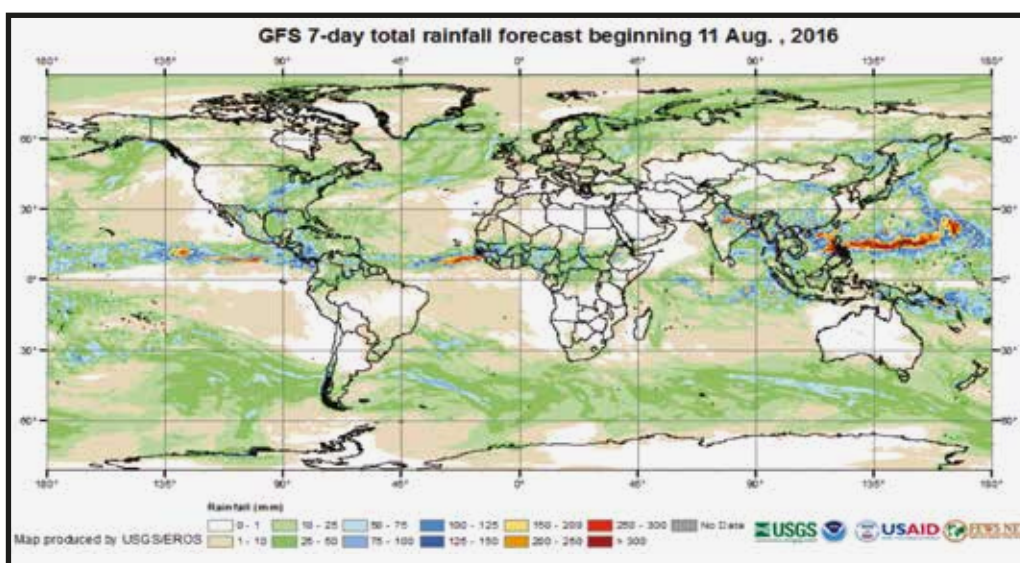


**FIGURE 15. Global seven-day accumulation data for the first day of the seven-day period.**



- **Dekadal RFE (also called RFE 1.0).** This product is the RFE algorithm that was operational from 1995 through 2000, prior to RFE version 2.0 (Herman *et al.*, 1997). RFE 1.0 used an interpolation method to combine Meteosat and GTS data, and included warm cloud information for the dekadal estimates.
- **Daily 30-day rain and dry days and anomalies.** These are derived from daily RFE data and consist of four products: the Number of Rain Days and Anomaly (Figure 16), the Consecutive Dry Days and Anomaly (Figure 17), the Total Rainfall and Anomaly (Figure 18), and the Days since Rain and Anomaly (Figure 19). The product is packaged into four pairs of graphics. Each graphic consists of a data image (left image) and its anomaly image (right image). The anomaly image illustrates the difference between the current day's image and the average for the same day from 2001 through 2009. The upper left image pair shows the number of days, over the last 30 days, in which at least 1 mm of rain fell and its anomaly. A "rain day" was defined as a day on which the rainfall amount was greater than or equal to 1 mm. The upper right image pair shows the maximum number of consecutive dry days over the past 30 days and its anomaly. A "dry day" was defined as a day on which the rainfall amount was less than 1 mm. The lower left image pair illustrates the total accumulated amount of rainfall over the past 30 days and its anomaly. The lower right image pair displays the number of days since a "rain day" and its anomaly, that is, the number of days since the rainfall in one day was equal or greater to 1 mm. The input data for each day of a 30-day cycle is the daily RFE as provided by NOAA-CPC.

**FIGURE 16. Maps of the number of rain days and relative anomaly.**

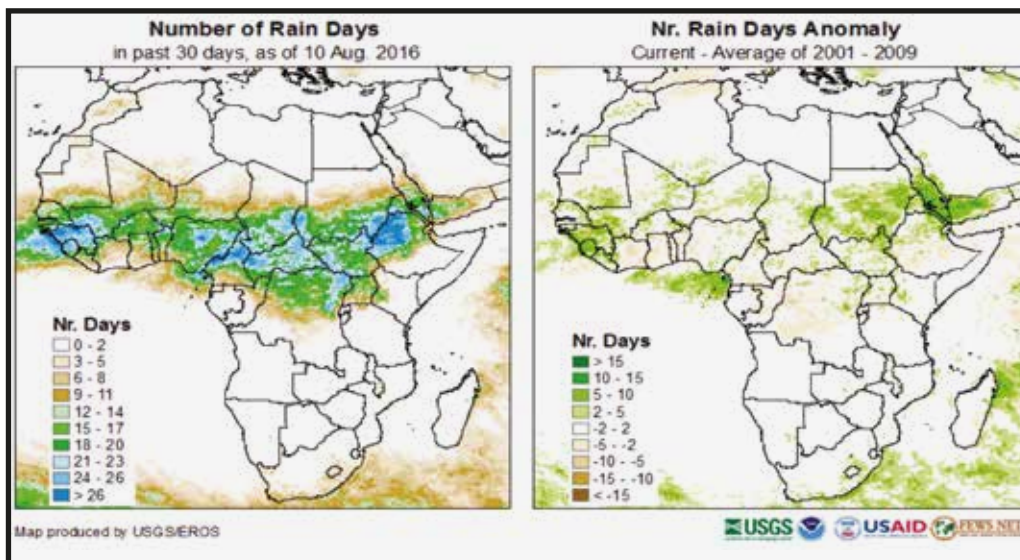


FIGURE 17. Maps of maximum consecutive dry days and relative anomaly.

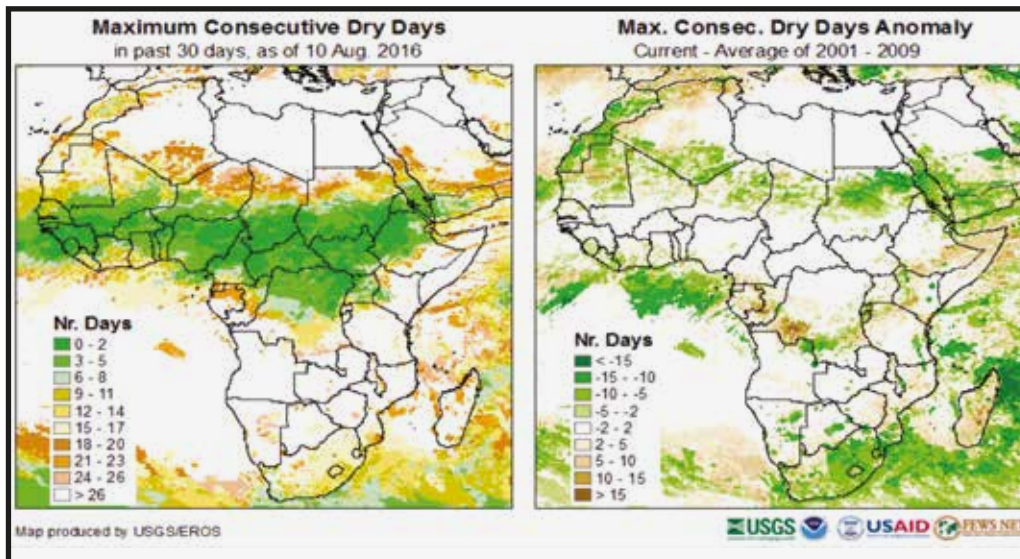
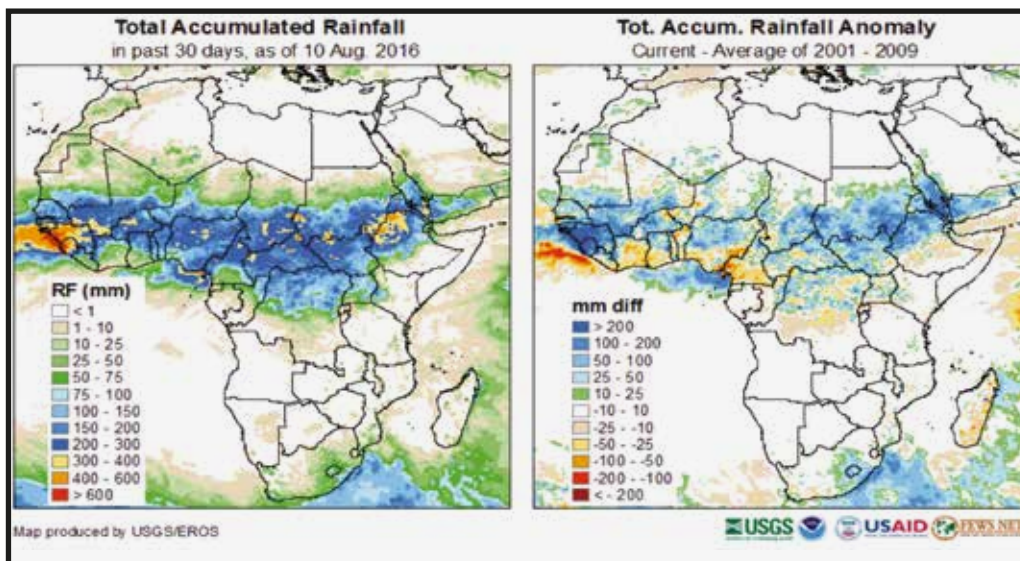
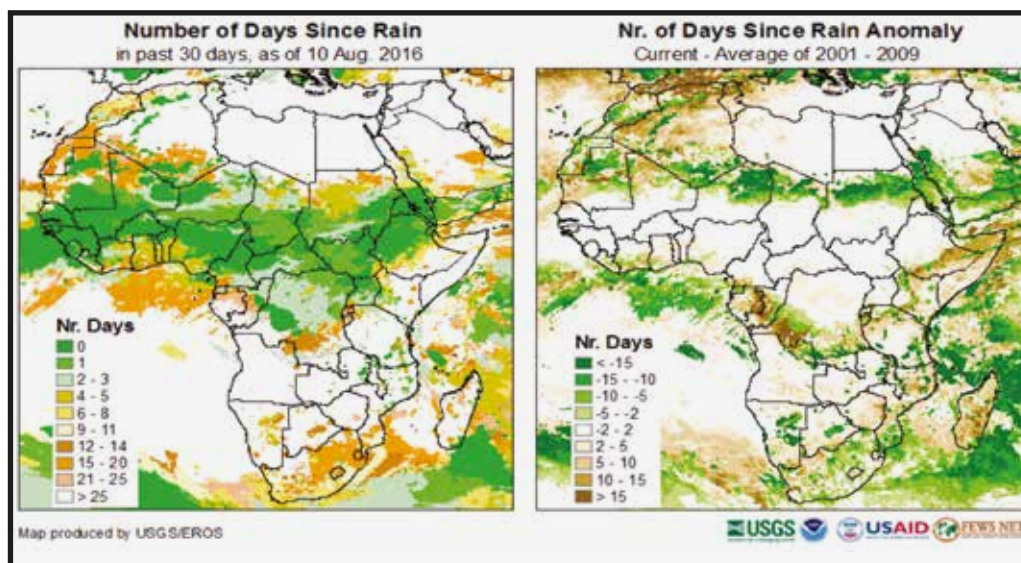


FIGURE 18. Maps of total accumulated rainfall and relative anomaly.



**FIGURE 19. Maps of number of days since rain and relative anomaly.**



- **Basin Excess Rainfall Maps (BERMs).** These are available in two product types, namely Basin Excess Rainfall Maps (BERM) Catchments (Figure 20) and BERM Rivers (Figure 21).

A simple method for identifying areas subject to flooding or excess moisture has been developed on the basis of the joint use of satellite RFEs and digital maps of basin boundaries and river networks. Maps are produced, which highlight the basins experiencing above-average rainfall over the previous ten-day period, as well as river reaches with potentially higher-than-average stream flow.

A straightforward application of the RFE images produced by NOAA images has been their use in conjunction with USGS digital maps of basins and river networks. These were derived from 1-km resolution topographic data, and are part of a topologically coded (Verdin and Verdin, 1999) global data set known as HYDRO1K. Rainfall estimates are added over river basin areas for each dekad and cumulatively, for the season. These sums are divided by the corresponding values for long-term average conditions (Hutchinson *et al.*, 1995). Excess rainfall scores are assigned to basin areas and river reaches accordingly – the higher the ratios, the greater the scores. Maps are then produced with colour codes indicating relative levels of excess precipitation. These products are called BERMs.

BERMs reveal situations of sustained heavy regional rains that adversely affect food security through flooding, and the consequent widespread disruption of agriculture, transportation, and market systems. The basin (or catchment) map highlights those sub-basins (out of approximately 3 000 across the continent) that receive above-average precipitation for the dekad, and cumulatively for the season, by colour-coding the relevant polygons.

The river segment (or stream) map highlights those reaches of river receiving above-average amounts of dekadal and seasonal cumulative precipitation, according to a similar scoring system. The difference is that a reach of river may receive rainfall

from a much larger upstream area than that of the sub-basin polygon in which it lies. Thus, a sub-basin may not be highlighted because only light rain is occurring locally, while the reach of river passing through it may be highlighted, due to heavy rains in upstream catchments.

**FIGURE 20. Excess rainfall map for the first dekad of August 2016 at catchment level.**

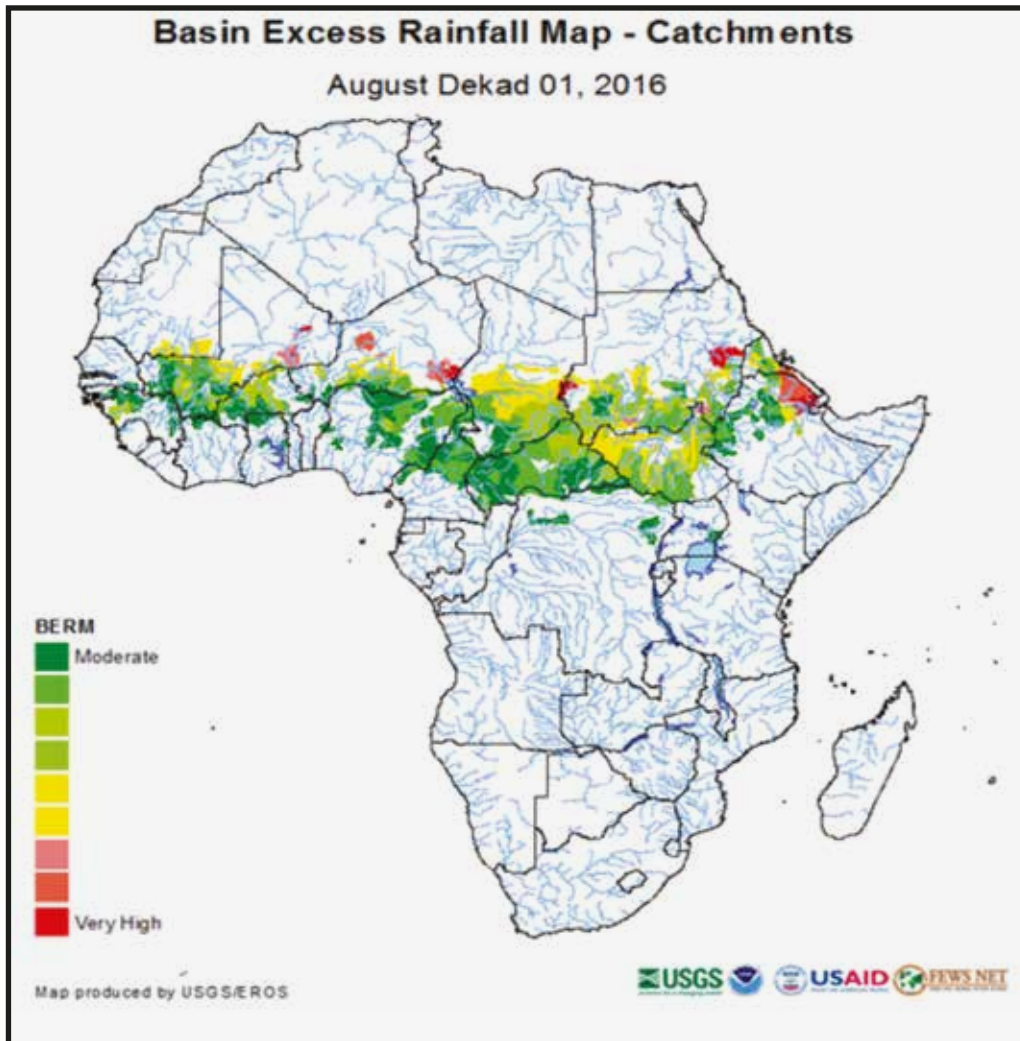
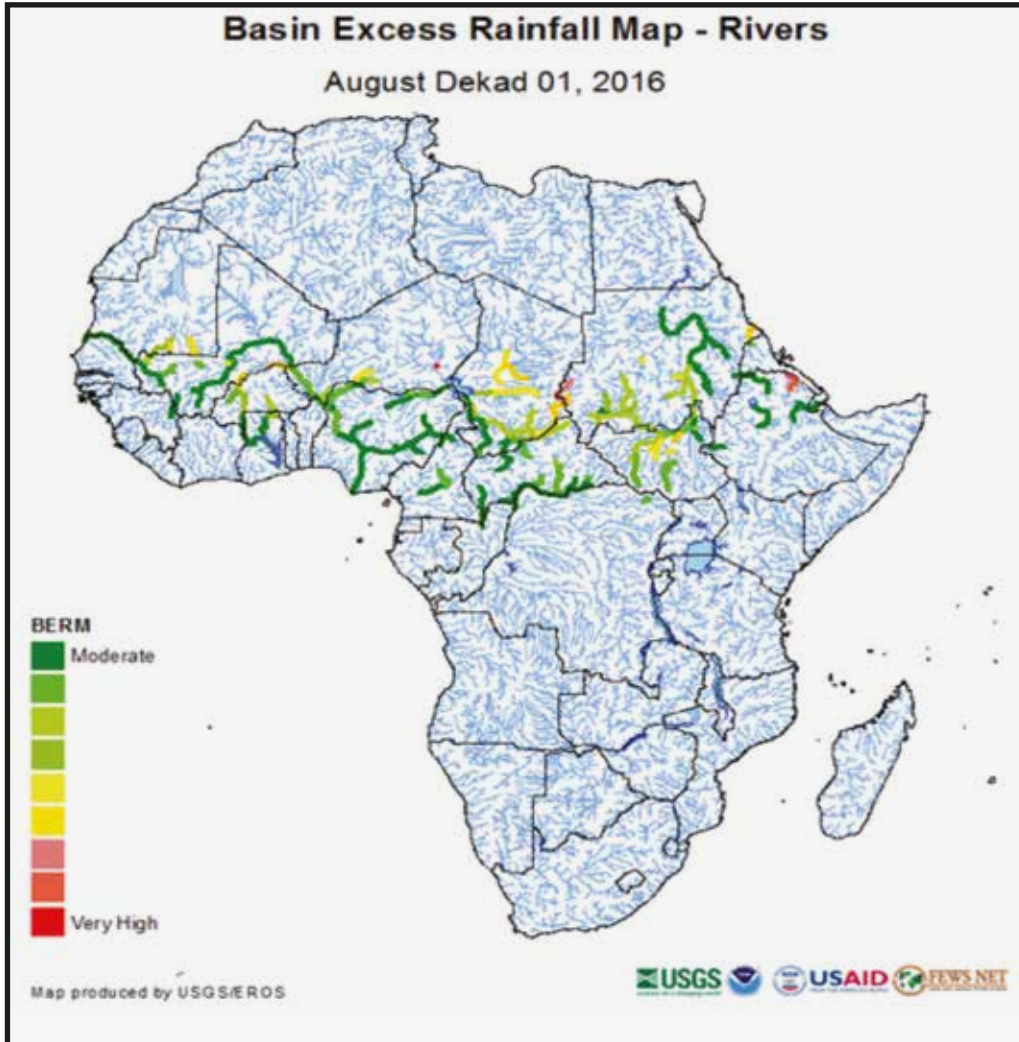


FIGURE 21. Excess rainfall map for the first dekad of August 2016 at river level.



- **Daily Runoff.** This is generated using the Soil Conservation Service's (SCS) Curve Number (CN) method. The model's primary input is the daily RFE, while its output is an estimate of the daily runoff (in mm), on a pixel-by-pixel basis, for the entire continent of Africa.

Surface runoff magnitude is determined using the SCS CN procedure (SCS, 1972), according to which infiltration losses are combined with surface storage with the relationship shown in Equation 1:

$$Q = (P - Ia)^2 / (P - Ia + S) \dots\dots\dots (1)$$

where  $Q$  is the accumulated runoff (rainfall excess) in mm ( $Q = 0$ , when  $P < I_a$ ).  $P$  is rainfall in mm,  $I_a$  is the initial abstraction in mm that accounts for surface storage, interception, and infiltration prior to runoff defined as:

$$I_a = 0.2 * S \dots\dots\dots (2)$$

$S$  is a parameter given by Equation 3:

$$S = 25,400/CN - 254 \dots\dots\dots (3)$$

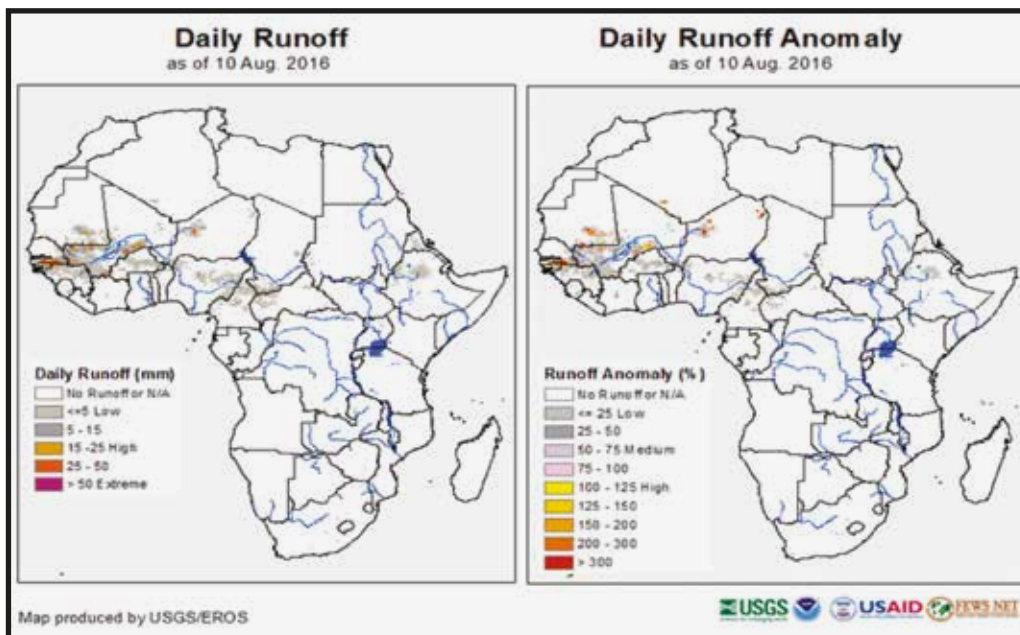
The CN's magnitude depends on soil hydraulic conductivity, land use and soil antecedent moisture conditions (AMC) at the start of the rainfall event. For this review, an Africa-wide CN for an average antecedent soil moisture condition (type II AMC), derived by Artan *et al.* (2001), is used. However, during daily simulations, CNs and the  $S$  variable are adjusted on the basis of five-day AMC values (Senay and Verdin, 2003).

Daily runoff is calculated for each pixel with a spatial resolution of 10 km. The Daily Runoff Anomaly graphic (Figure 22) shows the relative magnitude of the runoff on a given day compared to a historical maximum. To avoid extreme runoff caused by erroneous RFEs, the Daily Runoff Anomaly calculation uses the median of the maximum annual runoff (based on daily runoff values) from 1998 through the most recent year:

$$\text{Daily Runoff Anomaly (\%)} = \text{Daily Runoff} / (\text{median of annual maxima}) * 100$$

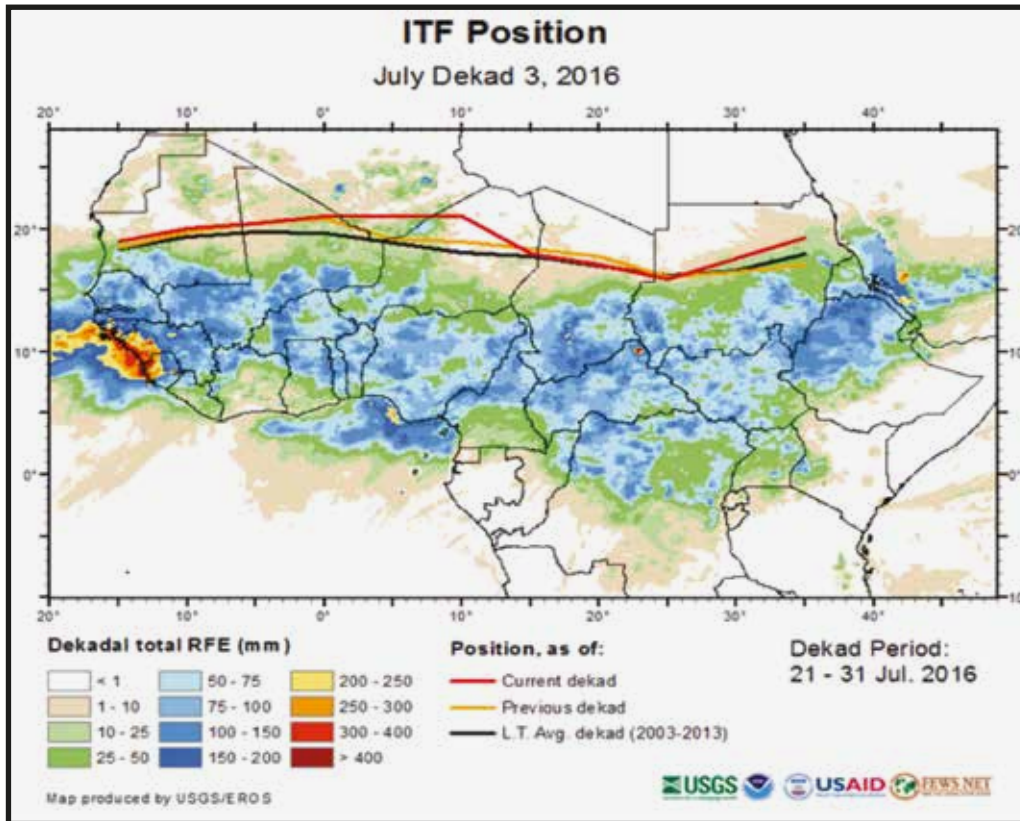
It should be noted that the daily runoff is being compared to the median of the annual maxima runoff values experienced during the period of historical data (1998-present). Thus, a magnitude close to 100 percent means that today's runoff for a given pixel is close to the maximum observed value for that pixel on any day in the past (time series).

FIGURE 22. Maps of daily runoff and anomaly as of 10 August 2016.



- Inter-Tropical Front (ITF) Position.** This graphic shows the 10-day average latitudinal position of the Africa Inter-Tropical Front (ITF) (formerly called the Inter-Tropical Convergence Zone (ITCZ)). The ITF data, and the subsequent information, are provided by the NOAA-CPC. The 10-day mean position of the Africa ITF has been monitored since 1988, for the region comprised between longitude 15° W to 35° E. Daily analyses of the ITF position are performed by hand interpolation of the 15° C surface dew point and the surface wind streamlines modelled by the Global Data Assimilation System (GDAS). Dekadal values are simple averages of the daily positions. Climatological means are computed using the previous year's analyses (Figure 23). Monitoring is performed from April through October. Current products may also be found online at <http://earlywarning.usgs.gov/fews/product/55> or <http://www.cpc.ncep.noaa.gov/products/fews/ITCZ/itcz.shtml>.

**FIGURE 23. ITF position map for the third dekad of July 2016, also showing the position during the previous dekad and the long-term average.**



- **Moisture Index (MI).** This agrometeorological indicator is defined by a simple supply/demand ratio, and then multiplied by 100 to provide a percentage value. The products are available at <http://earlywarning.usgs.gov/fews/product/52>. The MI is determined by the following equation:

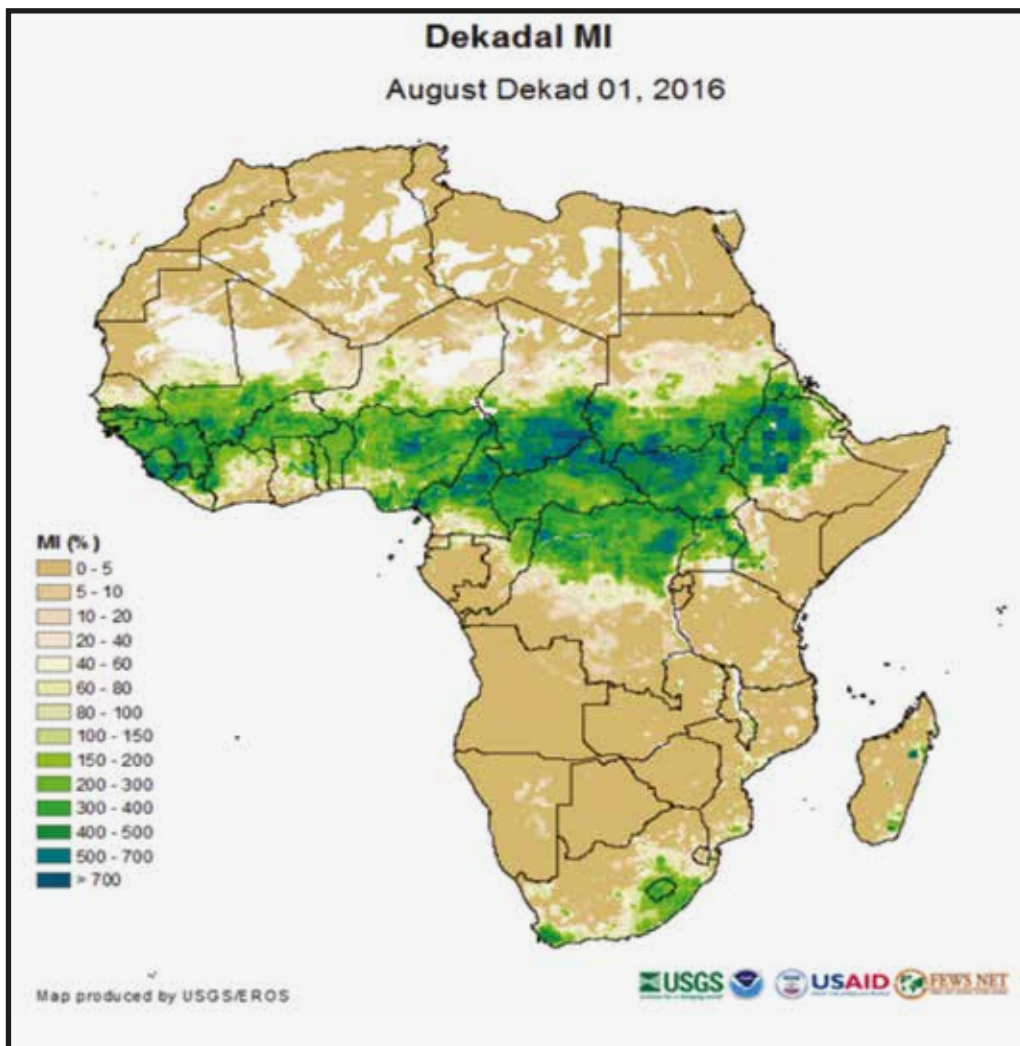
$$[(PPT + SW) / PET] * 100$$

where  $PPT$  is dekadal rainfall (mm),  $SW$  is available soil water (mm), and  $PET$  is dekadal potential evapotranspiration (mm). As a stand-alone product, the dekadal MI images (Figure 24) provide additional information concerning the moisture available to crops, thus enhancing the information provided by the RFE images. To calculate dekadal MI on a spatial basis, the RFE images are used directly for  $PPT$ , as  $PET$  grid values are computed from the GDAS analysis fields. A simple bucket model (defined by the soil's Water Holding Capacity (WHC) and the crop root depth) is used to calculate a new  $SW$  value for each dekad,  $i$ :

$$SW_i = SW_{i-1} + PPT_i - PET_i$$

where  $SW_i$  is subject to the constraint  $0 \leq SW_i \leq WHC$ . Soil water in excess of the WHC is assumed to be lost, as runoff or drainage out of the first 100 cm layer of soil.

FIGURE 24. MI map of the first dekad of August 2016.

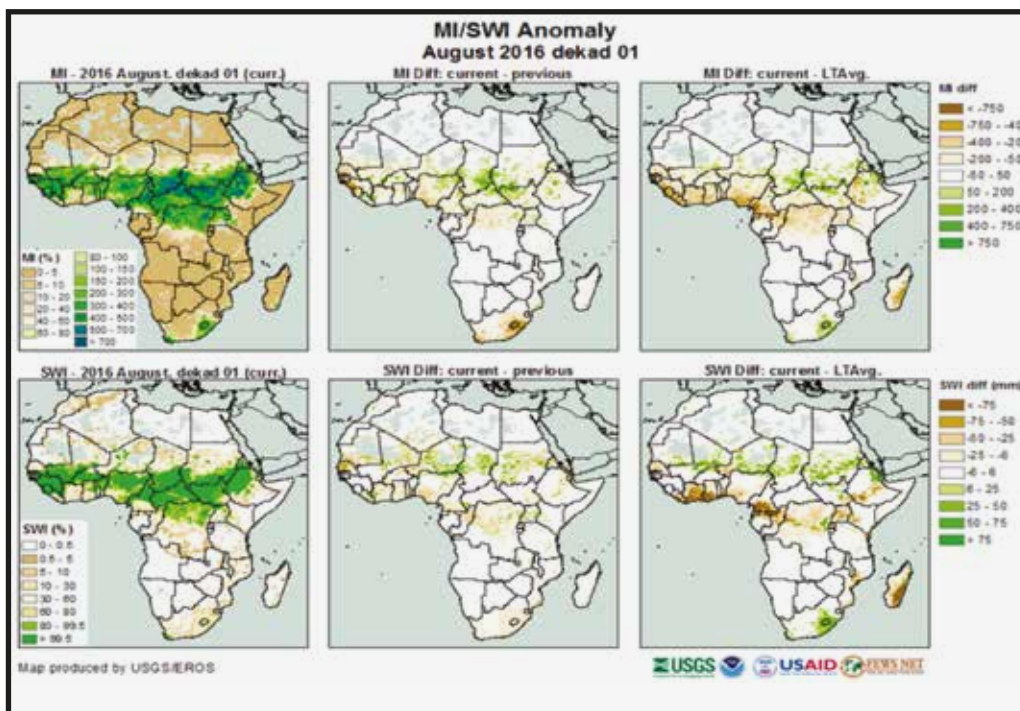


GDAS analysis fields, generated every six hours, are used to estimate dekadal PET on a spatial basis using the Penman-Monteith equation (the formulation suggested by Shuttleworth, 1992, for reference crop evaporation is used). The GDAS fields used include air temperature, atmospheric pressure at the surface, wind, relative humidity, and radiation (long-wave, short-wave, outgoing, and incoming). The PET is computed for each day, and appropriate sums are made to obtain dekadal totals. The spatial variation of soil WHC is characterized using the FAO Digital Soil Map of the World (FAO, 1994). The scale of the original mapping is 1:5 000 000, and the soil polygons carry attributes that include an estimate of easily available water capacity in the upper 100 cm, based on soil physical characteristics. These values were adopted to calculate soil water conditions. The FAO soil map has been rasterized at a scale that matches the 0.1-degree RFE grid.

- MI/SW Difference Images.** This graphic contains six images (Figure 25). The upper left part illustrates the current dekad MI and the lower left is the current dekad SWI. The upper and lower centre images show the differences between the current dekad and the preceding dekad for the MI and the SW respectively. The right-hand images illustrate the differences between the current dekad and the long-term average for the same dekad for the MI (upper) and the SW (lower). The products and related documentation are available at: <http://earlywarning.usgs.gov/fews/product/53>.

With regard to these data sets, it should be noted that: (i) the long-term average data for the MI and the SW were calculated from 1961–1990 FAO rainfall and potential evapotranspiration data; (ii) the MI differences are presented in units of percentage-point difference, i.e. simple subtractions of one image from the other – they should not be confused with ratios or percentage difference calculations; and (iii) differences in the SW are in actual mm of soil water. The SWI is presented as a ratio (percentage) of the soil’s WHC.

**FIGURE 25. MI/SW difference images of the first dekad of August 2016.**

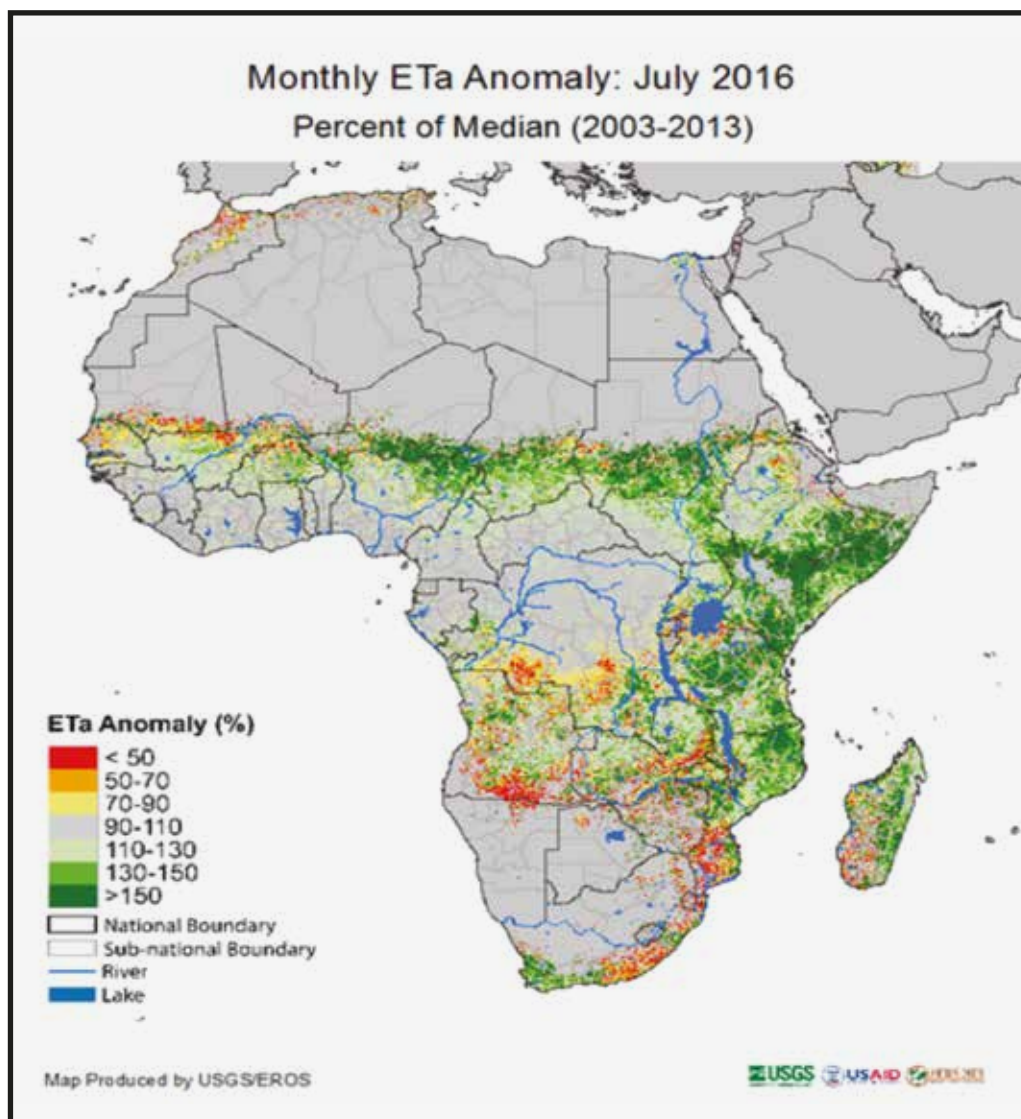


Monthly Evapotranspiration (ETa) Anomaly. Evapotranspiration (ET) is the combination of transpiration from vegetation (through the root system) and direct evaporation from soil-vegetation-water surfaces. Actual ET (ETa) is produced using the Operational Simplified Surface Energy Balance (SSEBop) model (Senay *et al.*, 2013) for the period from 2003 to date. The SSEBop set-up is based on the Simplified Surface Energy Balance (SSEB) approach (Senay *et al.*, 2007, 2011), with unique parameterization for operational applications. This approach combines ET fractions generated from remotely sensed MODIS thermal imagery, acquired every dekad, with reference ET using a thermal index approach. The ETa anomaly products are the ratio of the ETa and the corresponding median ETa, expressed as a percentage value. Arid regions with little or no vegetation (i.e. where the maximum NDVI < 0.25) are replaced with precipitation values for the corresponding period. In arid climates, the magnitude of ETa can be approximated by precipitation. The product and associated documentation are available at <http://earlywarning.usgs.gov/fews/product/66#documentation>. ETa anomaly products (current vs. 2003–2013) are also available at [http://earlywarning.usgs.gov/fews/datadownloads/Global/ETa Anomaly](http://earlywarning.usgs.gov/fews/datadownloads/Global/ETa%20Anomaly).

The ETa anomaly products offered are:

- Monthly ETa products: available for every month in a year (Figure 26).
- Cumulative ETa anomaly products: these are cumulative in intervals of dekads and grouped by the region's main growing season(s).

FIGURE 26. Monthly ETa anomaly product for July 2016.



- Standard Precipitation Index (SPI). This index presents a rainfall anomaly as a normalized variable that conveys the probabilistic significance of the observed or estimated rainfall (McKee, 1993). By expressing anomalies in terms of their likelihood of occurrence, it is easier to evaluate the rarity of the observed event, in the absence of a nuanced understanding of the rainfall regime at the location in question. This method offers a different, and complementary, perspective compared to anomalies (which may be relatively large, but not very significant in areas with highly variable rainfall) with respect to normal figures or the percentage thereof (these may be extreme, but not particularly significant in dry locations).

To evaluate the likelihood of occurrence, probability distribution functions (PDFs) are fit at each pixel for each accumulation interval. These PDFs are fit to the Collaborative Historical African Rainfall Model (CHARM) (Funk *et al.*, 2003), which provides a 36-year

time series with which to estimate gamma distribution parameters. The CHARM data establish the shape of the distribution, and provide an estimate of the variance.

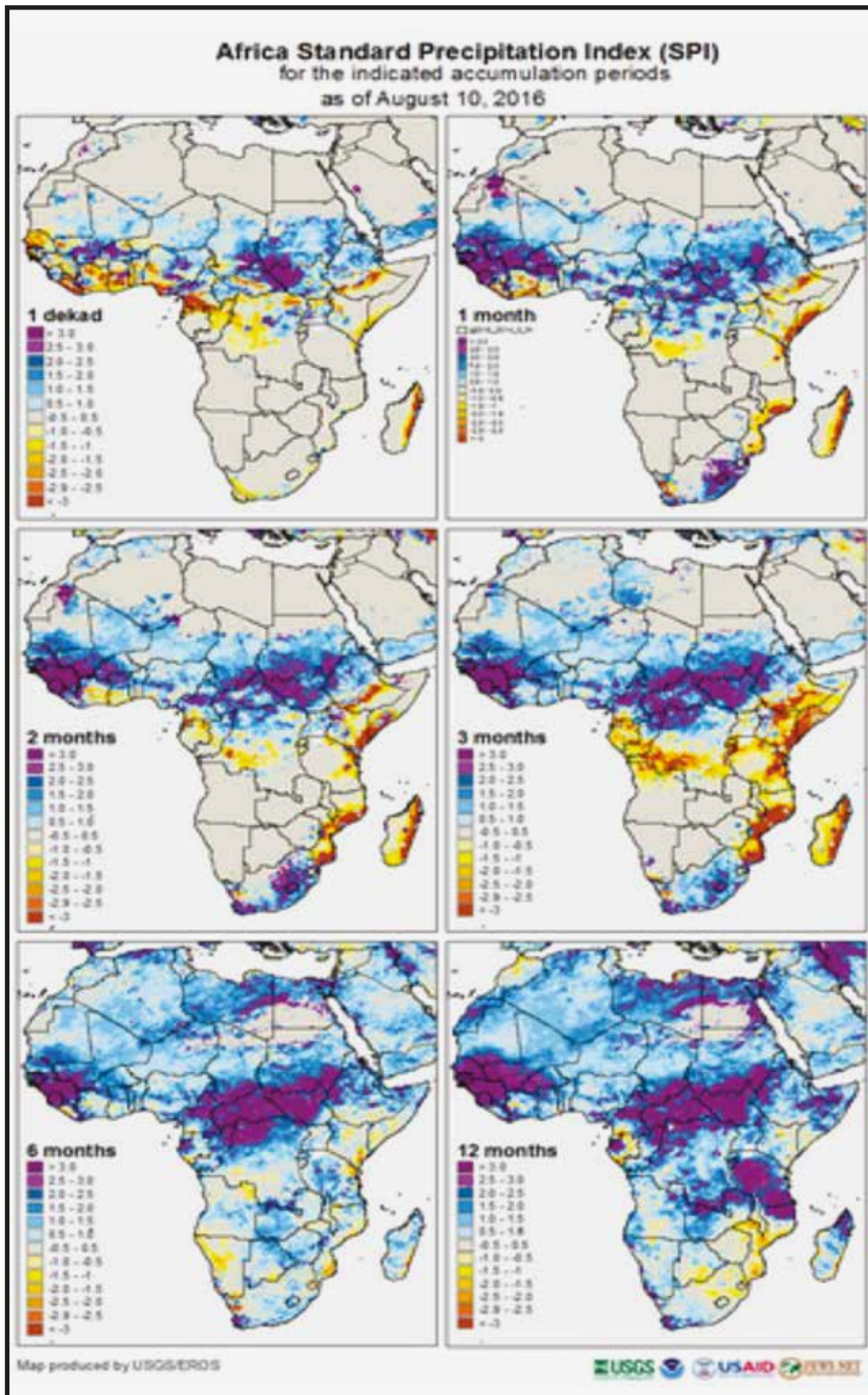
This research uses the gamma probability distribution to parameterize historical rainfall amounts. Gamma distribution parameters are fit to the CHARM estimates for each interval. The product of the gamma distribution parameters is equal to the mean. A difference in the mean of the historical record (CHARM) and of the real-time estimates will result in a bias in SPI values. To account for this, the estimated gamma distribution parameters are adjusted to match the mean provided by the African Rainfall Climatology data set (ARC; [http://www.cpc.ncep.noaa.gov/products/fews/AFR\\_CLIM/appl\\_clim.pdf](http://www.cpc.ncep.noaa.gov/products/fews/AFR_CLIM/appl_clim.pdf)).

As ARC estimates come in, the data are aggregated for the appropriate interval and compared to the adjusted PDF for that location. From this, the probability of exceedance is calculated and converted to a normalized variable representing the severity of the estimate.

SPI values over zero indicate conditions wetter than the median, while negative SPIs indicate conditions that are drier than the median (Figure 27). For drought analysis, an SPI lower than -1.0 indicates that the observation is approximately a one-in-six dry event; it is termed "moderate". An SPI lower than -1.5 indicates a one-in-fifteen dry event, and is termed "severe". Values lower than -2.0 are typically referred to as "extreme", indicating that the event falls within the driest 2 percent of all events.

The product and relative documentation is available at: <http://earlywarning.usgs.gov/fews/product/51>.

FIGURE 27. SPI products for accumulation periods.



Tools available via the FEWS NET data portal that are relevant to agricultural crop production and forecasting include:

- **Map Viewer.** This interactive map viewer allows users to visualize administrative and crop zone time series of NDVIs, dekadal rainfall and seasonal cumulative rainfall, and includes options for data download. The Map Viewer may be accessed at: <http://earlywarning.usgs.gov/fews/mapviewer/index.php?region=af>.
- **Early Warning eXplorer (EWX) software.** This software is an interactive web-based mapping tool that allows users to visualize continental-scale RFE, land surface temperature (LST) and total precipitable water (TPW) data and anomalies at varied time steps, as well as review time series analyses. The EWX may be accessed at <http://earlywarning.usgs.gov/fews/ewx/africa/index.html>.
- **Drought Status Monitor (DSM).** This is an experimental decision support tool based on weather and crop conditions. It incorporates drought monitoring rules that distinguish severity and provides a generalized drought indicator at national and subnational scales. The DSM is accessed at <http://earlywarning.usgs.gov/fews/dsm/index.php>.
- **GeoWRSI.** This program is a geospatial, stand-alone implementation of the WRSI as implemented by the USGS for FEWS NET activities. The program runs a crop-specific water balance model for a selected region in the world, using raster data inputs. The program produces a range of outputs that can either be used qualitatively, to help assess and monitor crop conditions during the crop growing season, or that can be regressed with yields to produce yield estimation models and yield estimates. Other tools are available to post-process the GeoWRSI outputs for use in yield estimation models. The GeoWRSI may be accessed at <http://chg.geog.ucsb.edu/tools/geowrsi/index.html>.
- **GeoCLIM.** This spatial analysis tool is designed for climatological analysis of historical rainfall and temperature data. GeoCLIM provides non-scientists with an array of accessible analysis tools for climate-smart agricultural development. These user-friendly tools can be used to obtain and analyse climate data, blend station data with satellite data to create more accurate data sets, analyse seasonal trends and historical climate data, create visual representations of climate data, create scripts (batch files) to quickly and efficiently analyse similar “batches” of climate data, view and edit shapefiles and raster files, and extract statistics from raster data sets to create time series. GeoCLIM is accessed via <http://chg.geog.ucsb.edu/tools/geoclim/index.html>.

### 3.3.1.4 VEGETATION/Proba-V Data Portals

The VEGETATION Programme was developed jointly by France, the European Commission, Belgium, Italy and Sweden. The programme's first satellite component (VEGETATION 1, also known as SPOT VEGETATION or SPOT VGT) was launched on 24 March 1998 on board of SPOT 4, while the second instrument was launched on board of SPOT 5 on 4 May 2002. Today, SPOT VEGETATION's successor flies on the European PROBA-V satellite. More similar data are expected via the Copernicus Programme, Sentinel 3 and others.

PROBA-V was developed both as a follow-up to the 15-year SPOT-VEGETATION mission, and as a preparation for the upcoming Copernicus' ESA (European Space Agency) Sentinel-3 land and ocean observation satellite mission. The SPOT-VEGETATION mission provided essential information on aspects such as crop yields, droughts and deforestation to a broad user community. To optimally serve the vegetation and land surface community, PROBA-V's spectral channels are similar to those of the SPOT-VGT instrument, thereby preserving maximum observational consistency with the SPOT-VGT era. Benefiting from the technological developments made since the launch of SPOT-VEGETATION in 1998, PROBA-V has a lean instrumental payload on a platform smaller than 1 m<sup>3</sup>. Using a constellation of three cameras, PROBA-V covers the entire Earth every two days and provides useful reflectance measurements for climate impact assessment, surface water resource management, agricultural monitoring and food security purposes.

VEGETATION data sets are available through various data portals, including the DevCoCast Data Portal (<http://www.devcoCast.eu/ViewContent.do?pagelD=1>), the Proba-V Data Portal (<http://proba-v.vgt.vito.be/content/products>), the VITO Data Portal (<http://www.vito-eodata.be/PDF/portal/Application.html#Home>), and the Copernicus Global Land Service <http://land.copernicus.vgt.vito.be/PDF/portal/Application.html#Home>). The data provided through these portals include NDVIs, Vegetation Productivity Indices (VPIs), VCIs, LAIs, fAPARs, Fraction of Vegetation Cover (FCover), Dry Matter Productivity (DMP), Normalized Difference Water Indices (NDWIs), and Burnt Area.

For the Proba-V data, it should be noted that all 1-km products are available free of charge through the ESA Earth Watch programme. Only 300-m products and L1C products older than one month are available free of charge; the newer versions may be accessed for a fee.

The NDVI is an indicator of the biomes' greenness. As such, it is closely linked to the fAPAR. Although the NDVI is not a physical property of the vegetation cover, its simple formulation has made it a popular indicator in monitoring ecosystems:

$$NDVI = (REF_{nir} - REF_{red}) / (REF_{nir} + REF_{red})$$

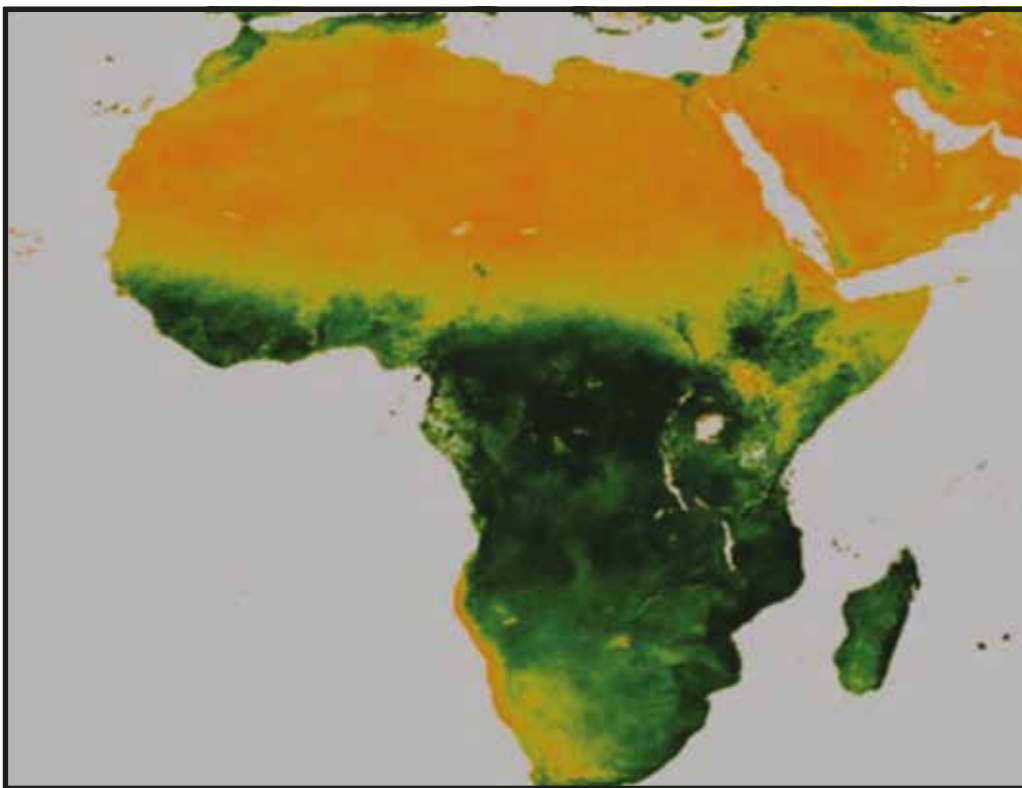
where  $REF_{nir}$  and  $REF_{red}$  are the spectral reflectances measured in the NIR and red wavebands respectively.

The VEGETATION instruments measure reflectances in four spectral bands: B0 (or "blue"), B2 ("red"), B3 ("Near-IR") and MIR (Shortwave-IR). The NDVI can then be calculated by using the B3 band for the NIR reflectance and B2 for the visible light reflectance:

$$NDVI = (B3 - B2)/(B3 + B2)$$

The outcome is a 10-day synthesis (Figure 28): it combines daily atmospherically corrected data of all VEGETATION segments (measurements) of the given dekad into a single image using the MVC (Maximum Value Composite) algorithm, which selects the pixels with the best ground reflectance values. There are two types of such S10 products, which are delivered by the CTIV (the VEGETATION image processing centre): S10s with all spectral bands, viewing and solar angles, and NDVI values; and S10s with only NDVI values, which are then called S10 NDVI. Within VGT4AFRICA (Vegetation for Africa), only S10 NDVI products are delivered to users.

**FIGURE 28. S10 NDVI product of the first dekad of May 2006.**

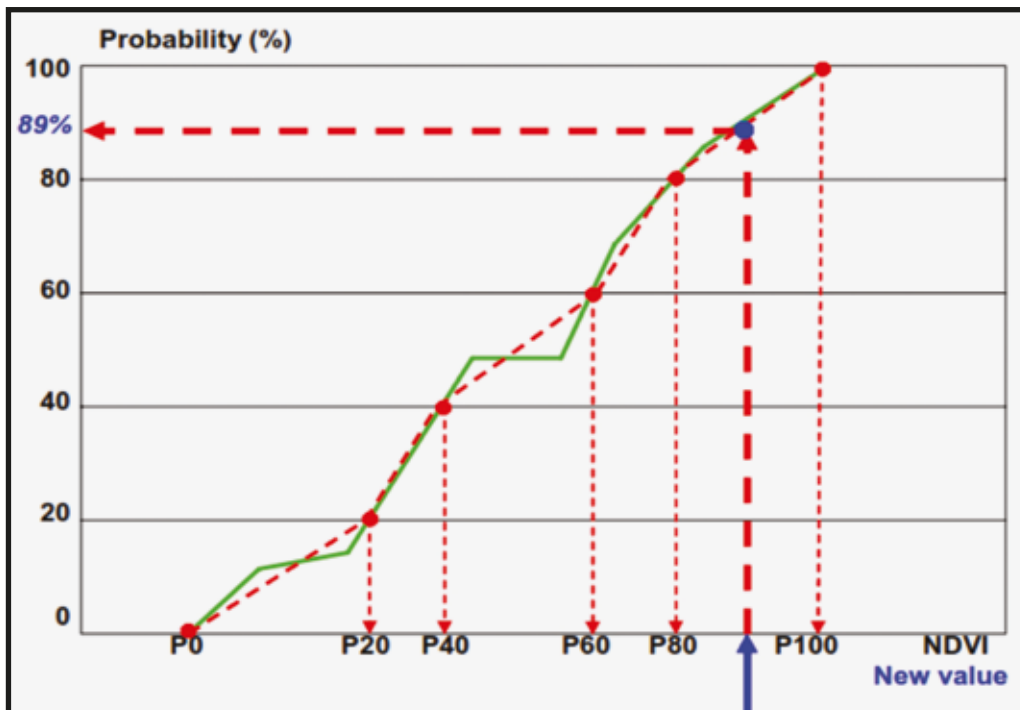


The VPI assesses the overall vegetation condition by referencing the current value of the NDVI with the long-term statistics for the same period. The VPI is a percentile ranking of the current NDVI value against its historical range of variability: values of 0 percent, 50 percent and 100 percent, respectively, indicate that the current observation corresponds with the historical minimum (worst vegetation state), median (normal) or maximum (best situation) ever observed.

The VPI method was originally developed by Sannier (1998) based on NOAA-AVHRR data for a study area in Zambia. It was later implemented by Eerens (2005) for Europe (for MARS-STAT) and Africa (MARS/FOOD-GMFS), on the basis of SPOT-VEGETATION data. The VPI method applies techniques that are commonly used in hydrology to predict extreme events.

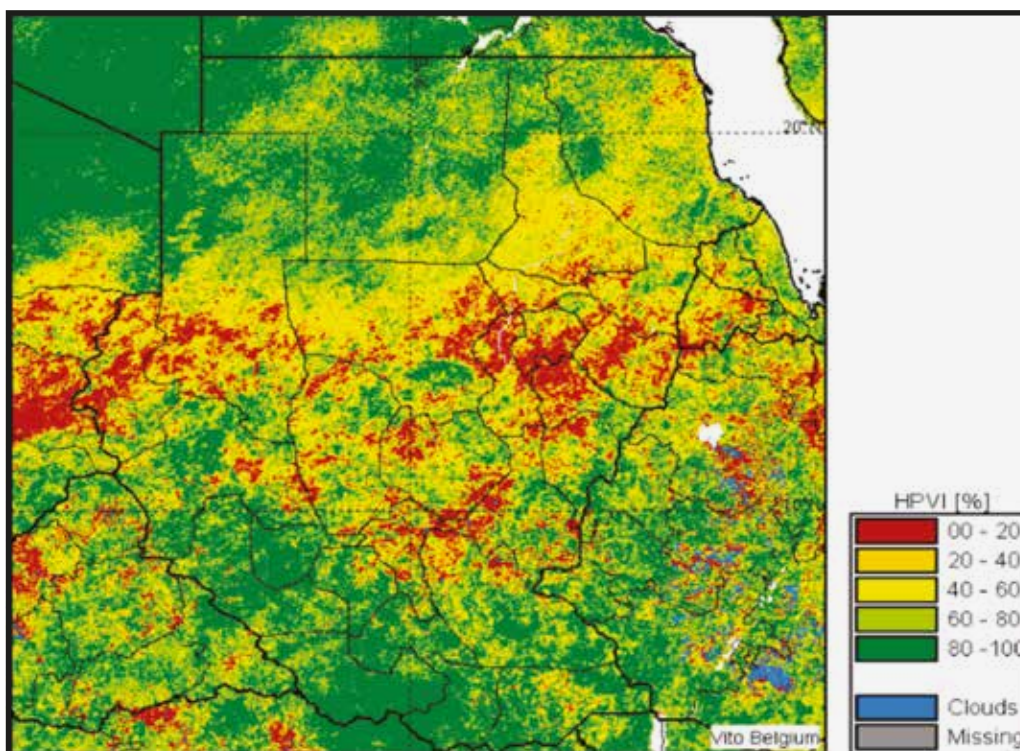
The general principle of the VPI method is explained in Figure 29 below. The green line represents the cumulative histogram, which is derived from the historical (in this case, NDVI) values available for the period under consideration. The red line, which connects the selected set of percentiles, forms an approximation of the true histogram. The figure only shows six percentiles (P0, P20, ..., P100); however, 11 deciles (P0, P10, ...) are used in the computations. New observations are referenced to the (approximate) histogram, which enables derivation of their historical probability. The example illustrated in Figure 29 (blue point) has a relatively high NDVI, and therefore a high probability (89 percent). Sannier *et al.*, 1998 immediately classified the probabilities into five groups (0-20 percent, ..., 80-100 percent). However, in this review, the original probabilities are retained.

**FIGURE 29. VPI illustration, showing an example of high NDVI and high probability.**



The VPI can be calculated on the basis of the DMP or NDVI values and for the main vegetation types, using the best land cover information available. The VPI delivered within the framework of VGT4AFRICA is produced on the basis of SPOT-VGT NDVI values (Figure 30).

**FIGURE 30. VPI product for Sudan for the second dekad of August 2016.**



The VCI compares the current NDVI to the range of values observed over the same period in previous years. The VCI is expressed in percentages and situates the observed value between the extreme values (the minimum and the maximum) recorded in the previous years. Lower and higher values indicate, respectively, bad and good vegetation state conditions.

The LAI is defined as half the total area of green elements of the canopy per unit horizontal ground area. The satellite-derived value corresponds to the total green LAI of all the canopy layers, including the understory; this may represent a very significant contribution, particularly for forests. In practical terms, the LAI quantifies the thickness of the vegetation cover. The Global Climate Observing System (GCOS) recognizes the LAI as an Essential Climate Variable (ECV).

The fAPAR quantifies the fraction of the solar radiation absorbed by live leaves for photosynthesis, and refers only to the green and alive elements of the canopy. The fAPAR depends on canopy structure, vegetation element optical properties, atmospheric conditions and angular configuration. To overcome dependency on the latter feature, a daily integrated fAPAR value is assessed. The GCOS also recognizes fAPAR as an ECV.

The FCover corresponds to the fraction of ground covered by green vegetation. In practical terms, it quantifies the spatial extent of the vegetation. The FCover is independent from the direction of illumination and is sensitive to the amount of vegetation. The product can validly replace the vegetation indices classically used to monitor ecosystems. It is also independent

of leaf and soil optical properties, although it is defined with reference to green elements. The FCover typically varies from 0 (bare soil) to 1 (full cover). The accuracy required should be consistent with that proposed for the fAPAR, and should be approximately 0.05. Similarly, the maximum encoding step should be 0.01.

The FCover is used to decouple vegetation and soil contributions in energy balance processes, with particular attention to temperature and evapotranspiration. Its interannual variations enable monitoring of the changes in land use.

The FCover algorithm is based on the transformation of the NDVI:

$$FCover = (NDVI - NDVI_{SOIL}) / (NDVI_{MAX} - NDVI_{SOIL})$$

This equation requires:

- Identification of the per-pixel based bare soil NDVI value. This is achieved by computing the minimum NDVI (NDVImin) value over time and for each pixel. The NDVImin over pixels mostly covered by vegetation will not be representative of bare soil; therefore, a bare soil value of 0.1 is assigned if the NDVImin = 0.2. This bare soil value is obtained from the peak of the frequency of the distribution of the maximum NDVI over time (NDVImax), which corresponds to the NDVI values observed over desert areas.
- Identification of the maximum NDVI value (NDVImax) to rescale the NDVI in an fCover percentage. This value is established as 0.85, based on the analysis of the annual NDVI's cumulative curve.

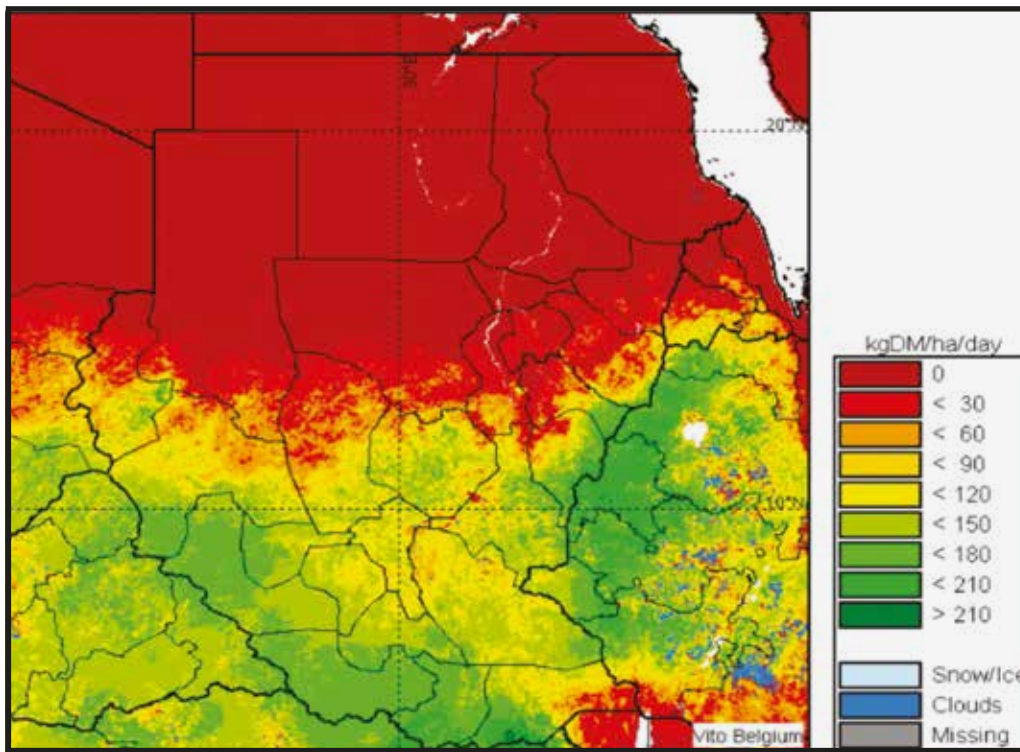
The DMP (Figure 31) represents the overall growth rate of or dry biomass increase in the vegetation, expressed in kilograms of dry matter per hectare per day (kgDM/ha/day). The DMP is directly related to the NPP (Net Primary Productivity, in gC/m<sup>2</sup>/day); however, its units are customized for agrostatistical purposes.

As described by Monteith (1972), the DMP can be calculated by combining the fAPAR – estimated from satellite imagery – with solar radiation and temperature information. According to Monteith, the increase in dry-matter biomass on a daily basis (subscript 1) can be formulated as:

$$DMP_1 = R_1 \cdot 0.48 \cdot fAPAR_1 \cdot e(T_1) \cdot 10,000$$

where  $R_1$  [J/m<sup>2</sup>/day] is the Sun's incoming short-wave radiation (2 003 000 nm) – averagely 48 percent of which consists of PAR (400-700 nm) – and  $fAPAR_1[-]$  is the PAR-fraction absorbed by green vegetation. The efficiency term  $e(T_1)$  [kgDM/JPAR] accounts for the conversion of this absorbed energy into biomass (radiation use efficiency) and for the losses related to the transport of photosynthetates, the maintenance of the standing phytomass, etc. The function  $e(T_1)$  is simplified and approximated as a function of daily temperature  $T_1$  (Veroustraete *et al.*, 2002). The function  $e(T_1)$  is non-linear and bell-shaped: it reaches a maximum at a temperature of 22°C and approaches zero for temperatures below 0°C and above 40°C. The factor 10 000 [m<sup>2</sup>/ha] transforms square metres into hectares, a more common unit in agrostatistics.

**FIGURE 31. The DMP product for Sudan for the second dekad of August 2016.**

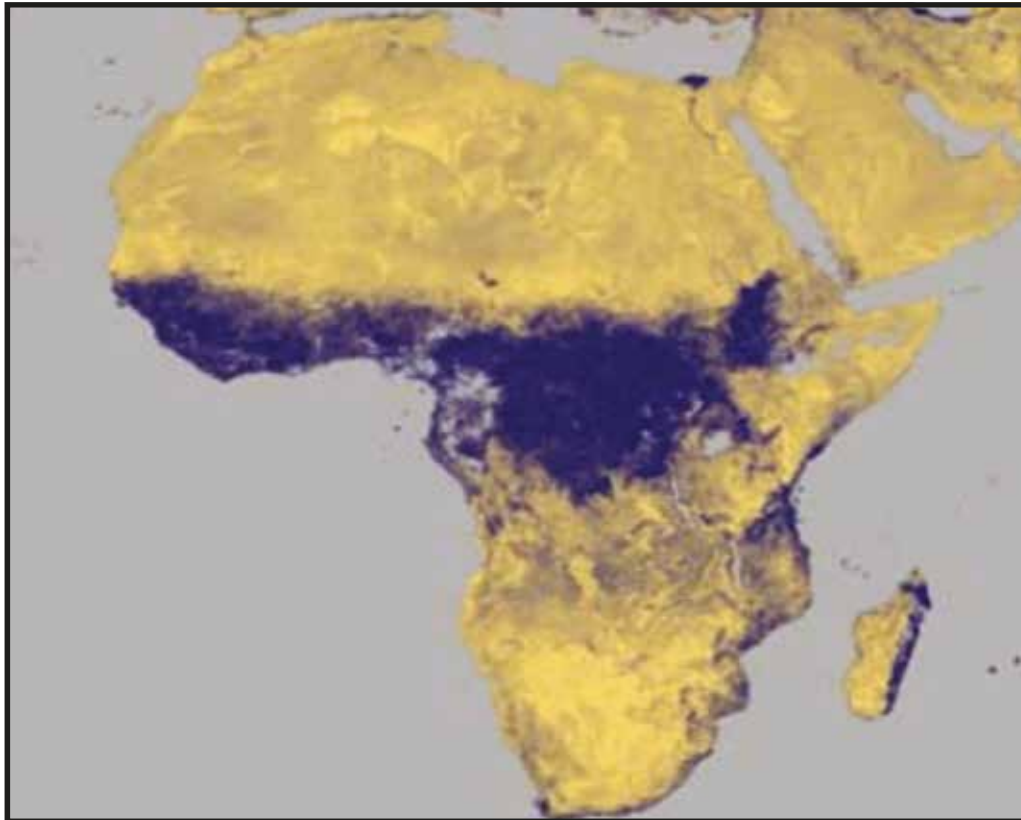


The **NDWI** (Figure 32) is a dimensionless index that indicates the presence or absence of water on the surface. It is calculated by comparing the shortwave and NIR sunlight reflected by the surface (reflectance). The NDWI is also sensitive to changes in the liquid water content of vegetation canopies. The NIR and Short-Wave Infrared (SWIR) reflectance bands can be combined to compute the NDWI, according to the formula:

$$NDWI = (\rho_3 - \rho_4) / (\rho_3 + \rho_4)$$

where  $\rho_3$  is the reflectance in the NIR band and  $\rho_4$  is the reflectance in the SWIR band. This formula is similar to that of the well-known NDVI, except that the NDWI formula considers the SWIR ( $\rho_4$ ) instead of the reflectance of visible (red) light. This usage of SWIR reflectance is precisely what makes the NDWI more sensitive to water content.

**FIGURE 32.** The NDWI product of the first dekad of July 2006.



Lastly, the **Burnt Area** product maps the burnt scars, and provides temporal information on the fire season. The GCOS also recognizes Burnt Area maps as an ECV. The burned area product includes the burned area itself and information about the temporal pattern of the fire activity, i.e. the start and end dates of the fire season. The product is a digital map, at full resolution, of the extent of the surfaces burned during a period of time (in this case, a dekad). Start- and end-of-season products provide dates for the occurrence of burned surfaces at a reduced resolution, typically half-degree by half-degree/ $0.5^\circ \times 0.5^\circ$ .

Burned area identification is carried out on a pixel basis. Detection is based on algorithms developed within the framework of the Global Burnt Area 2000 (GBA 2000) project and adapted for real-time monitoring application within the framework of the Global Daily Burned Area (GDBA) project coordinated by the EU-JRC. A complete description may be found in Tansey (2002). The output product is a daily map of burned surfaces.

The seasonality of the burnt areas is assessed by  $\frac{1}{2}^\circ \times \frac{1}{2}^\circ$  grid cells. This algorithm was developed within the framework of the Geoland project. The first step of the processing chain consists in generating 10-day syntheses at  $\frac{1}{2}^\circ$  resolution. The 10-day  $\frac{1}{2}^\circ \times \frac{1}{2}^\circ$  resolution images are assembled into time series, to identify the characteristics of the most recent season.

### **3.3.1.5 GEONETCast**

GEONETCast is a global network of satellite-based data dissemination systems providing environmental data to a global user community. GEONETCast is a milestone in the Global Earth Observation System of Systems (GEOSS), coordinated by the intergovernmental GEO group. GEONETCast is designed to make a vast range of essential environmental data readily available to users around the world. It is designed to be a user-driven, user-friendly, and low-cost information dissemination service providing global information for sound decision-making in a number of critical areas, including climate, agriculture, weather, water, public health, energy, natural disasters, and ecosystems. Accessing and sharing such a range of vital data is expected to yield societal benefits, through improved human health and well-being, as well as sound environment management and economic growth. Within the existing framework, GEONETCast is already partially realizing this goal with environmental data exchange and data delivery systems in Europe, Africa and the Americas. An additional data exchange service is now being established to cover the Asia-Pacific region. The following products are being made available to the GEONETCast user community: Meteosat image data; GOES East and West image data; FY-2 image data; Land and Ocean Sea Ice Satellite Application Facility (SAF) products; EUMETSAT meteorological products; NOAA-NESDIS meteorological products; NOAA-NESDIS Ocean colour and sea surface temperature products; VEGETATION products from VITO; MODIS Ocean colour products; and in situ and observational data.

EUMETCast is one of the three main components of the global GEONETCast infrastructure, an early GEOSS achievement. GEONETCast combines EUMETCast with GEONETCast-Americas (operated by NOAA) and FengYunCast (operated by the Chinese Meteorological Agency) to form the GEONETCast Networking Centres (GNC), capable of providing near-global dissemination.

### **3.3.1.6 EUMETSAT Data Portal**

<https://eoportal.eumetsat.int/userMgmt/protected/welcome.faces>

EUMETSAT delivers agreed data, products and support services to its Member States and users worldwide – both from their own programmes as well as third-party programmes. EUMETSAT provides data sets on key indicators of interest, including: faPAR; Fractional Vegetation Cover (FVC); LAI; Land Surface Albedo; Surface Soil Moisture; active fire monitoring product; Daily Evapotranspiration (ET); Fire Risk Map (FRM); LST; and Burnt Area products. The full list of data sets provided and descriptions thereof may be accessed at

[http://navigator.eumetsat.int/discovery/Start/DirectSearch/Extended.do?m\(c0\)=theme.par.Land](http://navigator.eumetsat.int/discovery/Start/DirectSearch/Extended.do?m(c0)=theme.par.Land).

### **3.3.1.7 The Earth Explorer**

<http://earthexplorer.usgs.gov/>

The USGS Earth Explorer is similar to the USGS Global Visualization Viewer (GloVis) in that users search catalogues of satellite and aerial imagery. The Earth Explorer provides data sets that include: the AVHRR (AVHRR Global 1 Km, AVHRR Composites); the NASA LPDAAC Collections (Aster collections, MODIS Gross Primary Productivity, MODIS LAI/fAPAR, MODIS Land Cover, MODIS Land Surface Reflectance, MODIS Land Surface Temperature/Emissivity, MODIS Thermal Anomalies and Fire, MODIS Vegetation Indices, and MODIS Water Mask); Vegetation Monitoring (AVHRR Phenology, eMODIS Global Land Surface Temperature, eMODIS NDVI, eMODIS Phenology, NOAA CDR NDVI, and VegDRI); the Landsat archive; and Sentinel 2 data (10-m resolution).

### **3.3.1.8 Copernicus – Sentinels Scientific Data Hub**

<https://scihub.copernicus.eu/>

The Copernicus – Sentinels Scientific Data Hub is a portal that provides complete, free and open access to the data collected through Copernicus missions. The Copernicus missions (Sentinel-1, Sentinel-2, and Sentinel-3) represent the EU's contribution to GEOSS. Data from all three Sentinels are available free of charge. The online registration process is open to all and grants access rights for searching and downloading Sentinel products.

Sentinel-1 is the European Radar Observatory, representing the first new space component of the GMES (Global Monitoring for Environment and Security) satellite family, which was designed and developed by ESA and funded by the European Commission (EC). Sentinel-1 is composed of a constellation of two satellites: Sentinel-1A and Sentinel-1B, which sharing the same orbital plane with a 180° orbital phasing difference. The mission provides independent operational capability for continuous radar mapping of the Earth, with enhanced revisit frequency, coverage, timeliness and reliability for operational services and applications that require long time series. The mission's objective is to ensure C-Band SAR data continuity following the retirement of ERS-2 and the end of the Envisat mission. For this purpose, the satellites carry a C-SAR sensor, which offers medium- and high-resolution imaging in all-weather conditions. The C-SAR is capable of obtaining night imagery and detecting small movements on the ground, which makes it useful for land and sea monitoring. Frequent revisits by Sentinel-1 over the same area enable close monitoring of changes in land cover; this is particularly useful for monitoring tropical forests – typically shrouded by cloud cover – and for detecting illegal timber harvesting worldwide. Information on land cover is also important for agricultural practices, in particular estimating crop acreage, providing information on soil moisture information and forecasting yields.

Sentinel-2 is a multispectral operational imaging mission within the GMES program. It is jointly implemented by the EC and ESA for global land observation, in particular to retrieve data on vegetation, soil and water cover for land, inland waterways and coastal areas, and to provide corrections of atmospheric absorption and distortion data. The images are captured at high resolution, with a wide swath width and high revisit capability: ten days at the Equator

with one satellite, and five days with two satellites under cloud-free conditions, resulting in two to three days at mid-latitudes. This enhances the continuity of data provided by SPOT-5 and Landsat-7, thus supporting the monitoring of changes occurring in the vegetation within the growing season, as well as many other applications.

To meet user needs, the data collected through the Sentinel-2 satellite supports the operational generation of several high-level products, including: generic land cover; land use and change detection maps (e.g. CORINE land cover maps updates, soil sealing maps, forest area maps); and maps of geophysical variables (e.g. the LAI, leaf chlorophyll content, leaf water content).

The Sentinel-2 mission comprises twin polar-orbiting satellites in the same orbit, phased at 180° to one other. Sentinel-2A was launched on 23 June 2015 and is already operational. Sentinel-2B is set for launch in 2017.

The ESA and EC Sentinel-3 mission is another element of the GMES program. It responds to the need for operational and near real-time monitoring of ocean, land and ice surfaces over a period of 20 years. The satellite measures sea surface topography, sea and land surface temperature, and ocean and land surface colour, with high accuracy and reliability. The data captured support ocean forecasting systems, and environmental, agricultural and climate monitoring.

The Sentinel-3 mission is designed as a constellation of two identical polar orbiting satellites, phased at 180° to one another, for the provision of long-term operational marine and land monitoring services. The mission's operational character implies that data products will be available at higher temporal resolution and that they will be delivered very quickly.

Sentinel-3A was launched on 16 February 2016. Sentinel-3B is scheduled for launch in 2017.

### **3.3.2 RS portals, tools, data and products available for a fee**

Various EO data portals provide commercial data (optical or SAR) that are useful for agricultural crop production and forecasting.

#### **3.3.2.1 DigitalGlobe imagery**

DigitalGlobe leverages its high-resolution multispectral satellites to provide Red-Edge detection. This enables the performance of vegetative analyses that can reveal plant type, age, health and diversity in unprecedented detail. RS solutions that include the Red-Edge band are sensitive enough to discriminate between young and mature plants, conifers and broad-leafed plants, and even subtle changes in plant health, before they are visible. Analysts rely on the sensitivity of WorldView-2's Red-Edge band to deliver granular field classifications and early-warning capabilities to industries that depend on the environment. In the context of precision agriculture, DigitalGlobe imagery support various activities, such as discrimination of weeds and field crops, the monitoring of effects of irrigation on crop health, and the calculation of yield by mapping crop health to market place.

Through its Seeing a Better World™ Program, DigitalGlobe partners with scientists of the STARS (Spurring a Transformation for Agriculture through Remote Sensing) Project to provide better information that can increase productivity and decrease vulnerability for millions of family farmers, whose plots of land (perhaps even held on an insecure tenure) may be no larger than a football field. Very High-Resolution (VHR) satellite imagery, such as that provided by DigitalGlobe, is considered the ultimate force multiplier for smallholder farmers, who currently have few avenues to diagnose crop health, identify appropriate responses, forecast expected production, or access credit and financial services to improve their productivity. DigitalGlobe's VHR, super-spectral imagery provides many key agricultural data points, such as water availability, plant nitrogen content, crop vigour and evidence of continued care of the land over time that could be used as collateral. Under the initiative that began in early 2014, DigitalGlobe provides information derived from its visible and very NIR satellite imagery to monitor crop growth at the level of the smallholder farm plots found in the SSA and South Asia. The ultimate goal is to improve the estimates of crop yield as the season progresses, and to generate better, evidence-based advisories for on-farm and around-farm practices such as those provided by extension services and the private farm inputs sector.

Pan, Sun and Li (2008) conducted a study using QuickBird imagery with a production efficiency model (PEM) to estimate crop yield in Zhonglianchuan, a hilly area on the Loess Plateau, China. In the PEM model, crop yield is a function of the PAR, the fAPAR and light-use efficiency (LUE). Based on QuickBird's high spatial resolution imagery, a land cover classification is used to attribute a class-specific LUE. The fAPAR is related to spectral vegetation indices (SVI), which can be derived from the satellite images. The LUE, fAPAR and incident PAR data were combined to estimate the crop yield. Farmer-reported crop yield data in 80 representative plots were used to validate the model output. The results indicated that QuickBird imagery is capable of improving the accuracy of predicted results, compared to the Landsat TM image. The predicted yield approximated well with the data reported by the farmers ( $r^2 = 0.86$ ;  $n = 80$ ).

DigitalGlobe imagery can be accessed via the DigitalGlobe Image Finder: <https://browse.digitalglobe.com/imagefinder/main.jsp>.

### **3.3.2.2 Imagery from Airbus Defence and Space**

Airbus Defence and Space offers various optical and SAR imagery that supports agricultural applications. The suite of satellite imagery includes SPOT, Pleiades, and TerraSAR.

SPOT satellites have been supplying high-resolution, wide-area optical imagery since 1986. The 30-year archive acquired by SPOT 1 through to SPOT 7 contains over 30 million images at resolutions of 20 to 1.5 m, all accessible from Geostore (<http://geostore.astrium-geo.com/>). This array of optical satellite imagery, as well as the SAR imagery offered by Airbus Defence and Space, are suitable for various agricultural applications, including crop acreage and other biophysical parameters that can support crop yield forecasting.

The Airbus Defence and Space Geostore for optical and SAR products (SPOT, Pleiades and TerraSAR) may be accessed at <http://www.intelligence-airbusds.com/en/4871-browse-and-order>.

### **3.3.2.3 Imagery from Planet Labs/BlackBridge (Rapid Eye)**

Each of RapidEye's five satellites contains identical sensors, are equally calibrated and travel on the same orbital plane (at an altitude of 630 km). Together, the five satellites are capable of collecting over 4 million km<sup>2</sup> of 5-m resolution, 5-band colour imagery daily. Each sensor aboard RapidEye is capable of collecting image data in five distinct bands of the electromagnetic spectrum: Blue (440-510 nm), Green (520-590 nm), Red (630-690 nm), Red-Edge (690-730 nm) and Near-Infrared (760-880 nm). The nominal resolution on the ground is 5 m, corresponding to NIIRS 2. RapidEye's satellites are the first commercial satellites to include the Red-Edge band, which is sensitive to changes in chlorophyll content. Studies show that this band can assist in monitoring vegetation health, improve species separation and help to measure protein and nitrogen content in biomass. Various studies have used RapidEye's multispectral data to estimate the LAI and biomass.

Planet Labs/BlackBridge/Rapid Eye imagery may be accessed at: <http://eyefind.rapideye.com/>.

### **3.3.2.4 Imagery from DMCii (DMC Constellation, NigeriaSAT-2)**

Disaster Monitoring Constellation for International Imaging (DMCii) delivers high-resolution Earth imaging services from coordinated satellites of the international DMC Constellation. DMCii specializes in rapid programmed campaigns. The first generation of Disaster Monitoring Constellation (DMC) was launched in 2002–2003 to create the first constellation that was designed to deliver daily repeat high-resolution imaging. Four satellites in phased sun-synchronous orbit delivered 650-km wide multispectral imagery with a ground sample distance (GSD) of 32 m. An additional satellite was launched in 2005, providing even greater imaging capacity, and a third 32-m sensor was added in 2012. The second generation of enhanced DMC satellites (launched in 2009) dramatically enhanced the imaging capacity, retaining the same 650-km swath width but with twice the pixel density, at 22-m GSD. In these second-generation DMC satellites, the radiometry was also improved. The satellites are routinely cross-calibrated within 1 percent of Landsat. Data continuity is ensured with the launch of additional capacity to capture 60 million km<sup>2</sup> of imagery per day (scheduled in 2014–2015). The DMC also delivers VHR capability, with 2.5-m GSD panchromatic and 5-m GSD multispectral imagery.

In addition to commercial activity, the DMC works actively within the International Charter on Space and Major Disasters to provide free-of-charge satellite imagery for humanitarian use in the event of major international disasters, such as tsunamis, hurricanes, fires and flooding.

DMCii imagery may be accessed at <http://catalogue.dmcii.com/>.

### 3.3.3 Other RS platforms that support agricultural applications

Other commercial sources of RS data that may be useful for the purposes of agricultural production and forecasting include renowned companies that offer aerial photography, LiDAR and drone services. Due to the sheer quantity of such companies, they will not be listed individually in this review. Suffice to note that while, in the context of agricultural statistics, aerial photography has been used for many years, LiDAR and drones have only recently been applied.

## 3.4 National agencies mandated to generate crop production statistics

In this assessment of the main national agencies mandated with the regular generation of reliable agricultural production statistics, the following key factors have been considered:

- Institutional infrastructure (prerequisites dimension);
- Technical and financial resources (input dimension);
- Statistical methods and practices (throughput dimension);
- Availability and reliability of statistical information (output dimension);
- Information-user needs, and packaging and dissemination.

A framework of the institutional SWOT analysis to be applied was endorsed and applied by the UN Statistical Commission in 2010, in support of the Global Strategy to Improve Agricultural and Rural Statistics (GSARS). The results of the analysis are documented in the 2010 AGRICAB report, which highlighted the following key findings with regard to SSA countries:

- Demand was increasing for reliable and objective agricultural production forecasts, to support decision-making and response planning.
- There was a need to determine best practices for national yield and acreage forecasting, in light of mixed and diverse farming systems occasioned by emerging climatic trends.
- It was necessary to enhance understanding of institutional capacities and gaps, to develop and recommend both short- and long-term action plans that could meet user demands.

In this review, a country-by-country capacity analysis is undertaken for the three pilot countries of Kenya, Senegal and Zimbabwe.

### 3.4.1 National institutional RS capacities and competencies in the pilot countries

In Kenya, Senegal and Zimbabwe, there are two basic kinds of crop production forecasting.

The most common approach relies on a large-scale administrative network of MoAs and field

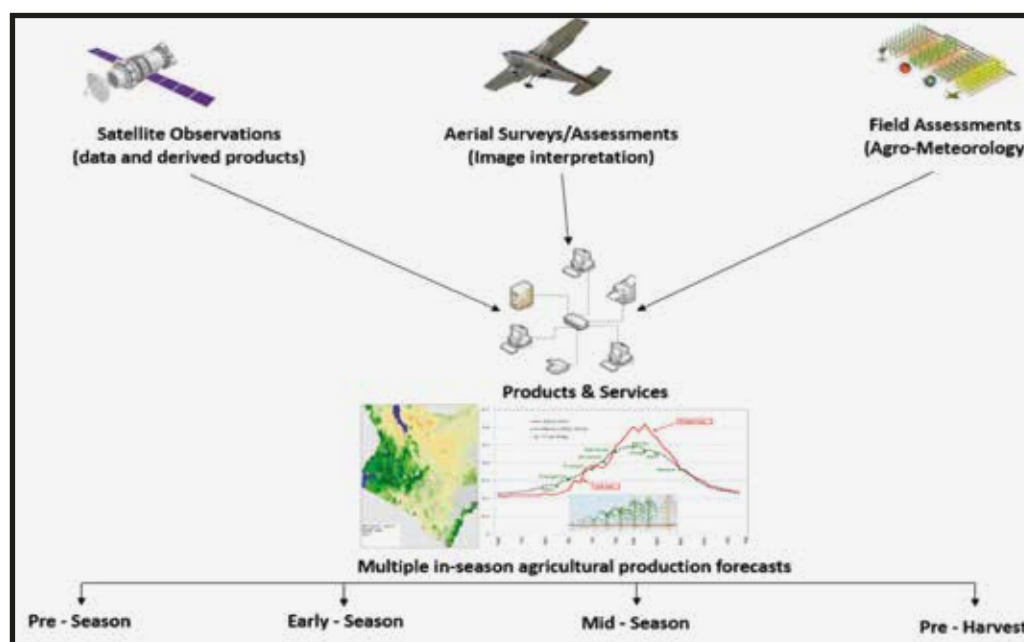
extension officers in rural areas. During each crop growing season, agriculture extension officers at the lowest administration level observe and record estimated area planted, yield and production based on their field experience. These observations are aggregated at district, county and national level as the official crop production estimates. However, this approach has several weaknesses, among which subjectivity and an absence of verification mechanisms.

The second approach is more objective and involves statistical practices, using field and aerial surveys. This approach is very demanding in terms of human and financial resources, and is usually not practiced regularly in the pilot countries.

The best practices leverage on a convergence of evidence from multilevel observation networks, which geospatially integrate field and remotely sensed data and products together with simple crop models to provide timely and reliable seasonal agricultural production forecasts, at critical timeframes for decision-making at subnational to national level.

Figure 33 depicts the integrated crop production forecasting system emerging from the best practices.

**FIGURE 33. Integrated crop production forecasting systems.**



This elaborate and fairly advanced agricultural production system requires multiagency collaboration at national, regional and international levels. It is against this system that national institutional capacities and gaps are assessed and determined for Kenya, Senegal and Zimbabwe.

### 3.4.1.1 Kenya

In Kenya, the MoA is mandated to provide agricultural production forecasts and statistics. It deploys over 5 000 agricultural extension officers to observe and estimate the area planted and the yield, and to compute agricultural production, at the lowest administrative levels. These estimates are aggregated at district, provincial or county and national levels to obtain national production estimates. This approach relies on the extension officers' field experience and informants from the local community.

These production estimates are affected by several inherent weaknesses:

- Overall, the methods used by each extension officer are subjective and impressionistic, and are largely based on informal interviews with local farmers and communities.
- Differentiating mono- and intercropped maize field sizes is problematic and inaccurate.
- Often, the area planted does not translate to harvested acreage, due to waterlogging, drought, pests and insufficient labour resources.
- The acreage planted is estimated as the difference with the previous year's estimate; this is a source of systematic error.
- Agricultural production estimates are often subject to upward or downward revision, for political reasons.

The MoA also collaborates with the Kenya Meteorological Department (KMD) and the Directorate of Resource Surveys and Remote Sensing (DRSRS) given their technical competencies in assessing prevailing agroclimatic conditions and statistically estimating agricultural production based on mid-season aerial surveys (the latter are undertaken by the DRSRS). Since 1984, crop forecasting has been one of the DRSRS's core activities, supporting informed decision- and policy-making in food security and relief supply. The DRSRS's work also supports forward planning ahead of actual harvest (for example, to inform export/import planning), strategic food reserves, and early warning taking into account production. The DRSRS is also mandated with the collection, storage, analysis, updating and dissemination of geospatial information on natural resources, to facilitate informed decision-making for the sustainable management of these resources and thus ultimately alleviate poverty and foster sound environmental management. The data collected form the basis for policies and development plans. The data also support decision-making in various government ministries, and resource planning and management agencies.

The DRSRS's main objectives are to:

- collect data on the numbers and distribution of livestock and wildlife and associated environmental and ecological attributes in the Kenya Rangelands;
- map and monitor the vegetation and habitats of livestock and wildlife in Kenya;
- undertake land cover/use assessment, mapping and monitoring (vegetation cover, forests, species composition, biofuel and land degradation);
- develop EWS for crop forecasting to be used in food security management and vegetation biomass productivity monitoring, for the purpose of range management;
- develop Land Information Management Systems (LIMS) from the geospatial data collected; and
- coordinate the application of RS technology in Kenya.

The DRSRS has a variety of up-to-date facilities and professional staff for resource surveys and mapping:

- GIS and RS laboratory – to support agricultural production forecasting
- Air Service – 2 Partenavia 168 and Cessna 208 (Caravan) aircrafts for wildlife and livestock aerial censuses, low-level reconnaissance flights and high-level aerial photography – to perform forest cover mapping, infrastructures and crop forecasting
- Cameras – 35mm vertical and oblique photo cameras to capture high-level aerial photography.
- Tape recorders – to archive aerial survey observations of wildlife and livestock populations
- Survey standard GPS devices – for location mapping and sampling
- Fieldwork motor vehicles – for field sampling and ground truthing
- Herbarium – a depository and inventory of plant specimens
- Library – this well-stocked facility holds several books, technical reports and articles relevant to the department's activities

The DRSRS deploys its own aircrafts and sensors to undertake yearly aerial surveys, which are interpreted to estimate crop acreage, density, yield and overall production for selected cereals. DRSRS outputs include:

- timely preharvest production forecasts or early warnings with regard to maize and wheat, which enable the Government to make appropriate contingency plans for storage and exports, if a bumper harvest is expected, or for imports and (localized or national) distribution strategies if a severe deficit is expected;
- long-term agricultural production databases for use in planning, management and policy formulation, with regard to production and national food security;
- research and development to improve the timeliness, accuracy and service delivery of its agricultural production estimations.

The KMD is responsible for:

- Generating seasonal climatic and short-term weather forecasts, which are disseminated to various end users with adequate lead time; the receiving parties include the MoA, which provides contextual interpretation of the data and issues agricultural advisories before and during the crop growing season.
- Collecting, collating and analysing agroclimatic observations and assessments. The KMD publishes monthly agrometeorological bulletins, which serve as regular inputs to the crop assessment reports and briefs compiled by the MoA and its partners.

The MoA also collaborates with other national, regional and international agencies, including FAO, WFP, WMO, IGAD Climate Prediction and Application Centre (ICPAC), FEWS NET and many other technical team members of the Kenya Food Security Steering Group (KFSSG). The MoA uses remotely sensed products – such as RFEs, Climate Hazards Group InfraRed Precipitation with Station data (CHIRPS), eMODIS and SPOT NDVI images – as inputs for agriculture and food security monitoring and vulnerability assessments.

### 3.4.1.2 Senegal

A large proportion of the Senegalese population lives in rural areas and relies on own food production from smallholder farms. To ensure food security for this vulnerable population, early estimations of agricultural production are crucial at all levels, from household to national. Agriculture is mainly rain-fed and depends, to a great extent, on seasonal rainfall amounts and distribution. However, its crop production is subject to drought and threats from pests such as desert locusts. The northern regions of Senegal are characterized by greater rainfall variability and low rainfall amounts, and are largely pastoral, with relatively lower crop production.

Agriculture employs 77 percent of the economically active population and accounts for 12.4 percent of the country's national gross domestic product (Funk *et al.*, 2012). Key food staples are millet, sorghum, maize and rice, which are grown for domestic consumption; cotton and groundnut are produced for export. However, Senegal is not self-sufficient and is a net importer of cereal crops. The average yields for sorghum, grain maize and millet are 0.7, 1.2 and 0.6 t.ha<sup>-1</sup> respectively, well below global average yields for these cereals. Agricultural production statistics are provided by the *Direction de l'Analyse, de la Prévision et des Statistiques Agricoles*.

The institutional framework of Senegal's agricultural sector is organized by two main ministries: the Ministry of Agriculture and the Ministry of Animal Husbandry.

The Ministry of Agriculture, Biofuels and Food Security includes the following substructures:

- The Directorate of Agriculture, which is responsible for the implementation of food grains and agro-industrial development policies and for overseeing field-based extension services;
- The Directorate of Horticulture, which coordinates government support to the horticultural sector;
- The Directorate of Agricultural Census; and
- The Directorate of Plant Protection, which is responsible for government pest control programs, including regulations, management of standards and various field interventions.

The Ministry of Animal Husbandry is mandated to provide several services and coordinate government support to the livestock, dairy and poultry subsectors.

These services are complemented by the following research and training institutions:

- The ISRA (*Institut Sénégalais de Recherches Agricoles*) – Senegalese Agricultural Research Institute) is the leading agricultural research institution and works on various issues related to crop and animal production
- The institute of Food Technology – *Institut de Technologie Alimentaire* (ITA)
- The Horticulture Development Centre (CDH)
- West Africa Rice Development Association (WARDA)

Senegal has several agricultural and veterinary training colleges, which provide most of the human resources used in the agricultural sector:

- The *Ecole Nationale Supérieure d'Agriculture* (ENSA) – the country's principal agricultural college;
- The *Ecole Inter-Etats des Sciences et Médecine Vétérinaires* (EISMV) – the inter-state veterinary college; and
- The Horticulture Development Centre (CDH).

The Centre de Suivi Ecologique (CSE) is a centre of excellence in agro-environmental monitoring. The CSE has key expertise in GIS and RS and has been mandated by the Government to provide RS-based information to monitor Senegal's environmental and agricultural resources.

The CSE also supports other government agencies, such as:

- The *Direction de l'Analyse, de la Prévision et des Statistiques Agricoles* (DAPSA) and the *Ministère de l'Agriculture et de l'Équipement Rural* (MAER) in generating agricultural statistics;
- The National Agency for Statistics and Demography of the Ministry of Finance and Economy, which uses agricultural statistics to calculate gross economic indicators for Senegal;
- The *Direction de l'Élevage* (DIREL) of the Ministry of Animal Husbandry; and
- The *Direction de l'Agriculture* (DA), which coordinates the campaigns and weekly meetings of the Ministry of Agriculture.

The CSE also participates in the *Groupe de Travail Pluridisciplinaire* (GTP), the body officially charged with monitoring the agricultural campaign in Senegal. It is coordinated by the *Agence nationale de l'aviation civile et de la météorologie* (ANACIM) and includes in principle all relevant parties (ministries, governmental agencies, international organizations, NGOs, etc.).

The CSE is a centre of excellence with regard to data management and the provision of derived information (Delcombel *et al.*, 2006). The Centre also plays an important role in terms of training and capacity building, and offers lectures for university students. The CSE's current responsibilities include:

- supporting the government in monitoring rain-fed crops, in response to the government policy to reduce dependency on imported cereals;
- improving the agricultural production statistics system by integrating RS observations;
- improving the current EWS; and
- improving grass biomass forecasting in pasturelands.

The main international development partners in Senegal's agricultural sector include; FAO, USAID, USDA, the World Bank, the African Development Bank, the West African Development Bank, the French Government, the Peace Corps and several other local and international NGOs. These are rather similar to Kenya's MoA partners.

To understand Senegal's livelihoods, the WFP, FAO, the CSE, the *Conseil National de la Sécurité Alimentaire* (CNSA) and FEWS NET collaborated to generate generalized livelihood zones and profiles for the country. The map is based on three aspects:

- i. geographic conditions (topography, height above sea level, soils, climate, vegetation and infrastructure (roads, railroads, telecommunications);
- ii. production (agricultural and pasture systems); and
- iii. access to commercial markets and labour. The characteristics of the production systems in each zone are described, including the main risks characterizing each region. For each zone, and for all of the main crops therein, agricultural calendars were made. After they were identified and characterized, different hazards (drought being the main climatic risk) and their order of importance were ascertained during regional workshops (WFP *et al.*, 2011).

Senegal relies on a combination of both field crop assessments undertaken by the MoA and in-line agency extension officers, remotely sensed products and crop model outputs, to generate multiseasonal agriculture production forecasts. Unfortunately, the integration of remotely sensed products into their forecasting systems is not operational; rather, it is mostly undertaken by its research and regional institutions, with the support of international technical partners such as FAO, WFP, FEWS NET and EU/JRC-MARS.

In Senegal, there are good opportunities to build on existing capacities within the MoA and related institutions to support operationalization of best practices in agricultural production forecasting systems.

#### **3.4.1.3 Zimbabwe**

Zimbabwe's National Statistical System (NSS) comprises of four essential components, which are coordinated by the Zimbabwe National Statistics Agency (ZIMSTAT) through the Census and Statistics Act (Chapter 10:29) of 2007. These components are:

##### **(a) Data producers**

The production and compilation of statistics in Zimbabwe can be considered to be decentralized, meaning that several institutions are involved in data collection and/or compilation, and ZIMSTAT is the main producer of official statistics. Some institutions involved in the production of statistics are government parastatal agencies, departments and line ministries. The role of data producers is to ensure a continuous stream of high-quality and accessible economic and social statistical data and information to meet the demands of different users.

##### **(b) Data users**

Data users are the most important component of an NSS, being those who demand and utilize statistical data and information. A sustainable NSS is user-focused and demand-driven. Data users play a major role in the NSS, such as by advancing a common understanding of policy issues and related data requirements, setting data priorities, clarifying the objectives for data collection, and agreeing on the best methods for collecting data. The main users of statistics and information include government agencies and parastatal organizations: these bodies use statistics for policy formulation, planning, administration, monitoring, evaluation, transparency governance and accountability.

Other statistics users are:

- The Parliament: national and local elected members need statistics to engage in evidence-based discussions, debates and planning.
- The private sector: economic agents use statistics to assess business and investment opportunities, risks and prospects. They also use statistics to plan, make decisions, monitor, evaluate and report on business activities.
- The media: these act as intermediaries in using and bringing statistics to the attention of key stakeholders and the general public.
- Civil society organizations: these include national and international non-governmental organizations and non-profit making bodies that work with disadvantaged communities such as the rural poor, women, the disabled, children, the displaced, etc. These organizations need and use demographic and other statistics to plan, implement, monitor and evaluate their activities.
- The general public: members of the general public use statistics for a variety of purposes, including public debate, making individual decisions and assessing the performance of the government.
- Development partners and international organizations: these bodies use statistics to assess requirements for providing assistance, for participating in development initiatives and for evaluating the effectiveness of their assistance programmes.

### **(c) Data suppliers**

Data suppliers include households, individuals, groups and business establishments that provide raw data. The Geo-Information and Remote Sensing Institute (GRSI) of the country's Scientific and Industrial Research and Development Centre (SIRDC) collects and analyses Earth Observation and geographic information for the development of Zimbabwe.

The Research Council of Zimbabwe administers Zimbabwe's membership in the GEO, a global coordinated initiative to enhance capacity for producing, managing and using Earth Observation data and enable participation in, and contribution to, the GEOSS. The GRSI is a founding member of the ZimGEO initiative.

Established in 2005, the GEO is a voluntary partnership of governments and organizations that envisions "a future wherein decisions and actions for the benefit of humankind are informed by coordinated, comprehensive and sustained Earth observations and information." The GEO Member Governments include 102 countries and the European Commission; it also envisages 103 Participating Organizations, comprising international bodies with a mandate in Earth Observation. Together, the GEO community creates the GEOSS, that will link Earth Observation resources worldwide across multiple societal benefit areas – Biodiversity and Ecosystem Sustainability, Disaster Resilience, Energy and Mineral Resources Management, Food Security and Sustainable Agriculture, Infrastructure and Transportation Management, Public Health Surveillance, Sustainable Urban Development, Water Resources Management – and make those resources available for better informed decision-making.

The University of Zimbabwe is a key source of satellite data for various applications. The university has a satellite-receiving station that receives data related to the services offered

in the SADC region via the MESA Project. These services fall within the three thematic areas of fire, agriculture and flood. These data sets are readily available for sharing with the government and the private sector. The main aim of these services is to improve decision- and policy-making through the use of Earth Observation data.

#### **(d) Research and training Institutions**

The main research institutions in the country are state and private universities, and research centres. To add value to data, researchers, academia, policy analysts and subject specialists undertake definitive policy-related analyses. Training institutions play the important role of developing and promoting appropriate statistical methodologies.

The GRSI is currently developing new Earth Observation and geodatabase products for government departments, and training forms a strong component in all of its projects. In addition, the University of Zimbabwe has been instrumental not only providing in data to government departments, but has also in capacity building in the areas of GIS and Earth Observation.

#### **Key institutional producers of agricultural statistics**

In Zimbabwe, the main institutions involved in producing agricultural statistics are ZIMSTAT; the Ministry of Agriculture, Mechanization and Irrigation Development (MoMID); the Department of Research and Specialist Services (DRSS); the Agriculture Technical and Extension Services (AGRITEX); the National Early Warning Unit (NEWU); the Ministry of Lands and Rural Resettlement (MLRR); the Food and Nutrition Council (FNC); the Cotton Company of Zimbabwe; the Zimbabwe Farmers' Union; the Zimbabwe Commercial Farmers' Union; the Meteorological Services Department (MSD); the Scientific and Industrial Research and Development Centre – Geo-Information; the Tobacco Industries Marketing Board (TIMB); the Agriculture and Rural Development Authority; the Grain Marketing Board; the Agriculture, Research and Extension Services; FEWS NET; and the Millers Association of Zimbabwe.

#### **Stakeholders in agricultural production forecasting**

The crop production forecasting committee is composed of the Main Committee, under which are subcommittees on grains and oil seeds, cotton, tobacco and methodology. A number of organizations are permanent members of every committee: ZIMSTAT, the Department of Meteorological Services, the National Early Warning Unit, AGRITEX, the University of Zimbabwe and the District Development Fund.

The members of the Main Committee are ZIMSTAT, the Grain Marketing Board, the Commercial Farmers' Union, the TIMB, the Cotton Company of Zimbabwe, the Ministry of Agriculture Mechanization and Irrigation Development, the Agriculture Economics and Markets, the Agriculture and Marketing Authority, the Meteorological Services Department, the National Early Warning Unit, AGRITEX, the DRSS, the District Development Fund (DDF), the University of Zimbabwe and the Ministry of Finance. ZIMSTAT is the chair of the Main Committee.

The members of the Methodology subcommittee are ZIMSTAT, the MSD, the NEWU, the University of Zimbabwe, AGRITEX, the DDF, the DRSS, the GRSI, the Ministry of Macroeconomic Planning and Investment Promotion, and the Food and Nutrition Council. ZIMSTAT is the chair of the Methodology subcommittee.

The Grains and Oil Seed subcommittee is chaired by the Grain Marketing Board. The members of the committee are the Commercial Farmers' Union (CFU), the Zimbabwe Farmers' Union (ZFU), the Commercial Oil Seed Producers Association and all permanent members. The Cotton subcommittee is chaired by the Cotton Company of Zimbabwe. The members are the CFU, the ZFU and all permanent members. The Tobacco subcommittee is chaired by the TIMB. The members are the Zimbabwe Tobacco Association and all permanent members.





## Key findings and conclusions

The operational RS systems used in the three pilot countries and in the SSA in general have the potential to improve agricultural crop forecasting. Linking these RS approaches with traditional crop forecasting systems has the capacity to improve both the spatial and the temporal resolution of current crop forecasts. Ancillary data sets and techniques will continue to be relied upon to improve mapping, particularly of growth stage and of crop yield. These include crop models, crop calendars, and calibration and validation data. To improve crop forecasting, an integrated system could be achieved by linking remotely sensed and contextual data, on one hand, with historical trends and model outputs, on the other, at spatial and temporal resolutions appropriate for farming industries.

The key findings of this review emphasize the following:

- There have been significant improvements in global remotely sensed observations, products and services, in terms of sensors and spatial and temporal resolution;
- An enhanced quality of the readily available suite of agricultural drought monitoring and early warning products;
- Most RS products and services are freely available on dedicated geoportals, however, their use and applications in the pilot countries is still very low.
- The available RS products must be validated and fine-tuned for wider application within the countries of interest;
- Africa's IT and communications systems are all at different levels of development, although they have significantly improved over the past decade and are generally capable of accessing and downloading low- to moderate-resolution RS data and products;
- There are gaps in the institutional capacity to integrate RS products with the field agroclimatic information available, to support a timely, reliable and cost-effective agricultural crop forecasting system;
- The rate of technological transfer is unsustainable, due to the uncoordinated and ad hoc funding initiatives by development partners, which in most cases end with

project funding, only to be replicated afresh without recognizing and building upon earlier initiatives;

- Kenya, Senegal and Zimbabwe show disparities in terms of the institutional development of the use of RS products and services, disparities that well reflect the challenges inherent in Africa. Successful implementation of the AMIS pilot project would inform the future scalability of improved agricultural forecasting systems across the continent.

The findings of this review will make a valuable contribution to the development of guidelines on using RS products, tools, methodologies and data to improve crop production forecasts. In particular, the findings form a useful basis that will inform the subsequent steps of this initiative, namely: reviewing and analysing the correlation between data from RS and crop production estimates (acreage and yield) using historical RS data and estimates from the three countries selected; identifying key data, products, methodologies and tools that can be easily used by statistical offices to improve crop production forecasts; developing guidelines and recommendations on the RS tools, products, methodologies and data; identifying training needs and developing appropriate training courses for key staff of the national agencies responsible for generating agricultural crop statistics and forecasts; and preparing the final report.

# References

- Atzberger, C.** 2013. Advances in Remote Sensing of Agriculture: Context Description, Existing Operational Monitoring Systems and Major Information Needs. *Remote Sensing*, 5(2): 949–981.
- Basso, B., Cammarano, D. & Carfagna, E.** *Review of Crop Yield Forecasting Methods and Early Warning Systems*. Paper prepared for the *First Meeting of the Scientific Advisory Committee of the Global Strategy to Improve Agricultural and Rural Statistics*, 18-19 July 2013. Rome, FAO.
- Copernicus.** 2015. *Copernicus global land service*. Available at: <http://land.copernicus.vgt.vito.be/PDF/portal/Application.html#Home>. Accessed on 16 July 2016.
- DevCoCast.** 2013. *GEONETCast for and by Developing Countries: DevCoCast*. Available at: <http://www.devcocast.eu/ViewContent.do?pagelId=1>. Accessed on 16 July 2016.
- Dorward, A., Chirwa, E., & Jayne, T.** 2010. The Malawi Agricultural Inputs Subsidy Programme, 2005/6 to 2008/9. In Chuhan-Pole, P. & Devarajan, S. (eds) *Yes Africa Can: Success Stories from a Dynamic Continent*. World Bank Publication: Washington, D.C.
- Dorward, A., Chirwa, E., Kelly, V., Jayne, T., Slater, R. & Boughton, D.** 2009. *Evaluation of the 2006/7 Agricultural Input Supply Programme, Malawi: Final report*, School of Oriental and African Studies (SOAS) Publication: London.
- Dugger, C.W.** 2007. "Ending Famine, Simply by Ignoring the Experts". New York Times. 2 December 2007. Available at <http://www.nytimes.com/2007/12/02/world/africa/02malawi.html?pagewanted=print>. Accessed on 16 July 2016.
- EUMETSAT.** *EUMETSAT: Monitoring weather and climate from space*. Available at: <https://eoportal.eumetsat.int/userMgmt/protected/welcome.faces>. Accessed on 17 July 2016.
- FAO.** 2009. *Strategic Framework 2010-2019*. Strategic Framework document presented at the 36<sup>th</sup> Session of the FAO Conference, 18-23 November 2009. Rome, FAO. Available at: <http://www.fao.org/docrep/meeting/029/k5864e01.pdf>. Accessed on 11 July 2016.
- \_\_\_\_\_. 2016. Agricultural Stress Index System (ASIS). Available at <http://www/fao.org/giews/earthobservation/>. Accessed on 4 July 2016.

**FAO, UN & World Bank.** 2010. *Global Strategy to Improve Agricultural and Rural Statistics*. Report Number 56719-GLB. World Bank Publication: Washington, D.C.

**FEWS NET.** *Famine and Early Warning System Network*. Data portal. Available at: <http://earlywarning.usgs.gov/fews>. Accessed on 15 July 2016.

**FEWS NET.** 2008. *Report on the Joint Field Trip on Post-Harvest Food Security and Maize Marketing Monitoring, 16<sup>th</sup>–25<sup>th</sup> June 2008*. Available at <http://reliefweb.int/report/malawi/report-joint-trip-post-harvest-food-security-and-maize-marketing-monitoring-16-25-jun>. Accessed on 16 July 2016.

**FEWS NET.** 2009. *Informal Cross Border Food Trade in Southern Africa*. Washington D.C.

**Gasser, W.R.** 1967. *Aerial Photography for Agriculture*. Studies in Intelligence series. Available at [https://www.cia.gov/library/readingroom/docs/DOC\\_0000609171.pdf](https://www.cia.gov/library/readingroom/docs/DOC_0000609171.pdf). Accessed on 24 July 2016.

**Global Strategy to improve Agricultural and Rural Statistics (GSARS).** 2015. *Technical Report on Cost-Effectiveness of Remote Sensing for Agricultural Statistics in Developing and Emerging Economies*. GSARS Report: Rome.

\_\_\_\_\_. 2016. *Crop Yield Forecasting: Methodological and Institutional Aspects*. GSARS Publication: Rome.

**Hagblade, S. & Nyembe, M.** 2008. *Commercial Dynamics in Zambia's Cassava Value Chain*. Food Security Research Project. Working Paper No. 32. Available at <http://www.aec.msu.edu/agecon/fs2/zambia/index.htm>. Accessed on 17 July 2017.

**Hoefsloot, P., Ines, A., van Dam, J., Duveiller, G., Kayitakire, F. & Hansen, J.** 2012. *Combining crop models and remote sensing for yield prediction: Concepts, applications and challenges for heterogeneous, smallholder environments*. Report of CCFAS - JRC Workshop at Joint Research Centre, Ispra, Italy, 13 – 14 June 2012. European Union Publication: Luxembourg. Available at: <http://publications.jrc.ec.europa.eu/repository/bitstream/111111111/31230/1/lbna25643enn.pdf>. Accessed on 7 May 2017.

**Jayne, T.S., Sitko, N., Ricker-Gilbert, J. & Mangisoni, J.** 2010. *Malawi's Maize Marketing System. Lilongwe: The World Bank and Government of Malawi/Ministry of Agriculture*. [http://fsg.afre.msu.edu/malawi/Malawi\\_maize\\_markets\\_Report\\_to-DFID-SOAS.pdf](http://fsg.afre.msu.edu/malawi/Malawi_maize_markets_Report_to-DFID-SOAS.pdf). Accessed on 7 May 2017.

**Jovanović, D., Sabo, F., Govedarica, M. & Marinković, B.** 2014. Crop Yield Estimation in 2014 for Vojvodina Using Methods of Remote Sensing. *Ratarstvo i povrtarstvo*, 51(3): 145-153. Available at <http://scindeks-clanci.ceon.rs/data/pdf/1821-3944/2014/1821-39441403145J.pdf>. Accessed on 13 July 2016.

**Lea, N. & Hanmer, L.** 2009. *Constraints to Growth in Malawi*. Policy Research Working Paper No. 5097. World Bank Publication: Washington, D.C.

**Megill, D.** 2005. *Recommendations for Adjusting Weights for Zambia Post Harvest Survey Data Series and Improving Estimation Methodology for Future Surveys*. Food Security Research Project. Working Paper No. 13. Available at: [http://fsg.afre.msu.edu/zambia/wp13\\_zambia.pdf](http://fsg.afre.msu.edu/zambia/wp13_zambia.pdf). Accessed on 21 July 2016.

**National Oceanic and Atmospheric Administration (NOAA).** 2016. *National Weather Service Climate Prediction Center*. Available at: <http://www.cpc.ncep.noaa.gov>. Accessed on 15 July 2016.

**Pan, G., Sun, G.-J. & Li, F.-M.** 2009. Using QuickBird Imagery and a Production Efficiency Model to Improve Crop Yield Estimation in the Semi-Arid Hilly Loess Plateau, China. *Environmental Modelling & Software*, 24(4): 510-516. Available at <http://www.sciencedirect.com/science/article/pii/S1364815208001746>. Accessed on 7 July 2017.

**Proba-V.** 2016. *proba-VEGETATION: the small satellite for global vegetation monitoring*. Available at: <http://proba-v.vgt.vito.be/content/products>. Accessed on 16 July 2016.

**Randall, L., Bruce, S., Nikolova, S. & Lawson, K.** 2011. *A review of the use of remote sensing for crop forecasting in Australia*. Paper prepared for the 34<sup>th</sup> International Symposium on Remote Sensing of Environment, 10-15 April 2011. Sydney, Australia, International Society for Photogrammetry and Remote Sensing (ISPRS).

**Rashid, S., Minot, N. & Taffesse, A.** 2008. *Assessment of Cereal Production and Availability Forecasts in Ethiopia: A Review of Existing Studies*. International Food Policy Research Institute (IFPRI) Publication: Washington D.C.

**Ray, S.S., Neetu, Mamatha, S. & Gupta, S.** *Use of Remote Sensing in Crop Forecasting and Assessment of Impact of Natural Disasters: Operational Approaches in India*. Paper prepared for the Expert Meeting on Crop Monitoring for Improved Food Security, 17 February 2014. Vientiane, FAO.

**Shang, J., Liu, J., Huffman, T., Qian, B., Pattey, E., Wang, J., Zhao, T., Geng, X., Kroetsch, D., Dong, T. & Lantz, N.** 2014. Estimating plant area index for monitoring crop growth dynamics using Landsat-8 and RapidEye images. *Journal of Applied Remote Sensing*, 8(1). Available at [https://www.researchgate.net/publication/268504936\\_Estimating\\_plant\\_area\\_index\\_for\\_monitoring\\_crop\\_growth\\_dynamics\\_using\\_Landsat-8\\_and\\_RapidEye\\_images](https://www.researchgate.net/publication/268504936_Estimating_plant_area_index_for_monitoring_crop_growth_dynamics_using_Landsat-8_and_RapidEye_images). Accessed on 23 July 2016.

**Soria-Ruiz, J., Fernandez-Ordonez, Y. & McNairn, H.** 2009. Corn Monitoring and Crop Yield Using Optical and Microwave Remote Sensing, in Ho, P.G.P. (ed.), *Geoscience and Remote Sensing*. Intech. Available at <http://www.intechopen.com/books/geoscience-and-remote-sensing/corn-monitoring-and-crop-yield-using-optical-and-microwave-remote-sensing>. Accessed on 10 July 2016

**Ustuner, M., Sanli, F.B., Abdikan, S., Esetlili, M.T. & Kurucu, Y.** 2014. *Crop Type Classification using Vegetation Indices of Rapid Eye Imagery*. Paper prepared for the ISPRS Technical Commission VII Symposium, 29 September–2 October 2014. Istanbul, ISPRS. Available at <http://www.int-arch-photogramm-remote-sens-spatial-inf-sci.net/XL-7/195/2014/isprsarchives-XL-7-195-2014.pdf>. Accessed on 22 July 2016.

**Whitcraft, A.K., McNairn, H., Lemoine, G., LeToan, T. & Sobue, S.-I.** 2016. *The Power of Synthetic Aperture Radar for Global Agricultural Monitoring*. Publication of the CEOS Ad Hoc Working Group on GEOGLAM. Available at [http://ceos.org/document\\_management/Ad\\_Hoc\\_Teams/GEOGLAM/AHTGEOGLAM\\_Power-of-Synthetic-Aperture-Radar-for-Global-Agricultural-Monitoring\\_Apr2016.pdf](http://ceos.org/document_management/Ad_Hoc_Teams/GEOGLAM/AHTGEOGLAM_Power-of-Synthetic-Aperture-Radar-for-Global-Agricultural-Monitoring_Apr2016.pdf). Accessed on 6 July 2016.

**Wu, J., Wang, D. & Bauer, M.E.** 2007. Assessing broadband vegetation indices and QuickBird data in estimating leaf area index of corn and potato canopies. *Field Crops Research*, 102(1): 33-42. Available at [http://rsl.gis.umn.edu/sites/rsl.gis.umn.edu/files/LAI\\_broadband%2520VI\\_QuickBird.pdf](http://rsl.gis.umn.edu/sites/rsl.gis.umn.edu/files/LAI_broadband%2520VI_QuickBird.pdf). Accessed on 6 July 2016.

**Zhang, L. & Grift, T.E.** 2012. A LIDAR-based crop height measurement system for *Miscanthus giganteus*. *Computers and Electronics in Agriculture*, 85: 70-76. Available at [http://abe-research.illinois.edu/pubs/T\\_Grift/A%20LIDAR-based%20crop%20height%20measurement%20system%20for%20Miscanthus%20giganteus.pdf](http://abe-research.illinois.edu/pubs/T_Grift/A%20LIDAR-based%20crop%20height%20measurement%20system%20for%20Miscanthus%20giganteus.pdf). Accessed on 24 July 2016.



This publication was prepared with the financial support  
of the Bill & Melinda Gates Foundation  
Comments and suggestions are welcome and may be sent to: [info@gsars.org](mailto:info@gsars.org)

#### CONTACT

### **Agricultural Market Information System (AMIS) project Statistics Division (ESS)**

Food and Agriculture Organization of the United Nations (FAO)  
Viale delle Terme di Caracalla, 00153 Rome, Italy

ISBN 978-92-5-109840-0



9 789251 098400

17569EN/1/07.17